

NPS ARCHIVE
1997.09
WONNACOTT, W.

NAVAL POSTGRADUATE SCHOOL Monterey, California



THESIS

MODELING IN THE DESIGN AND ANALYSIS OF A HIT-TO-KILL ROCKET GUIDANCE KIT

by

W. Mark Wonnacott

September, 1997

Thesis Advisor:
Second Reader:

Conrad F. Newberry
Louis V. Schmidt

Thesis
W757

Approved for public release; distribution is unlimited.

DUDLEY KNOX LIBRARY
NAVAL POSTGRADUATE SCHOOL
MONTEREY, CA 93943-5101

DUDLEY KNOX LIBRARY
NAVAL POSTGRADUATE SCHOOL
MONTEREY, CA 93943-5101

REPORT DOCUMENTATION PAGE			Form Approved OMB No. 0704-0188	
Public reporting burden for this collection of information is estimated to average 1 hour per response, including the time for reviewing instruction, searching existing data sources, gathering and maintaining the data needed, and completing and reviewing the collection of information. Send comments regarding this burden estimate or any other aspect of this collection of information, including suggestions for reducing this burden, to Washington headquarters Services, Directorate for Information Operations and Reports, 1215 Jefferson Davis Highway, Suite 1204, Arlington, VA 22202-4302, and to the Office of Management and Budget, Paperwork Reduction Project (0704-0188) Washington DC 20503.				
1. AGENCY USE ONLY (Leave blank)		2. REPORT DATE September 1997		3. REPORT TYPE AND DATES COVERED Master's Thesis
4. TITLE AND SUBTITLE MODELING IN THE DESIGN AND ANALYSIS OF A HIT-TO-KILL ROCKET GUIDANCE KIT				5. FUNDING NUMBERS
6. AUTHOR(S) Wonnacott, W. Mark				
7. PERFORMING ORGANIZATION NAME(S) AND ADDRESS(ES) Naval Postgraduate School Monterey, CA 93943-5000				8. PERFORMING ORGANIZATION REPORT NUMBER
9. SPONSORING / MONITORING AGENCY NAME(S) AND ADDRESS(ES)				10. SPONSORING / MONITORING AGENCY REPORT NUMBER
11. SUPPLEMENTARY NOTES The views expressed in this thesis are those of the author and do not reflect the official policy or position of the Department of Defense or the U.S. Government.				
12a. DISTRIBUTION / AVAILABILITY STATEMENT Approved for public release; distribution unlimited.				12b. DISTRIBUTION CODE
13. ABSTRACT (<i>maximum 200 words</i>) This thesis presents several computer models used in the design and analysis of a Hit-to-Kill Rocket Guidance Kit (HRGK). The HRGK—proposed as an inexpensive add-on kit—has the potential of converting unguided 2.75" diameter rockets into precision weapons against non-tank targets. A Naval Postgraduate School design team recently participated in a nation-wide graduate student competition for the design of such a kit. The design and analysis process led the author to develop and use various computer models and simulations. This thesis documents three distinct types of computer models found useful in the design. The first, operational effectiveness modeling, established the cost effectiveness of the NPS HRGK. The second was related to the preliminary sizing of various design aspects—ensuring the proper flow-down of system requirements into design specifications. The third was a six-degree of freedom (6DOF) simulation, developed to perform detailed analyses of the HRGK's performance. Although the models presented in this thesis pertain to the HRGK, the basic principles apply to the design or evaluation of other missile systems, and this thesis provides general insights regarding the benefits and limitations of computer modeling in missile design.				
14. SUBJECT TERMS Rocket Guidance Kit, Missile Design, Missile Modeling and Simulation				15. NUMBER OF PAGES 106
				16. PRICE CODE
17. SECURITY CLASSIFICATION OF REPORT Unclassified		18. SECURITY CLASSIFICATION OF THIS PAGE Unclassified		19. SECURITY CLASSIFICATION OF ABSTRACT Unclassified
				20. LIMITATION OF ABSTRACT UL

Approved for public release; distribution is unlimited

**MODELING IN THE DESIGN AND ANALYSIS OF A
HIT-TO-KILL ROCKET GUIDANCE KIT**

W. Mark Wonnacott
B.S.M.E., Brigham Young University, 1989

Submitted in partial fulfillment of the
requirements for the degree of

MASTER OF SCIENCE IN AERONAUTICAL ENGINEERING

from the

**NAVAL POSTGRADUATE SCHOOL
September 1997**

NPS Archive
1997.09
Wonnacott, W.

~~Thompson~~
~~W 757~~
~~C. 2~~

ABSTRACT

This thesis presents several computer models used in the design and analysis of a Hit-to-Kill Rocket Guidance Kit (HRGK). The HRGK—proposed as an inexpensive add-on kit—has the potential of converting unguided 2.75” diameter rockets into precision weapons against non-tank targets. A Naval Postgraduate School design team recently participated in a nation-wide graduate student competition for the design of such a kit. The design and analysis process led the author to develop and use various computer models and simulations. This thesis documents three distinct types of computer models found useful in the design.

The first, operational effectiveness modeling, established the cost effectiveness of the NPS HRGK. The second was related to the preliminary sizing of various design aspects—ensuring the proper flow-down of system requirements into design specifications. The third was a six-degree of freedom (6DOF) simulation, developed to perform detailed analyses of the HRGK’s performance.

Although the models presented in this thesis pertain to the HRGK, the basic principles apply to the design or evaluation of other missile systems, and this thesis provides general insights regarding the benefits and limitations of computer modeling in missile design.

Table 1: Summary of the data used in the study.	
Variable	Description
Age	Age in years
Gender	Male, Female
Education	High School, College, Graduate
Income	Low, Medium, High
Health	Good, Fair, Poor
Marital Status	Married, Single, Divorced, Widowed
Employment	Employed, Unemployed
Religion	Christian, Muslim, Hindu, Other
Political Affiliation	Democrat, Republican, Independent
Residence	Urban, Suburban, Rural
Travel Frequency	Frequently, Occasionally, Rarely
Travel Mode	Car, Plane, Train, Bus
Travel Duration	Short, Medium, Long
Travel Purpose	Business, Leisure, Family, Other
Travel Satisfaction	Satisfied, Dissatisfied
Travel Frequency (by Age)	Frequency of travel by age group
Travel Mode (by Age)	Mode of travel by age group
Travel Duration (by Age)	Duration of travel by age group
Travel Purpose (by Age)	Purpose of travel by age group
Travel Satisfaction (by Age)	Satisfaction with travel by age group

TABLE OF CONTENTS

I. INTRODUCTION.....	1
A. BACKGROUND.....	1
B. NPS HRGK DESIGN.....	2
C. THESIS SCOPE AND OUTLINE	4
II. COST OF OPERATIONAL EFFECTIVENESS ANALYSES	7
A. SIMPLIFYING ASSUMPTIONS	7
B. COST PER KILL.....	10
C. KILLS PER SORTIE	15
D. COST PER MISSION	15
E. OBSERVATIONS.....	20
III. PRELIMINARY SIZING ANALYSES	23
A. LENGTH, WEIGHT, AND CENTER OF GRAVITY	23
B. MANEUVERABILITY	26
C. SEEKER FIELD OF VIEW	39
D. COMMENTS AND OBSERVATIONS	46
IV. SIX-DEGREE OF FREEDOM SIMULATION	51
A. SIMULATION OVERVIEW.....	51
B. SIMULATION COMPONENTS.....	54
C. EQUATIONS OF MOTION	55
D. NPS HRGK RESULTS.....	58
E. OBSERVATIONS.....	60
V. CONCLUSIONS AND RECOMMENDATIONS.....	61
APPENDIX A. MISSILE AERODYNAMICS NOMENCLATURE	63
APPENDIX B. NOTES ON MATLAB AND SIMULINK.....	65
APPENDIX C. MATLAB CODE LISTINGS.....	67
LIST OF REFERENCES	89
INITIAL DISTRIBUTION LIST	91

LIST OF FIGURES

1. Sample Normal Plane View for a 12 mil, One-Dimensional Dispersion at 5 km Downrange.	3
2. Schematic View of the NPS HRGK Design.	5
3. Projected Area for Light Armored Vehicles.	9
4. Single-Shot P_K and Number of Rockets Required per Target as a Function of CEP.	13
5. Relative Cost per Kill against Various Targets.	14
6. AH-64 Apache Attack Helicopter Sorties Required to Achieve Mission Objective. ..	19
7. Number of Weapons Fired to Achieve Mission Objective.	19
8. Number of Targets Killed by Category, Weapon, and Loadout Option.	20
9. Physical Size and Center of Gravity Design Space.	25
10. Graphical Representation of Maneuverability Model Inputs.	27
11. Closed-Form Solution for Maneuverability Specifications with a Stationary Target..	29
12. Moving Target Scenario for Maneuverability Analysis.	31
13. Maximum Turn Rate Required to Hit Target (95% Probability).	33
14. Minimum Turn Radius Required to Hit Target (95% Probability).....	33
15. Plane-View, Free-Body Diagram for Steady-Turn Maneuver.	35
16. Required Thrust and Angle of Attack for Maximum Turn Rate or Minimum Turn Radius.	38
17. Required Field of View. Results for 95% Probability of Target Staying in Field of View with Worst Case Target Motion.	40
18. Target Distribution Model.	42
19. Illustrative Case for Probabilistic Seeker Field of View Analysis.	43
20. Possible Target Locations.	44
21. Alternative Method for Computing Target Distribution Area within Seeker Field of View Limits.	45
22. Probability Density Functions. (a) Rocket cross-track error, (b) Target cross-track position, and (c) Probability of acquisition.....	45
23. Probability of Target in Field of View for Maximum Launch Range (6 km).	47
24. Sensitivity Analysis of the Steady-Turn Maneuver Model for Thruster Sizing.	49
25. HRGK 6DOF Simulation Overall Block Diagram.	52
26. Detailed View of the Rocket Dynamics Block.	53
27. Detailed View of the Parameters and Coefficients Block.	53
28. Future 6DOF Architecture.	54
29. HRGK-Equipped Rocket Ballistic Trajectories.	59
30. Sustained and Pulsed Thruster Maneuvers.	59

LIST OF TABLES

1. Measures of Merit and Their Associated Objectives and Requirements.	3
2. COEA Target Set with Assumed Dimensions, Desired P_K , and P_{KH}	9
3. Single-Shot Probability of Kill Computer Model Inputs.	11
4. Cost per Kill.	14
5. Kills per AH-64 Apache Sortie against Light Armor Targets.	15
6. Weight, Length, and Center of Gravity Model Inputs.	24
7. Maneuverability Model Inputs.	26
8. Steady-Turn Maneuver Computer Model Inputs.	36
9. Seeker Field of View Analysis Inputs.	41

ACKNOWLEDGMENT

I am grateful for the support of my thesis advisor, Dr. Conrad Newberry, and the second reader, Dr. Lou Schmidt, for their help and guidance. Dr. Robert Ball, Aeronautics and Astronautics Department, and Major Vince Tobin and Captain Pat Mason, U.S. Army, were also very helpful with the cost of operational effectiveness portion of this thesis. I am very appreciative of the sacrifices of Major Boaz Pomerantz, Israeli Air Force; Major Silvino L. Silva, Brazilian Air Force; and Lieutenant Nigel A. Nurse, U.S. Navy who served on the NPS Hit-to-Kill Rocket Guidance Kit Design Team.

I am indeed indebted to my management at the Naval Air Warfare Center Weapons Division and the NAWCWPNS Long-Term Fellowship Committee for their continued support of my studies. I wish to specifically acknowledge Tomma Bersie, Doug Savage, John Freeman, Lee Gilbert, Paul Homer, and Ron Derr for allowing me this time at the Naval Postgraduate School. Special thanks also go to Ted Fincher and Ken Morton for inspiring me to pursue a graduate education.

But, my most tender and heart-felt gratitude is reserved for my sweet wife Diane and our dear children: Andrea, Jared, Nathan, Melissa, Marsha, Jennifer, and Kayla. Without their love and sacrifice, this thesis would not have been possible.

TABLE I		TABLE II	
Year	Value	Year	Value
1980	100	1985	120
1981	110	1986	130
1982	120	1987	140
1983	130	1988	150
1984	140	1989	160
1985	150	1990	170
1986	160	1991	180
1987	170	1992	190
1988	180	1993	200
1989	190	1994	210
1990	200	1995	220
1991	210	1996	230
1992	220	1997	240
1993	230	1998	250
1994	240	1999	260
1995	250	2000	270
1996	260	2001	280
1997	270	2002	290
1998	280	2003	300
1999	290	2004	310
2000	300	2005	320
2001	310	2006	330
2002	320	2007	340
2003	330	2008	350
2004	340	2009	360
2005	350	2010	370
2006	360	2011	380
2007	370	2012	390
2008	380	2013	400
2009	390	2014	410
2010	400	2015	420
2011	410	2016	430
2012	420	2017	440
2013	430	2018	450
2014	440	2019	460
2015	450	2020	470
2016	460		
2017	470		
2018	480		
2019	490		
2020	500		

I. INTRODUCTION

During the first half of the 1996-1997 Naval Postgraduate School (NPS) academic year, a team of aeronautical engineering graduate students was assembled to perform the conceptual design of a hit-to-kill guided rocket kit (HRGK). (The kit attaches to existing unguided rockets to give them precision strike capability.) As part of the design team, the author developed several computer codes or models to facilitate the design and analysis of the HRGK. Since the completion of the design project, many of these codes have been expanded or refined.

This thesis documents the theory used in the development of the improved computer models. It also describes the process of using the models and presents the modeling results for the NPS HRGK design. These descriptions provide an example of the type of modeling that can be used in the design and analysis of missiles.

This introductory chapter provides background information about the HRGK and pertinent details of the NPS HRGK design. It also outlines the remaining chapters of the thesis.

A. BACKGROUND

In the mid 1990s, US Army Aviation identified the need for a low cost, precision kill weapon system for use against soft or light-armor targets (such as trucks, armored personnel carriers, artillery, air defense systems, command posts, amphibious landing vehicles, or patrol boats). The objective of such a system would be to minimize the cost per kill for these types of targets. The 2.75-inch rocket (Mark-66) with a unitary, high-explosive (HE) warhead (M151) and a point detonation fuze (M423) was subsequently identified as a promising candidate for this low-cost mission.

These unguided rockets cost only about \$1,000 per unit, and large inventories are already available to the military services. The 2.75-inch rockets are launched from helicopters, fixed-wing aircraft, surface combat vehicles, and naval vessels. U.S. Army Helicopters carry the rockets in either a 7- or 19-tube launcher pod as part of the Hydra-70 weapon system. The Hydra-70 system includes the weapon (rocket, fuze, and warhead), launch pod, and an armament management system. With this system, the rockets can be fired in single-shot mode or in various sized ripple or salvo shots. The rockets can carry various warheads or payloads (including HE, kinetic energy flechettes, multi-purpose

submunitions, illumination flare, marking smoke, and chaff) with various fuzing options (including remotely set timed burst and super-quick or delayed contact fuzes).

The Mark-66 rocket with warhead and fuze is spin stabilized to provide some degree of accuracy. The rocket uses a fluted single throat nozzle to achieve approximately a 10 Hz spin by the time it exits the launcher. By motor burnout, the spin rate has increased to approximately 35 Hz. After motor burn out, the rocket's wrap-around fins de-spin the projectile and cause a significant spin rate (15-20 Hz) in the reverse direction. The spinning characteristics of the rocket played a significant role in the NPS design as will be discussed in the following section.

The baseline rocket configuration chosen for the kit (HE warhead and super-quick contact fuze) is an *area* suppression weapon. The unguided rocket has a total 12 milliradians (mill), one-dimensional dispersion, meaning that for every thousand meters of down range flyout a 12 m error results (1σ or 68%). For example, a nominal 5 km range launch would result in a normal-plane¹, radial miss of up to 60 m (5×12)—with 39% probability (see Figure 1). This level of accuracy is far from that required for single-shot, precision kills. To achieve point target accuracy, the rocket needs to be fitted with some type of guidance and control kit. The conceptual NPS HRGK, described in the next section, was designed to serve this purpose.

B. NPS HRGK DESIGN

The NPS HRGK was designed to meet certain requirements. The following subsections summarize these requirements and the pertinent aspects of the NPS HRGK design.

1. HRGK Design Specifications

The NPS HRGK design requirements were prepared by the American Institute of Aeronautics and Astronautics (AIAA) Missile Systems Technical Committee and were used for the 1996/1997 Graduate Team Missile Design Competition sponsored by the AIAA and Northrop Grumman Corporation [Ref. 1]. Table 1 summarizes the HRGK's measures of merit with their associated objectives and pertinent requirements.

¹ For the purposes of this thesis, all accuracies are in terms of the plane normal to the rocket trajectory rather than in the ground plane. This convention is typical for guided missiles.

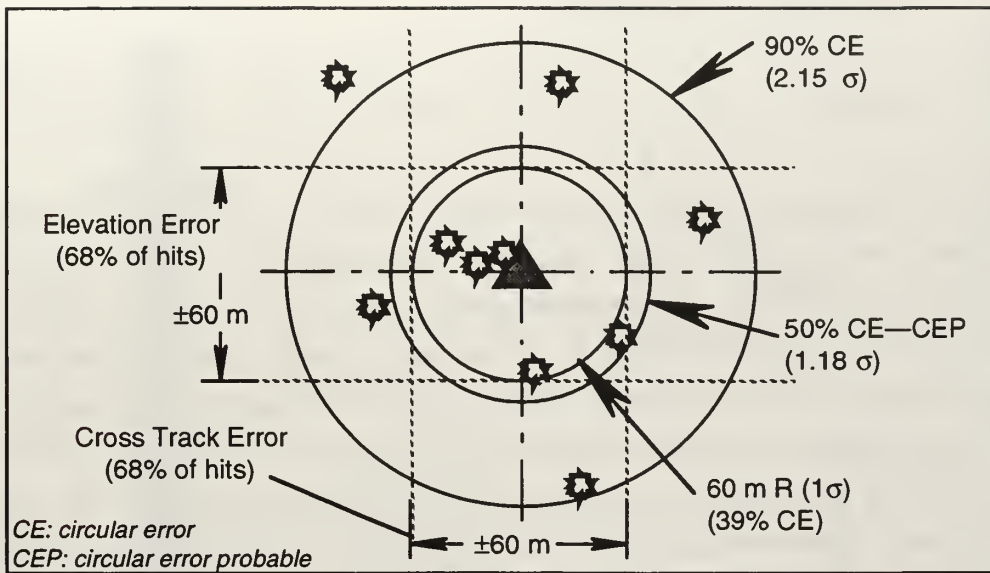


Figure 1. Sample Normal Plane View for a 12 mil, One-Dimensional Dispersion at 5 km Downrange. $[(12 \text{ m} / 1000 \text{ m}) \cdot 5000 \text{ m} = 60 \text{ m} (1\sigma)]$.

Table 1. Measures of Merit and Their Associated Objectives and Requirements.

<i>Measure of Merit and Objective</i>	<i>Specific Requirements</i>
Cost Maximize Units Bought	<ul style="list-style-type: none"> • \$10,000 Avg. Unit Cost (5,000 Unit LRIP^a) • Maximum \$1 Billion Total 5 Year Production Buy
Current Systems Computability Maximize Operability & Reduce Life Cycle Cost	<ul style="list-style-type: none"> • Existing Rocket, Fuze, Warhead, & Launch Pod <ul style="list-style-type: none"> — 72 inch total system maximum length — loaded pod center of gravity between lugs • Laser Designator Compatibility
Accuracy Provide Hit-to-Kill Accuracy	<ul style="list-style-type: none"> • 0.5 m CEP • 60 mph target speed
Weight Maximize Kits Deliverable via Airlift	<ul style="list-style-type: none"> • 30 pound Total System Maximum Weight
Maximum Range Maximize Platform Standoff Survivability	<ul style="list-style-type: none"> • 6 km (or More) Maximum Range (Maneuverability at Maximum Range)
Minimum Range Maximize Launch Acceptable Region	<ul style="list-style-type: none"> • 1 km (or Less) Minimum Range (Guidance, Fuzing, and Launch Transients)
Adverse Weather Performance Maximize Operability and Combat Flexibility	<ul style="list-style-type: none"> • 99% Worldwide Weather Capable
Time to Target Minimize Time (Improve Survivability)	<ul style="list-style-type: none"> • 16 seconds or Less to 5 km Range

^a Low Rate Initial Production

2. NPS Design Highlights

The following paragraphs briefly describe the major features of the NPS HRGK design. The design team's proposal gives a more detailed description of the design [Ref. 2].

The HRGK attaches over the fuze at the front end of a 2.75 inch rocket. It utilizes a strapped-down, four-quadrant silicon detector for semi-active laser spot homing. The HRGK employs three hot gas reaction jets (thrusters) to control the rocket's attitude and trajectory. A solid propellant burning in an insulated pressure chamber generates the thruster gas. The kit uses a look-up table scheme to control the thrusters based solely on the seeker outputs. Fast-cycle solenoid valves open and close the "on-off" thrusters. The thruster nozzles are inter-spaced between three fixed, wrap-around canards. The canards provide increased maneuverability (by reducing the rocket's static stability) and help constrain any jet and air stream interaction effects. The canards also contribute significantly to the HRGK's roll stability.

Thrust and radial needle rollers effectively isolate the NPS HRGK from the spinning motion of the rocket. Simulations show the kit's roll rate to be less than 9 degrees per second after the first seconds of flight. The kit's low spin rate and the simplistic pursuit navigation scheme eliminate the need for inertial sensors and greatly reduce the kit's signal processing requirements.

As shown in Figure 2, the basic kit is 19.0 inches long. It has a diameter of 2.75 inches (with canards wrapped in) and weighs 7.0 pounds. The NPS HRGK attaches to the 2.75 inch rocket between the M151 high-explosive warhead and M423 point detonation fuze. The all-up round is 68.75 inches long and weighs 30 lb. The guided rocket is compatible with the Hydra-70 rocket system.

C. THESIS SCOPE AND OUTLINE

The NPS HRGK design was achieved and verified with the aid of several original computer codes and models. The codes and models developed by the author and described in this thesis fall into the following three major categories:

- cost of operational effectiveness analyses,
- preliminary sizing analyses, and
- six-degree of freedom simulation.

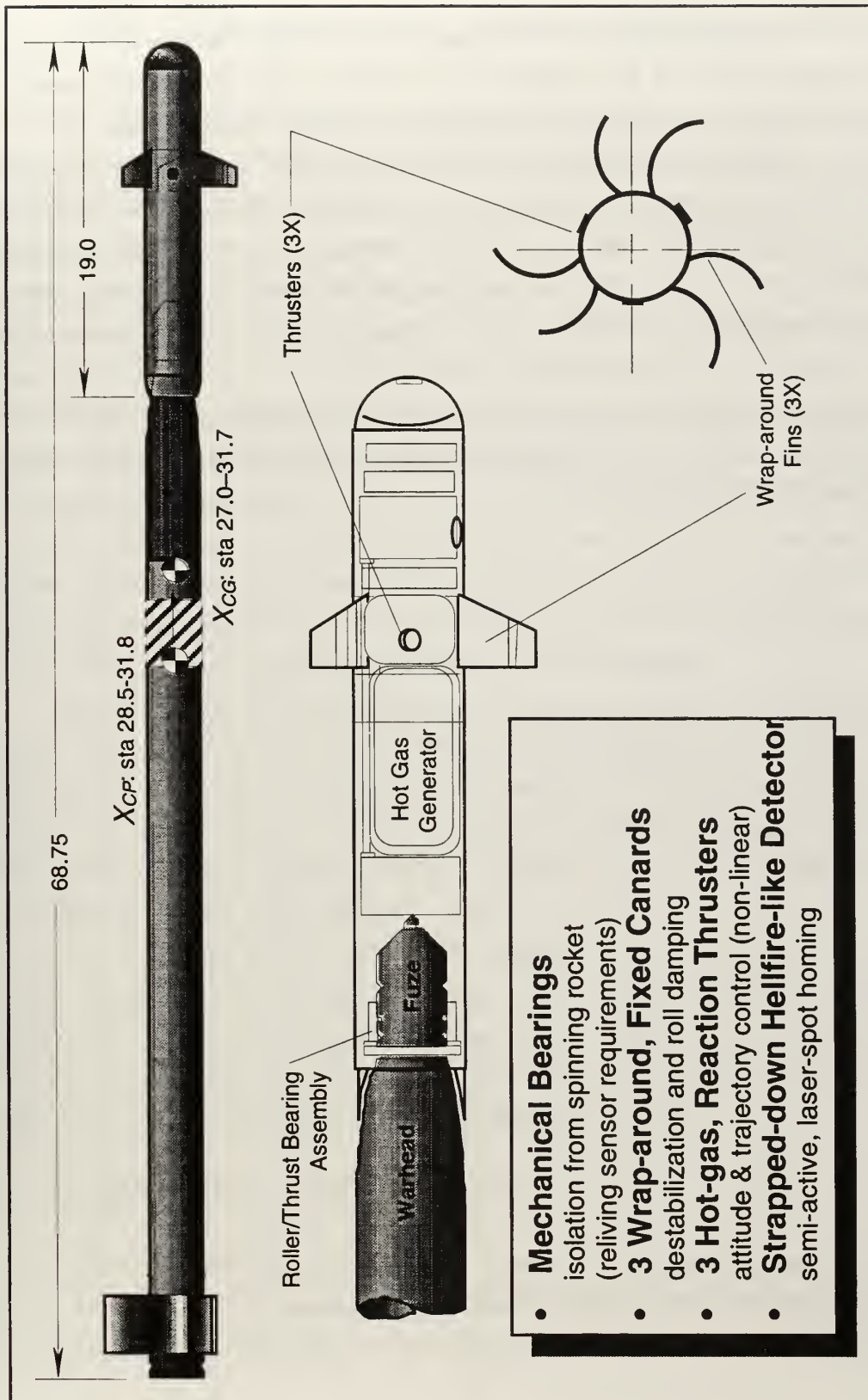


Figure 2. Schematic View of the NPS HRGK Design. Top drawing shows HRGK in place on Mark-66 Rocket with warhead and fuze. The in-flight ranges of the guided rocket's center of gravity and center of pressure are also indicated on the top drawing.

The following three chapters provide descriptions of the modeling processes in the respective categories. Each of these chapters (1) includes a description of the modeling methodology, (2) gives example results specific to the NPS HRGK design, and (3) discusses observations regarding the general use of the models. The final thesis chapter summarizes these conclusions and provides recommendations for additional work with the computer models. Appendices that contain the computer code listings and additional background have also been included. The appendices include a brief description of missile aerodynamics nomenclature (Appendix A) and a discussion concerning the use of the computer software MATLAB® and SIMULINK® (Appendix B).

In general, this thesis is not intended to be read from cover to cover. Instead this thesis is offered as a reference to possible analysis types and modeling methods for use in future conceptual design of missile systems.

® MATLAB and SIMULINK are registered trademarks of The MathWorks, Inc.

II. COST OF OPERATIONAL EFFECTIVENESS ANALYSES

Cost of operational effectiveness analysis (COEA) must be an important part of the design process. First, COEAs provide justification for the design based on operational effectiveness cost savings. But, just as importantly, COEA-type analyses provide the designer with focus and insight into the truly important aspects of the design. Basic COEA models with many simplifying assumptions can be used early in the process to focus design decisions. As the design matures, refined models can be used to evaluate major design iterations.

The COEA modeling developed for the NPS HRGK provided the justification for a HRGK-like system. The overall objective of the HRGK was to minimize the total cost per kill against appropriate targets. From the analysis, guided rockets showed a decreased cost per target kill and increased target kills per sortie when compared to alternative weapon systems. Additional modeling showed that guided rockets resulted in a reduction of sorties and weapon costs required to achieve a specific mission objective. The final NPS HRGK was an attempt to provide the lowest possible cost per kill design.

The COEA modeling discussed in this chapter provides several different levels of results. The low level results of the modeling include single-shot probabilities of kill and the number of weapons required per kill as a function of circular error probable (CEP). These values are then used to derive the cost per kill and the sorties per mission results. The number of weapons required per kill results also provide some additional insights that was critical to the NPS HRGK design.

The following section describes the simplifying assumptions used in the NPS HRGK COEA models. Subsequent sections provide more detailed descriptions of the model methodologies and the results. The chapter ends with a discussion of some observations concerning the use of COEA modeling in design. (Listings of the computer codes used in the NPS HRGK COEA are included in Appendix C.)

A. SIMPLIFYING ASSUMPTIONS

Several simplifying assumptions were made to facilitate the early NPS HRGK COEA modeling. These assumptions included defining guided and unguided weapon trajectories and costs, establishing a target set with desired probabilities of kill (P_k) for each

target, and estimating each target's vulnerability in terms of the conditional probability of kill given a hit (P_{KH}).

1. Weapon Accuracies

The accuracies for the unguided rocket were taken as a function of launch range and were based on a 12 milliradian accuracy [Ref. 1]. As a baseline for the comparison, a mid-range, 3-km shot was used with a resulting 42.4 m normal-plane CEP (36 m 1-dimensional, standard deviation multiplied by 1.1774—see Figure 1, for example). For the guided rockets, three different normal-plane CEP accuracies were assumed for comparison purposes—0.5 m, 1.0 m, 1.5 m, and 3.0 m.

For both the unguided and guided rockets, a 20° terminal dive angle (relative to the horizontal) was assumed as a best estimate¹. The shallow dive caused an increase in the rocket's ground plane down-track error but did not affect the cross-track error. These effects were accounted for implicitly in determining the probability of hitting the target.

For simple comparison purposes, the AGM-114 laser Hellfire's accuracy was assumed to be such that if it was shot at a target it would achieve the desired kill.

2. Target Set

The effectiveness analysis used four representative targets (mobile air defense unit, armored personnel carrier, support vehicle, and patrol boat). These targets were each assumed to be simple blocks of appropriate length, width, and height dimensions (see Figure 3). Table 2 lists the four targets with their associated dimensions [Ref. 3, 4, 5, and 6]. The dimensions are representative for targets found in the references. Table 2 also lists a desired P_K for each of the targets. These desired probabilities were assumed, based on the typical importance of the target.

The probability of each target being hit (P_H) was computed as the joint probability of the rocket being within both the top-to-bottom and the side-to-side dimensions of the target. The projected dimensions of the targets (normal to the flight trajectory) were computed for both a head-on and a broad-side attack. The two attack approaches gave the extremes in the target's presented area as shown in Figure 3. The P_H 's for the two extreme cases were computed and then equal-weight averaged as an estimate of the P_H for uniformly distributed attack approaches (0°-360°).

¹ Later analysis showed that unguided rockets may have even more shallow dive angles, making them even more inaccurate in the ground-plane.

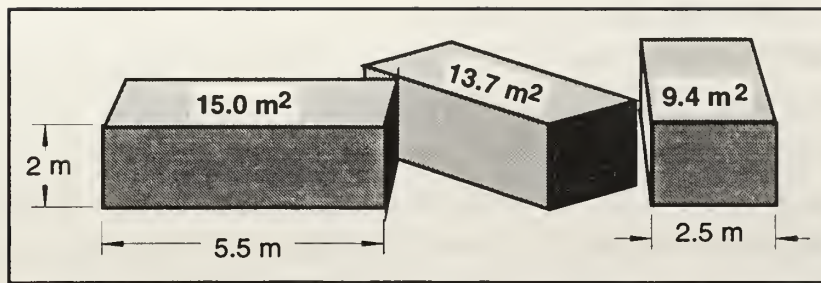


Figure 3. Projected Area for Light Armored Vehicles (head-on, 45°, and broad-side attacks with 20° dive angle).

Table 2. COEA Target Set with Assumed Dimensions, Desired P_K , and $P_{K/H}$.

<i>Target Description</i>	<i>Dimensions L x W x H</i>	<i>Desired P_K</i>	<i>$P_{K/H}$</i>
Mobile Air Defense Unit (Light Armor)	5 x 2.5 x 2 m	95%	90%
Armored Personnel Carrier (APC)	5 x 2.5 x 2 m	60%	80%
Support Vehicle (Large Truck)	8 x 2.5 x 2.5 m	50%	100%
Patrol Boat	14 x 4.5 x 1.5 m	75%	70%

3. Target Vulnerabilities

For each target a “cookie-cutter” model [Ref. 7] was used in determining the single-shot P_K (P_{Kss}). With the cookie cutter model, the target suffers a kill (according to an assumed $P_{K/H}$) if and only if it is actually hit. “Near misses” do not provide any P_K . Thus the value for P_K was the simple product of $P_{K/H}$ and P_H . The assumed values of $P_{K/H}$ are best estimates and are shown in the last column of Table 2. These high values of $P_{K/H}$ reflect the facts that (1) the targets were relatively soft, (2) the rocket is actually impacting the target to score a hit, and (3) the desired type of kill (firepower, mobility, catastrophic, etc.), which was not specified, may only require minor damage to the target.

4. Weapon Costs and Additional P_K 's

The per unit cost of the guided rocket concepts was assumed to be \$10,000—the upper threshold cost from the AIAA design contest, and the unguided, unitary warhead round (M151) was assumed to cost \$1,000 [Ref. 1]. A multipurpose submunitions (MPSM) round was assumed to cost \$2,000 and have a 10% P_K against non-tank targets. The Hellfire missile was assumed to have a per unit cost of \$40,000 [Ref. 8] and a single-shot kill capability against all four representative targets ($P_K = 80\%$ for tanks and $P_K = 100\%$ for all others).

5. Additional Assumptions

Additionally, the assumption was made that all weapons functioned during launch, flyout, and fuzing; with 100% reliability. The aimpoint was assumed to be the centroid of the target block without any bias errors in designation or flyout. It was also assumed that all rocket accuracy errors had a bivariate normal distribution with independent, equi-variance (σ^2) distributions along any two orthogonal axes normal to the flyout. Furthermore, the errors were assumed independent from rocket to rocket. Thus, the CEP was 1.1774σ and the P_K for n multiple rockets was $1 - (1 - P_{K \text{ single shot}})^n$.

The simplifying assumptions discussed in this section are reasonably valid under many conditions. The last section of this chapter (II.E. *Observations*) includes a brief discussion on the affect of some of the assumptions.

B. COST PER KILL

The overall objective of the HRGK was to minimize the total cost per kill against appropriate targets. To determine the cost per kill, the probability of kill per single weapon had to be established using the assumptions discussed above. This single-shot probability of kill, P_{Kss} , with the additional assumptions above, could then be used to determine the number of weapons required to achieve the desired P_K . From the number of weapons required per kill and the assumed cost per weapon, the estimated cost per kill could then be established. The process for determining the cost per kill and the results for the HRGK analysis are discussed in the following subsections.

1. Methodology

The methodology for determining the cost per kill involves determining the P_{Kss} for each weapon against each target and then determining the number of weapons required to achieve the desired P_K . A computer program was written in MATLAB to compute the P_{Kss} and number of weapons required per kill as a function of CEP. This program, which also computes a relative cost per kill tradeoff plot, is described in the following paragraphs.

a. Model Inputs

Only a small number of inputs are required for the single-shot probability of kill computer model. These inputs can be divided into descriptions of the target and of the weapon trajectory. Table 3 lists these two types of required inputs.

Table 3. Single-Shot Probability of Kill Computer Model Inputs.

<i>Input Name</i>	<i>Input Description</i>
<i>Target</i>	
L, H, and W	Effective Target Length, Height, and Width (unit of length)
Pkh	Probability of Kill given a Hit within the Effective Target Dimensions
PkD	Desired Probability of Kill for the Target
<i>Weapon Trajectory</i>	
dive	Dive Angle Relative to Horizontal (degrees)— θ
CEP_min	Minimum CEP to Be Used in Computations (unit of length)
CEP_max	Maximum CEP to Be Used in Computations (unit of length)

b. Single-Shot Probability of Kill

The first step in estimating the single-shot probability of kill is to establish the end-on and broad-side projected edges of the target normal to the weapon trajectory. The side-to-side dimensions for the two cases are simply $X_1 = W$ and $X_2 = L$, for the end-on and broad-side cases, respectively. The top-to-bottom dimensions are given by the following equations:

$$Y_1 = H \cos \theta + L \sin \theta \quad (\text{end-on})$$

$$Y_2 = H \cos \theta + W \sin \theta \quad (\text{broad-side})$$

Next, the probability of hit, P_H , was determined by estimating the probability of the weapon striking within the projected edges of the target—the joint probability of being within $\pm \frac{X_i}{2}$ and $\pm \frac{Y_i}{2}$ of the aimpoint, where $i = 1$ or 2 depending on the approach case. Given the assumed, independent bivariate nature of the weapon errors, the joint probability could be computed as the product of the two—cross-track (X -direction) and elevation (Y -direction)—probabilities. The `erf` function in MATLAB is defined as the following:

$$P = \frac{2}{\sqrt{\pi}} \int_0^x e^{-t^2} dt,$$

so the joint probability described above is given by the following MATLAB expression where the argument to `erf` is normalized by $\sqrt{2}$:

$$P_{H_i} \left(\pm \frac{X_i}{2}, \pm \frac{Y_i}{2} \right) = \text{erf} \left(\frac{X_i}{2} \frac{1}{\sqrt{2}\sigma} \right) \cdot \text{erf} \left(\frac{Y_i}{2} \frac{1}{\sqrt{2}\sigma} \right)$$

and where $i = 1$ or 2 and σ is the $CEP/1.1774$. The total P_H is then the equal weighted average of P_{H_1} and P_{H_2} . In other words, $P_H = (P_{H_1} + P_{H_2})/2$.

With the probability of hit, P_H , and the input $P_{K/H}$, the single-shot probability of kill is estimated as the product of the two.

$$P_{Kss} = P_{K/H} \cdot P_H.$$

c. *Number of Weapons per Kill*

With the P_{Kss} and the assumption that flyout errors for each weapon shot are unbiased and independent, the number of weapons required to achieve a desired P_K can be calculated.

The probability of the target surviving a single shot is given as the complement of P_{Kss} , $1 - P_{Kss}$. The probability of surviving n , independent shots is that quantity raised to the n th power, $(1 - P_{Kss})^n$. Thus, the probability of kill for n , independent shots is the complement to the latter probability of survival, namely:

$$P_K = 1 - (1 - P_{Kss})^n$$

The number of shots, n , to achieve a desired P_K can be determined by solving the above equation for n as is shown in the following equation.

$$n = \frac{\ln(1 - P_K)}{\ln(1 - P_{Kss})}.$$

d. *Accuracy and Relative Cost Trade-off Chart*

Knowing the number of weapons, n , required to achieve a desired probability of kill (P_K) against a specific target, the relative weapon costs to give equal cost per kill can be computed. For example, if two weapons (A) with a 0.5 m CEP or six weapons (B) with a 2.0 m CEP would be required to achieve a desired P_K , then if the cost of weapon B was one-third the cost or less of weapon A , weapon B would have a lower cost per kill against the specified target.

In the computer model, weapon costs are normalized relative to the cost of the minimum input CEP, CEP_{min} , weapon. Also, the number of weapons required to achieve a desired P_K are considered only as integer values.

e. Cost per Kill Calculations

The absolute cost per kill can easily be computed from the results of the computer model described above. The cost per kill for a specified target and weapon is simply the integer number of weapons required to achieve the desired P_K against that target multiplied by the assumed cost of that weapon.

2. Results

The results of the computer model described above are shown for the targets and weapons described above in section II.A. *Simplifying Assumptions*. The results include both the P_{Kss} and the cost per kill.

a. Direct Model Outputs

The combined single shot probability of kill and the number of weapons required to achieve a desired P_K are shown as a function of CEP in Figure 4. Various assumed accuracies for the unguided rockets are also marked on the plot with their corresponding launch ranges.

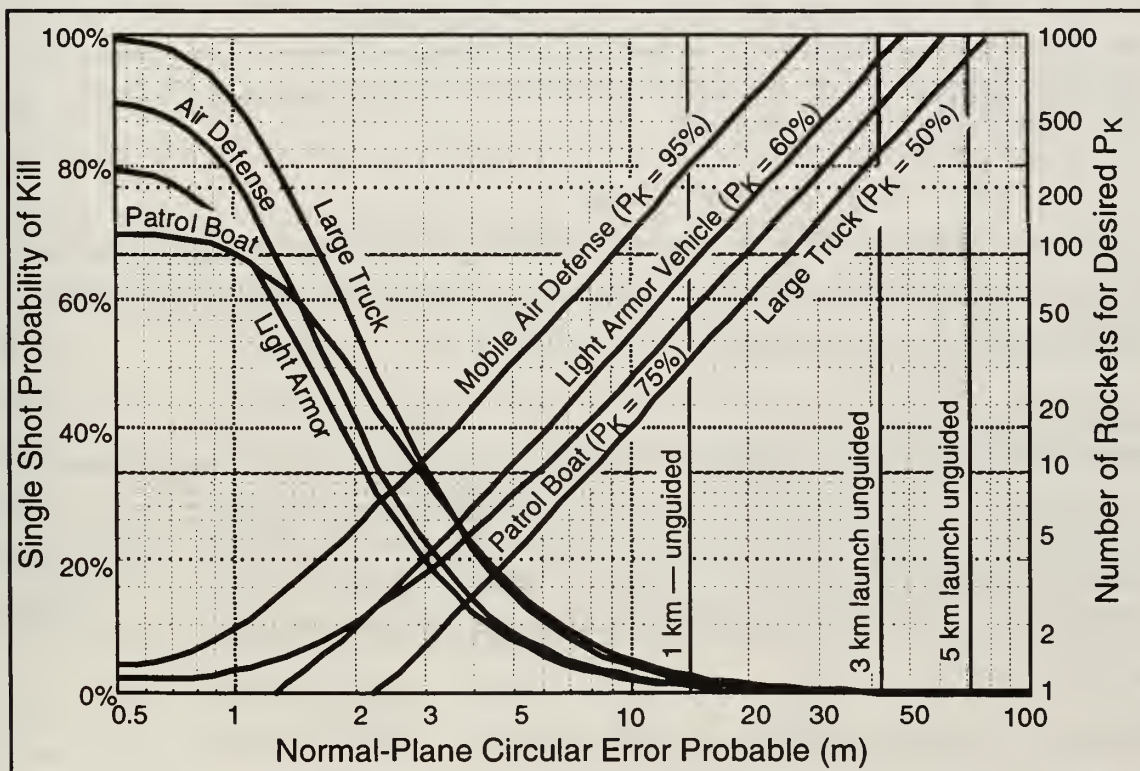


Figure 4. Single-Shot P_K and Number of Rockets Required per Target as a Function of CEP. (P_{Kss} curves slope down from upper left; number of rockets curves slope up to upper right.)

Figure 5 shows the relative weapon costs for equal cost per kill as a function of CEP. In this chart the weapon costs are relative to the 0.5 m CEP weapon cost. From the chart it appears that a weapon with a 2 m CEP (*B*) would have an improved cost per kill against all targets if the weapon cost were less than 33% of the 0.5 m CEP weapon (*A*). Weapon *C*, at half the cost of *A*, has the highest cost per kill at 4 m CEP.

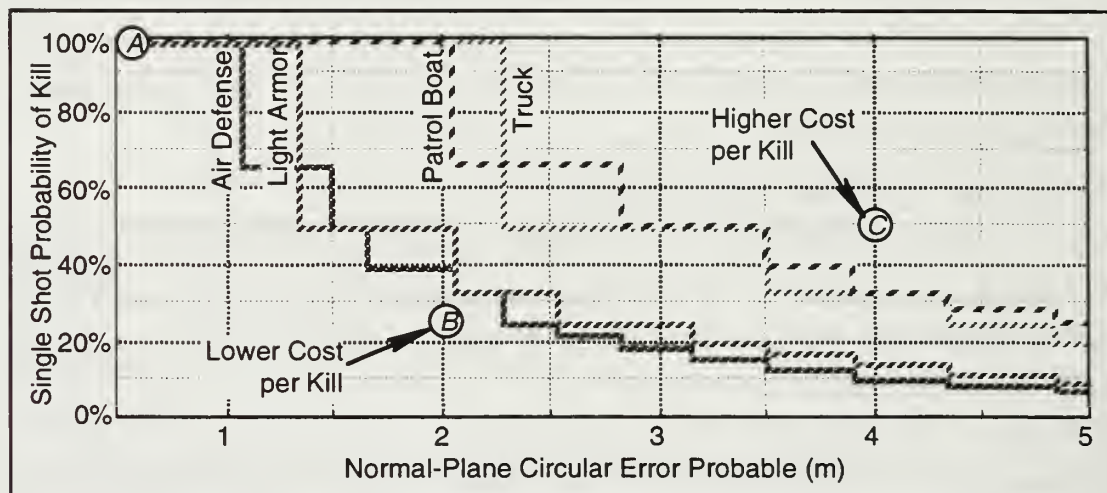


Figure 5. Relative Cost per Kill against Various Targets. Lettered design points (*A*, *B*, and *C*) are shown for illustration only.

b. Cost per Kill Results

From the number of weapons required per target kill, the costs per kill for each of the weapons can be computed. The results for the HRGK analysis based on the single assumed guided rocket cost are shown in Table 4.

Table 4. Cost per Kill.

<i>Target</i>	<i>Unguided Rocket</i>	<i>Guided Rocket</i>				<i>Hellfire</i>
		<i>0.5 m</i>	<i>1.0 m</i>	<i>1.5 m</i>	<i>3.0 m</i>	
Mobile Air Defense Unit	\$2,219k	\$20k	\$20k	\$40k	\$120k	\$40k
Light Armor	\$764k	\$10k	\$10k	\$20k	\$50k	\$40k
Large Truck	\$294k	\$10k	\$10k	\$10k	\$20k	\$40k
Patrol Boat	\$467k	\$20k	\$20k	\$20k	\$40k	\$40k

C. KILLS PER SORTIE

A shortcoming of the cost per kill analysis previously presented is illustrated in the following example. A weapon with a 2.0 m CEP (such as *B* in Figure 5) and a quarter of the cost of a 0.5 m CEP weapon has a lower cost per kill than the 0.5 m CEP weapon (such as *A* in Figure 5). However, it would take three times as many of the less accurate (but inexpensive) weapons to achieve the same number of kills against mobile air defense targets. The number of weapons available for a given mission would be limited by the number of launch platforms sorties. The importance of kills per sortie is completely ignored in the cost per kill data. A kills per sortie analysis helps to illustrate the importance of precision in strike warfare.

The kills per sortie analysis performed for the HRGK was based on AH-64 Apache attack helicopter sorties. The helicopters were assumed to have either pure or mixed weapon payloads or loadouts. The pure loadouts were either 16 Hellfires or 76 rockets (four 19-tube rocket launchers). The mixed loadouts combined eight Hellfires with a limited number of unitary warhead (M151) rockets (guided or unguided) and additional MPSM-equipped rockets. The number of kills per sortie were calculated based on the P_{Kss} data in Figure 4 and the assumed P_K 's from the sub-section II.A.4. *Weapon Costs and Additional PK's*. The results are tabulated in Table 5 for the light armor target case.

Table 5. Kills per AH-64 Apache Sortie against Light Armor Targets.

<i>Weapon</i>	<i>Maximum Load</i>		<i>Mixed Load</i>	
Hellfire	16 Hellfires	16 Kills	8 Hellfires & 38 MPSM	9.90 Kills
HRGK (0.5m)	76 HRGKs	60.7 Kills	8 Hellfires, 24 MPSM, & 14 HRGKs	20.4 Kills
HRGK (1.0m)	76 HRGKs	52.5 Kills	8 Hellfires, 24 MPSM, & 14 HRGKs	18.9 Kills
HRGK (1.5m)	76 HRGKs	38.7 Kills	8 Hellfires, 24 MPSM, & 14 HRGKs	16.3 Kills
HRGK (3.0m)	76 HRGKs	15.1 Kills	8 Hellfires, 24 MPSM, & 14 HRGKs	12.0 Kills
Unguided	76 Rockets	0.09 Kills	8 Hellfires, 24 MPSM, & 14 Rockets	9.22 Kills

D. COST PER MISSION

A final type of modeling performed by the author for the NPS HRGK design combines the attributes of the cost per kill and the kills per sortie analyses. This analysis assesses the cost (in terms of sorties and cost of weapons fired) to achieve a mission

objective. The following subsections outline the analysis and present the results for the HRGK.

1. Mission Definition

The cost per mission analysis was based on a specific assumed mission scenario. This scenario defined the target matrix with a set priority on the target types as well as a mission objective. The scenario also defined the attacking helicopter loadouts. The assumed scenario is defined in the following paragraphs.

a. Target Matrix

The assumed target was an assembly area with the following targets types listed by priority and with the target quantities in parentheses:

- Mobile Air Defense Units (8)
- Main Battle Tanks (40)
- Light Armored Vehicles (150)
- Support Vehicles (250)

The mission objective was to destroy half of the vehicles in each combatant category.

b. Weapon Loadouts

The assumed initial strike force was a flight of five AH-64 Apache attack helicopters. As additional helicopters were needed they were added to the attack force one at a time. Each Apache carried a nominal load of eight Hellfires and two 19-rocket launcher pods. Each pod (which could be divided into zones) was loaded with twelve M261 MPASM-equipped rockets and seven guided or unguided M151 unitary warhead equipped-rockets. [Ref. 9]

The limited number of HRGK-equipped weapons (14) per helicopter was based on the assumption that only six to eight laser-designated flyouts could be made from a firing position before the helicopters would be forced to relocate. With eight Hellfires and 14 HRGKs, three firing positions would be required for the attack. This was considered to be the upper limit for a deep strike mission. The MPASM rockets would not require laser designation, yet they would still be effective against clusters of light armor, material, or personnel. [Ref. 9]

2. Example Calculation

The following provides an example of the process used to model the mission engagement. The 1.0 m CEP case is illustrated.

a. First Five Helicopters

The weapons loadout of the first five helicopters consists of the following:

- 40 Hellfire Missiles (each at a tank)
 - $40 \times 0.8 = 32$ tank kills
- 70 HRGK Rockets (16 at air defense units—2 per unit, 54 at light armor)
 - 16—8 air defense unit kills with $P_K = 95\%$
 - $54 \times 0.6909 = 37.31$ light armor kills
- 120 MPSM Rockets ($120 \times 0.1 = 12$ kills divided between non-tank targets)
 - 6 light armor kills
 - 6 support vehicle kills

In summary, after five helicopters, 8 air defense units are killed (exceeding objective), 32 tanks are killed (exceeding objective), 43.31 light armor vehicles are killed (31.69 short of the objective), and 6 support vehicles are killed (exceeding objective).

b. Sixth Helicopter

The following delineates the use of the sixth helicopter's weapons:

- 8 Hellfire Missiles (each at a tank)
 - $8 \times 0.8 = 6.4$ tank kills
- 14 HRGK Rockets (each at light armor)
 - $14 \times 0.6909 = 9.67$ light armor kills
- 24 MPSM Rockets ($24 \times 0.1 = 2.4$ kills divided between non-tank targets)
 - 1.2 light armor kills
 - 1.2 support vehicle kills

In summary, after the sixth helicopter, 8 air defense units are killed (exceeding objective), 38.4 tanks are killed (exceeding objective), 54.18 light armor vehicles are killed (20.82 short of the objective), and 7.2 support vehicles are killed (exceeding objective).

c. Seventh Helicopter

The following is for the seventh helicopter:

- 8 Hellfire Missiles (2—each at a tank, 6 at light armor)
 - $2 \times 0.8 = 1.6$ tank kills
 - $6 \times 1.0 = 6$ light armor kills
- 14 HRGK Rockets (each at light armor)
 - $14 \times 0.6909 = 9.67$ light armor kills
- 24 MPSM Rockets ($24 \times 0.1 = 2.4$ kills divided between non-tank targets)
 - 1.2 light armor kills
 - 1.2 support vehicle kills

After the seventh helicopter, 8 air defense units are killed (exceeding objective), 40 tanks are killed (exceeding objective), 71.05 light armor vehicles are killed (3.95 short of the objective), and 8.4 support vehicles are killed (exceeding objective).

d. Subsequent Helicopters

For any subsequent helicopters the weapons would be used as follows:

- 8 Hellfire Missiles (each at light armor)
 - $8 \times 1.0 = 8$ light armor kills
- 14 HRGK Rockets (each at light armor)
 - $14 \times 0.6909 = 9.67$ light armor kills
- 24 MPSM Rockets ($24 \times 0.1 = 2.4$ kills divided between non-tank targets)
 - 1.2 light armor kills
 - 1.2 support vehicle kills

This gives 18.87 light armor kills per sortie; therefore, the number of sorties, after the seventh, to reach the objective of 75 light armor kills is $3.95/18.87 = 0.21$, and the total number of sorties required for the mission is 7.21.

e. Summary

After 7.21 sorties the following number of weapons have been fired with the indicated assumed weapon cost:

- 57.67 Hellfires (\$2.3M)
- 100.9 HRGKs (\$1.0M)
- 173.0 MPSMs (\$0.35M)

for a total weapon cost of \$3.66M. The total targets killed were:

- 8 air defense units
- 40 tanks
- 75 light armor vehicles
- 8.65 support vehicles.

3. Results

Figures 6, 7, and 8 illustrate the results for the HRGK mission analysis. Figure 6 shows the number of sorties required to achieve the mission objective. With an assumed cost per sortie, these numbers could be directly applied to the weapon's cost per kill. The inclusion of a helicopter attrition rate would also make the cost per kill more realistic. Note that the 1.0 m CEP rocket does not require many more sorties than does the 0.5 m CEP.

Figure 7 shows the number of weapons fired during the mission for each of the different weapon cases. The total weapon cost in millions of dollars is also indicated on the graph.

Figure 8 summarizes which weapons killed which targets. It is interesting to note that with accurate HRGKs, the more expensive Hellfire missile could be used almost exclusively on tanks. On the other hand, when unguided rockets were used, nearly all the

target kills were from the Hellfire, and the unguided unitary (M151) rocket only registered 0.242 light armor and 0.474 support vehicle kills.

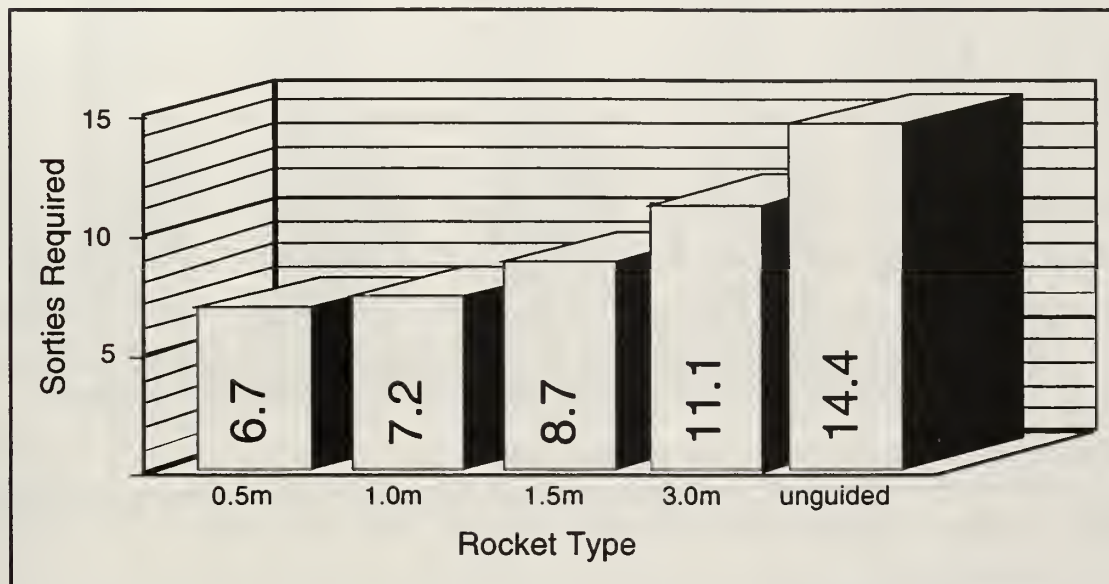


Figure 6. AH-64 Apache Attack Helicopter Sorties Required to Achieve Mission Objective.

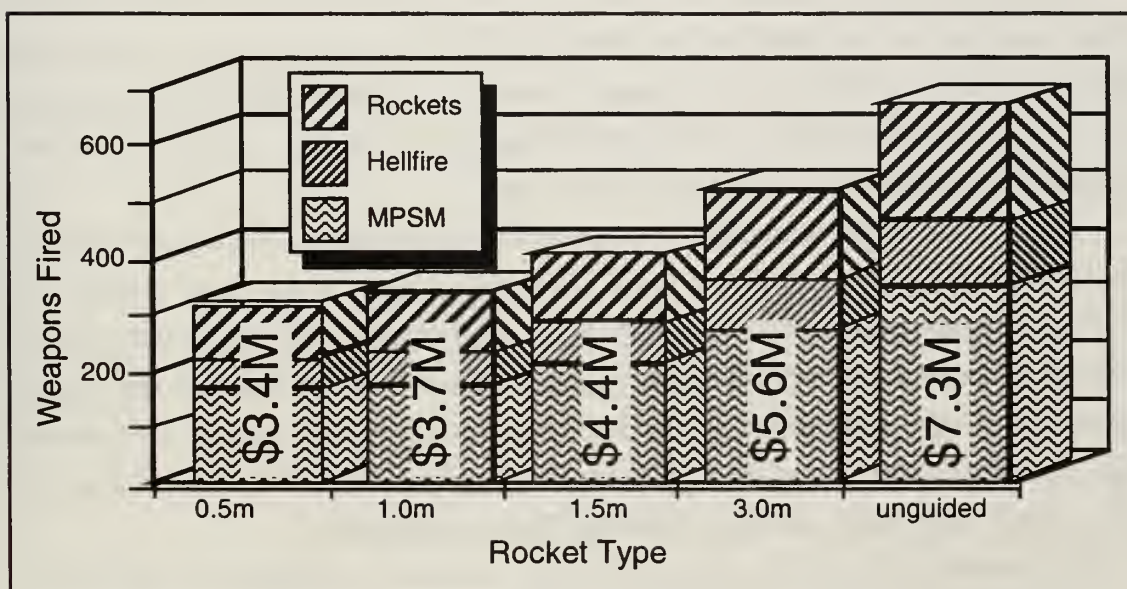


Figure 7. Number of Weapons Fired to Achieve Mission Objective. Total weapon costs indicated on graph in millions of dollars..

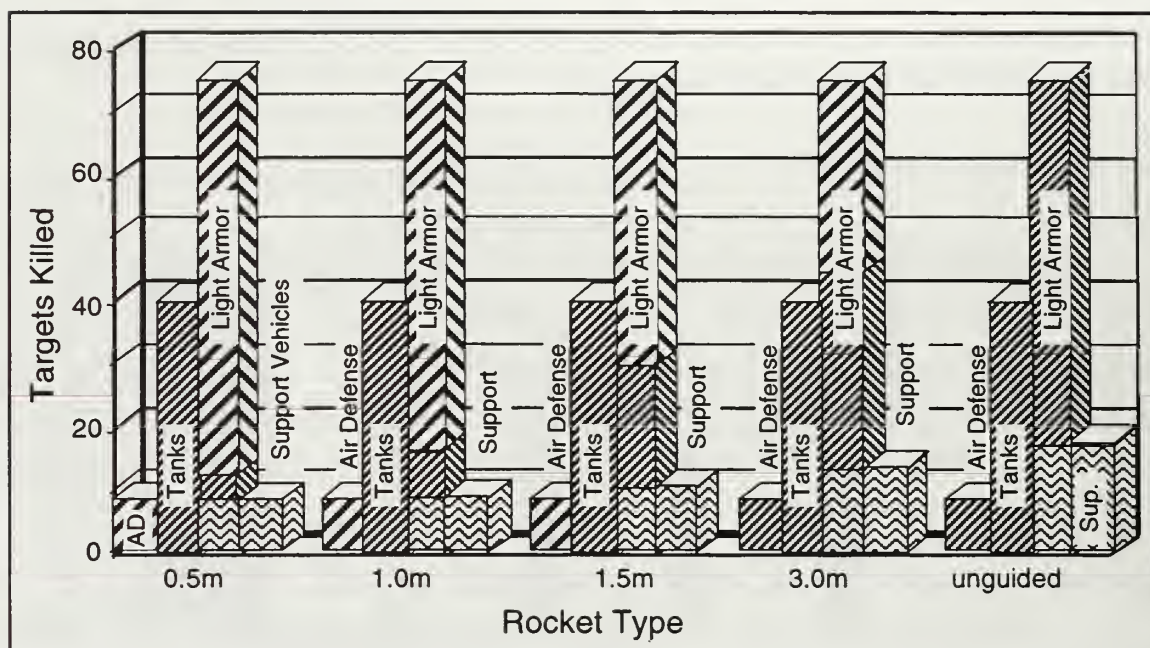


Figure 8. Number of Targets Killed by Category, Weapon, and Loadout Option.

E. OBSERVATIONS

Simple COEA type modeling is essential to the design process. Besides assuring that the design can be cost effective, the results from early analyses provide focus for the design team. COEA results can show general trends that might otherwise go unnoticed. COEA type modeling continues to be useful throughout the design process as refined-model analyses can help in verifying design decisions.

An example of how unexpected information can come from a COEA study occurred in the NPS HRGK analysis. Figure 4 (page 13) shows a “knee in the curve” around 1 m CEP. That is the approximate CEP where the P_{Kss} ’s begin to drop off significantly and the number of weapons needed per kill begins a steep increase. From the figure, it appears that weapons achieving a CEP much smaller than 1 m are not needed against the assumed targets. Therefore, as a result of the COEA modeling, designs that achieve tighter than 1 m CEPs at significantly higher costs are eliminated from consideration.

On the other hand, COEA results can be very sensitive to underlying assumptions. The possibility of invalid assumptions can make COEA modeling too unreliable for confident design decisions. For example, small changes in the low-level target set assumptions can result in important changes in P_{Kss} values. These values, in turn, will

impact sortie rates. Likewise, high-level assumptions like the mission definition used in the sorties per mission analysis will also impact the final COEA results. The validity of the assumptions involved in both low- and high-level models must be continuously assessed.

Specific examples of COEA sensitivities to underlying assumptions in the NPS HRGK models include two opposing possibilities. If the assumed target set were expanded to include a smaller point target, the “knee” of the P_{Kss} curve would shift to a smaller CEP. Then a more expensive, 0.5 m CEP weapon might become more cost effective than less expensive, 1 m CEP rockets. Conversely, if the centered, unbiased aimpoint assumption (discussed on page 10) were not valid, the general cost effectiveness advantage of the high precision rocket would become smaller, and guided rockets with slightly larger dispersion could become more cost efficient.

Ideally, COEA studies will include sensitivity analyses to determine the range of results depending on changes in the assumed inputs. With these sensitivities in mind, the designer can use the COEA models as powerful design tools.

III. PRELIMINARY SIZING ANALYSES

Several aspects of any design require preliminary sizing. For the NPS HRGK design, the physical dimensions (length, weight, and center of gravity), the thruster, and the seeker's field of view each needed to be sized early in the design process.

The author developed several computer codes to allow the sizing of the kit, its control mechanisms, and the seeker's field of view. These codes each use top-level requirements to generate lower-level design specifications. This flow down of specifications helps to assure that the final design meets the system requirements.

The following sections describe the methodology used in developing the computer models and describe some results specific to the NPS HRGK design. The chapter ends with observations regarding the models and the flow-down of design requirements.

A. LENGTH, WEIGHT, AND CENTER OF GRAVITY

The HRGK design weight and center of gravity affects the overall center of gravity of the guided rocket. The guided rocket's center of gravity is a critical design consideration in that it affects the rocket's stability in flight. Additionally, the guided rocket's center of gravity must be such that a fully loaded launcher pod's center of gravity is kept between the pod's two mounting lugs. Furthermore, the length and weight of the HRGK are constrained by limits specified for the overall length and weight of the guided rocket.

A MATLAB code was written by the author to help visualize the relationships between the HRGK size and the rocket's center of gravity. The code also maps the useable design space bounded by the maximum length and weight as well as the launcher's center of gravity constraints. This code is briefly described and some results are presented in the following subsections. The code listing is included in Appendix C.

1. Methodology

The computer code used for the length, weight, and center of gravity analysis is based on the simple equation defining a composite center of gravity, X_{CG} , based on the component weights, W_i , and component centers of gravity, x_{CG_i} . Namely,

$$X_{CG} = \frac{\sum (x_{CG_i} \cdot W_i)}{\sum W_i}.$$

a. Inputs

The user-defined parameters in the code are either design or constraint parameters as listed in Table 6. Additional model parameters needed for the model include the weight and center of gravity locations for the live and fired rocket and for the empty launcher. The length of the rocket and the location of the pod's front lug are also required. These parameters for the Hydra-70 rocket system were available from [Ref. 10 and 11].

Table 6. Weight, Length, and Center of Gravity Model Inputs.

<i>Input Name</i>	<i>Input Description</i>
<i>Design Space Parameter</i>	
Wk1	Range of kit weights (evenly-spaced vector) (lb)
Lk1	Specific kit lengths to be plotted (vector) (in)
Dk1	Specific kit densities to be plotted (vector) (lbm/in ³)
Cgk1	Assumed kit center of gravity (fraction of kit length back from nose)
dia	Assumed kit diameter (in)
<i>Constraint Parameters</i>	
Lmax	Maximum total length (in)
Wmax	Maximum total weight (lb)
CgL	Pod forward Cg limit (fraction of lug spacing back from front lug)

The kit's length is defined as the length extending forward from the tip of the rocket's fuze to the forward tip of the kit. The kit's center of gravity is based on that length; therefore, if the kit's center of gravity were behind the tip of the fuze, the value for *Cgk1* would be greater than unity.

b. Outputs

The computer code creates a plot of the rocket's center of gravity¹ as a function of guidance kit weight. The design space is marked with various curves indicating user specified guidance kit densities and lengths. With any two parameters defined (kit weight, density, length, or guided rocket center of gravity), the other two parameters are fixed on the plot. The usable design space is bounded by the maximum total length and weight as well as the loaded launcher's center of gravity constraints. The code generates the described plots for both the live and the fired rocket cases.

¹ Measured in calibers (missile diameters) from the forward tip of the guidance kit.

2. Results

Figure 9 shows the output from the computer model for the live rocket case. The solid lines represent the case where the kit's center of gravity is located at the kit's defined mid-length. The cross-hatched markings around the lines allow for the kit's center of gravity to travel within the middle third of the kit's defined length. The upper edge of the cross-hatched regions represents the kit's center of gravity being two-thirds of the length back from the nose, and the lower edge is for the center of gravity at the one-third mark. The bold lines represent the indicated design constraints. The NPS HRGK design point (7 pounds and 13.625 inches longer than the fuze) is marked on the plot as a reference.

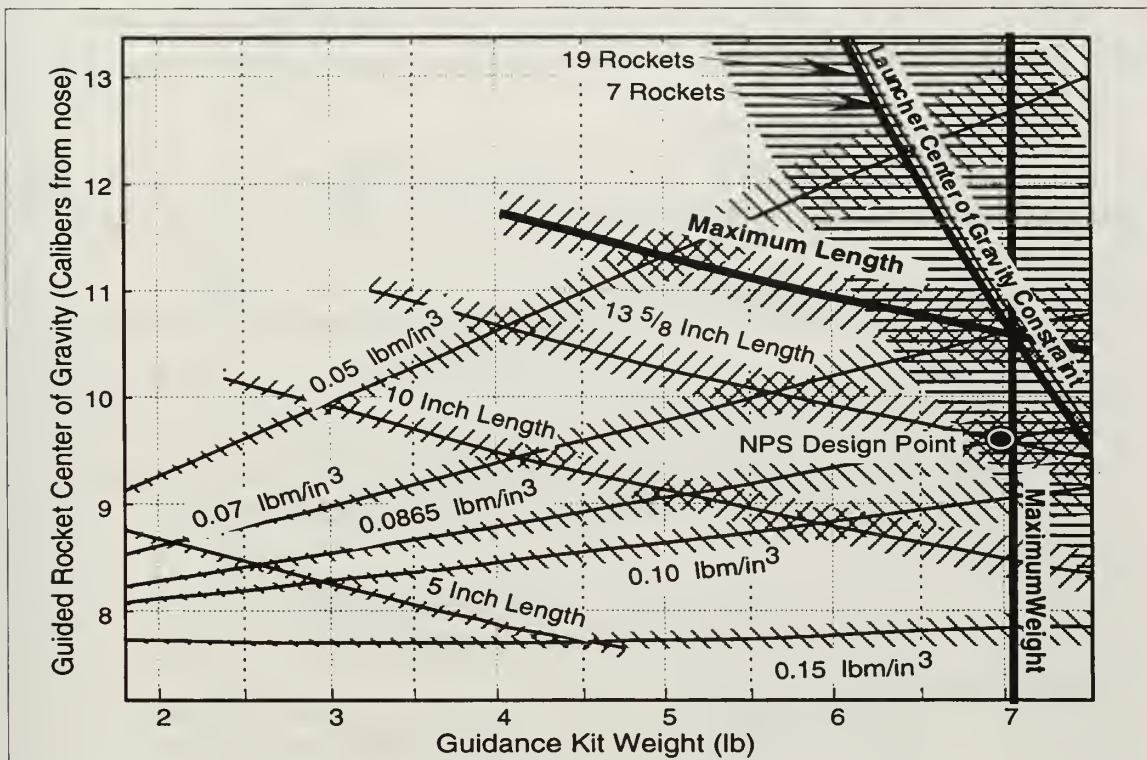


Figure 9. Physical Size and Center of Gravity Design Space. Kit length is defined from the tip of the rocket fuze forward. The launcher center of gravity constraint is tighter than specified for illustrative purposes.

From the plot it appears that the loaded launcher's center of gravity requirement (keeping the pod's center of gravity behind the launcher's front mounting lug) is not binding for most conditions. Indeed, for Figure 9, the constraint was tightened to keeping the pod's center of gravity within the *middle third* of the 14 inch lug spacing so that the constraint could even be seen in the plot.

B. MANEUVERABILITY

Another computer model was developed in MATLAB to define—based on the system requirements—the HRGK's maximum maneuverability specifications. An additional computer program uses a steady maneuver to determine the angles of attack and thruster forces needed to achieve the specified maneuverability. This latter code sizes the HRGK's thrusters. The following subsections describe these computer models and their results.

1. Turn Rate and Turn Radius Methodology

The maneuverability analysis determines the maximum turn rate in g's or minimum turn radius in kilometers needed to hit a target over various launch and seeker acquisition ranges. The two-dimensional model used in this analysis is described in this subsection.

a. Model Inputs

The maneuverability model requires several user-defined inputs. These inputs are listed and described in Table 7 and are illustrated graphically in Figure 10.

Table 7. Maneuverability Model Inputs.

<i>Input Name</i>	<i>Input Description</i>
<i>Launch and Seeker Acquisition Ranges</i>	
Rmin, Rmax	Minimum and maximum range to target at launch (km)
R _{acq}	Specific seeker's maximum target acquisition range (vector) (km)
<i>Unguided Errors</i>	
Pnt	Launcher pointing error at time of launch—1 σ (degrees)
B	Ballistic unguided flyout error—1 σ (milliradians)
<i>Weapon System Delays and Limitations</i>	
G _D	Guidance delay (time after launch before guidance is possible) (sec)
t _D	Target identification delay (from initial acquisition until start of turn) (sec)
S _F	Straight final flight distance (terminal non-maneuvering zone) (m)
<i>Missile and Target Motion</i>	
Time	Time values for missile range and velocity time profiles (vector) (sec)
Dist	Missile range profile (distances corresponding to <i>Time</i>) (vector) (m)
V _M	Missile velocity profile (velocities corresponding to <i>Time</i>) (vector) (m/s)
V _T	Target speed (mph)
<i>Statistical Confidence</i>	
sig	Number of sigma's confidence (e.g., sig=2 gives $\pm 2\sigma$ or 95% confidence)

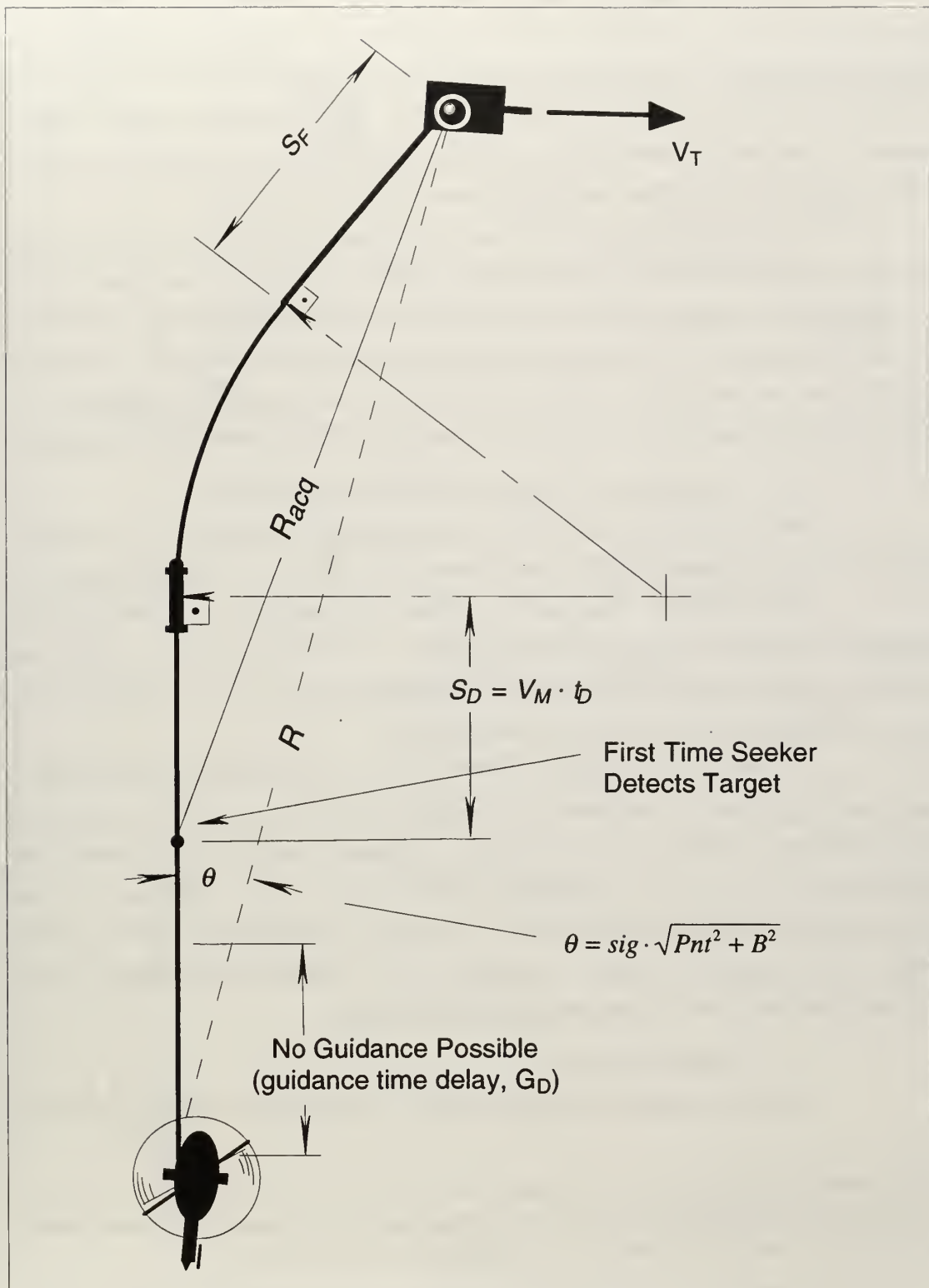


Figure 10. Graphical Representation of Maneuverability Model Inputs.

The two-dimensional model assumes that the rocket flies a straight path toward the initial target location but with an azimuth error angle, θ . This angle is a statistical combination¹ of the launcher pointing error and the ballistic flyout dispersion error of the rocket. After both the initial guidance delay², G_D , and after the rocket is within the assumed seeker acquisition range, R_{acq} , of the target; the rocket can begin a turn toward the target—correcting any cross-track errors due to θ or target motion.

A target identification delay time, t_D , between the first detection of the target and the start of the turn can also be included in the model. The distance associated with t_D , S_D , is based on the rocket velocity at the time of first detection (or the end of guidance delay, whichever is later). The model also allows for a terminal non-maneuver zone—some radius, S_F , from the target. For modeling purposes, this zone around the target forces the rocket to have completed its turn to the target and align itself for a final straight approach.

b. Stationary Target—Closed-Form Solution

With a stationary target, the inputs described above can provide a closed-form solution for the maneuverability specifications. This process is laid out in Figure 11.

The equations illustrated in Figure 11 provide the maneuverability requirements in terms of both required turn radius, r_T , and turn rate, n_{max} . (They also provide the solution to the minimum required seeker field of view—*FOV*. This part of the analysis will be described more fully in a later section.)

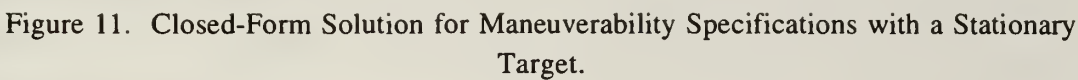
For the $\pm 2\sigma$ unguided error case ($sig = 2$), the resulting maneuverability values (r_T and n_{max}) could be interpreted as the biggest turn radius or slowest turn rate that would still ensure a 95% probability of hitting a stationary target. In other words, any larger or slower turns, than those specified, would not give a 95% confidence with the provided inputs. On the other hand, tighter or faster turns would give a higher than 95% confidence. Therefore, if the system is specified to 95% confidence, the computed values are the *maximum* turn rate and *minimum* turn radius required.

c. Moving Target

The basic equations shown in Figure 11 can be applied to the moving target

¹ The standard deviation, σ , of θ is the square root of the sum of the variances Pnt^2 and B^2 — $\sigma = \sqrt{Pnt^2 + B^2}$ —where Pnt and B are the standard deviations for the pointing error and the ballistic dispersion errors, respectively. The angle θ is some user-defined multiple (*sig*) of σ .

² The range associated with G_D is calculated based on the user-supplied range time profile for the rocket.



scenario shown in Figure 12. The moving target scenario assumes a “worst-case” target motion. The target moves with a crossing velocity in the direction opposite the flyout error. Then, after it is detected, the target turns in at 45° making the rocket’s turn tighter.

The moving target scenario precludes a closed-form solution of the maneuverability specifications. However, the equations in Figure 11 can be used with an iterative step at each of the flight milestones (target detection, start of turn, and end of turn). The MATLAB code listing in Appendix C uses this approach. The following description provides an example of the iterative process used in the computer code.

After R_D is calculated using the appropriate stationary target equations (see Figure 11), the time required to fly that distance is available from the range time profile. Using the time and the target speed, the new target location can be computed. The value for R_D can then be re-calculated based on the updated target location. These iterations continue until the change in R_D between iterations is less than some set tolerance (such as 1 m).

2. NPS HRGK Turn Rate and Turn Radius Analysis

This subsection discusses the maneuverability analysis performed specifically for the design of the NPS HRGK. The following paragraphs describe the inputs used for the computer model and present the analysis results.

a. NPS HRGK Model Inputs

The NPS HRGK analysis used the full gamut of specified launch ranges (1 to 6 kilometers) and various seeker acquisition ranges (0.75, 1.0, 1.15, 2.0, 3.0, and 6.0 km). The assumed 1σ values for launcher pointing error and ballistic dispersion were 3° and 12 mils, respectively. (Using a 95% confidence level— $\text{sig} = 2$, the angular flyout error was internally computed to be 6.16° .) The target speed was 60 mph per the system requirements. Initial guidance was delayed as a linear function of launch range (0.5 seconds for 1 km, up to 1.0 second for 6 km). The target identification delay was 0.625 seconds (arbitrarily chosen to correspond to 5 laser pulses at 8 Hertz), and the terminal non-maneuvering distance was arbitrarily chosen to be 200 meters.

The rocket’s velocity and distance time profiles used in the analysis were based on an early simulation of a HRGK-equipped rocket using a ballistic trajectory. Specifically, the simulation used the 150°F propellant thrust profile [Ref. 11] and a generic, hemispherical-nosed guidance kit with three canards. The aerodynamic coefficients and derivatives used in the simulation were determined using the software code, Advanced Design of Aerodynamic Missiles—ADAM [Ref. 12].

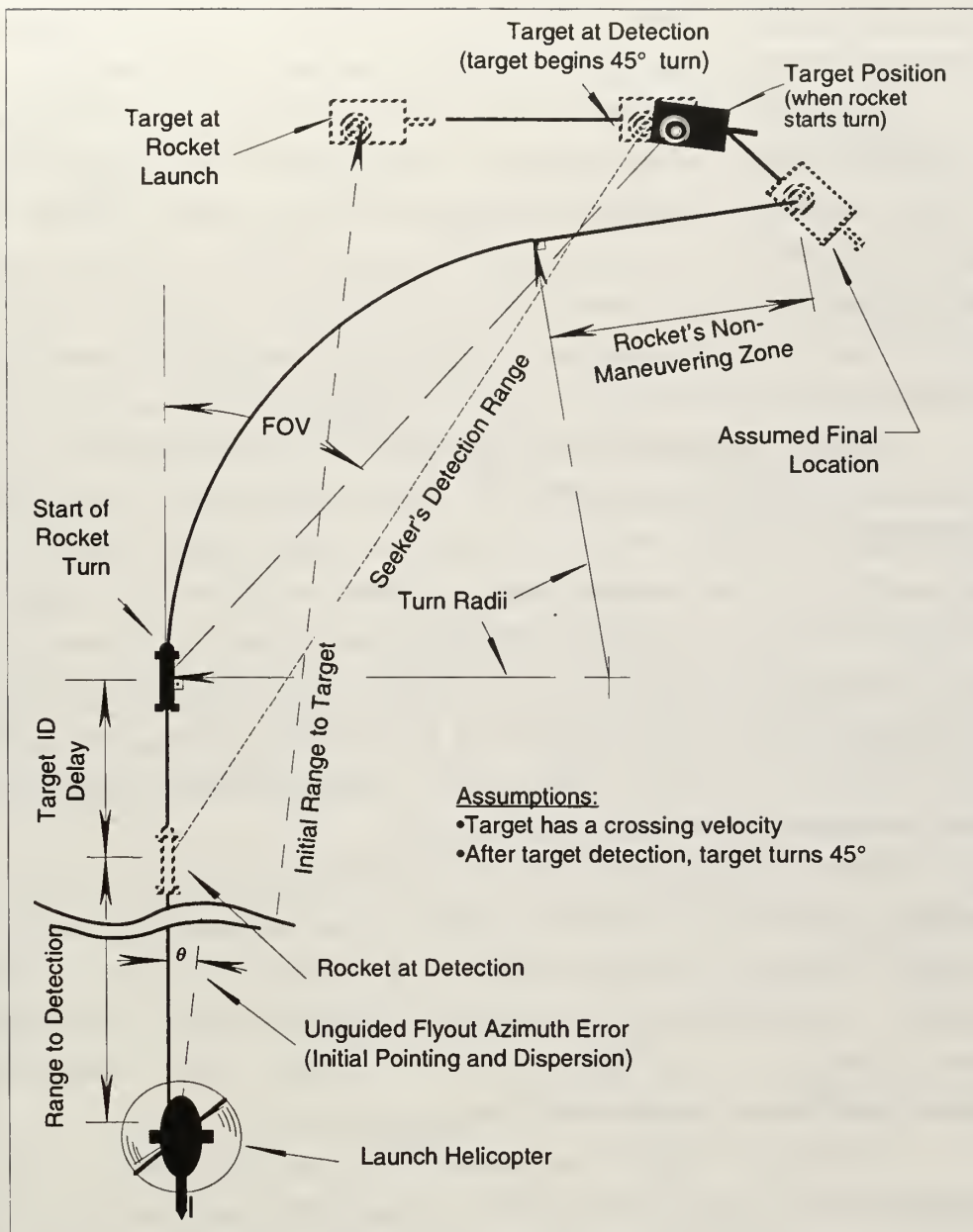


Figure 12. Moving Target Scenario for Maneuverability Analysis.

b. NPS HRGK Analysis Results

Based on the inputs described above, the maximum turn rate and minimum turn radius specifications for the NPS HRGK are shown in Figure 13 and Figure 14, respectively. The results are shown as a function of launch range for several seeker acquisition ranges. The analysis results show that as long as the seeker can initially detect

the target at 1.15 kilometers or more, the hardest g-loading maneuver for the rocket would be less than 15 g's and tightest turn radius would be greater than 1.83 kilometers.

The maximum turn rate is a strong function of launch range with short range launches requiring higher g-loading maneuvers. This is primarily due to higher rocket speeds at shorter ranges. For example, after flying 0.5 km, the rocket's velocity is 1.8 times higher than it is after coasting out to 5 km. For equal turn radii, a 1.8 factor increase in velocity yields a 3.2 (or 1.8^2) factor increase in turn rate. The guidance delay also increases the turn rate at shorter launch ranges. Target identification delays primarily impact the shorter seeker acquisition range cases—longer delays causing higher turn rates.

Unlike the maximum required turn *rate*, the minimum required turn *radius* is almost independent of rocket speed¹. Once the launch range places the target initially outside the seeker's acquisition range, the turn radius curves remain fairly flat with increasing launch range. For example, with a 1.15-km-acquisition-range seeker, the minimum required turn radius changes less than 59% across the spectrum of launch ranges (1.83 km at 1 km launch to 2.90 km at 6 km launch). Conversely, if the seeker has sufficient detection range to take advantage of it, the longer range launches allow significantly wider turns. For example, only a gentle 12.9 km turn radius is required with a 6 km seeker acquisition range and a 6 km launch range.

By either measure (turn rate or turn radius), the most stressing case for the maneuverability requirement is the short range launch, because of rocket speed and the lack of reaction time. The seeker's acquisition range can also significantly impact the HRGK maneuverability requirements—shorter range seekers forcing higher maneuverability requirements. Conversely, long range seekers can alleviate some maneuverability requirements by detecting the target earlier and allowing gentler turns.

An additional benefit of the maneuverability analysis is that the minimum required seeker acquisition range is shown to be 1.15 km. With shorter acquisition ranges and long launch ranges, the target's cross-track position relative to the rocket (due to θ and target motion) exceeds the seeker's range. For example, with a 4.1 km launch range, the rocket's closest unguided approach to the target is 0.75 km (2σ). For longer launch ranges, the closest approach distance would be greater than 0.75 km; therefore, a 0.75-km-detection-range seeker would not have a 95% probability of detecting the target.

¹ Rocket speed indirectly affects the turn radius since it partially determines the distance the target can travel before it is detected or impacted.

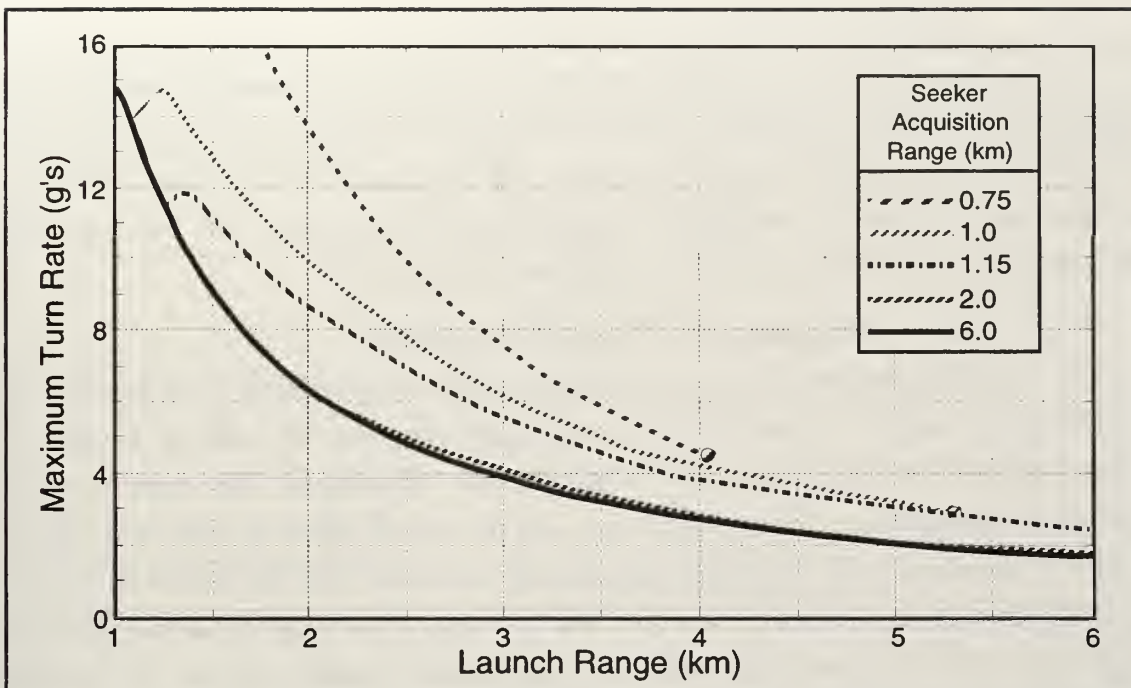


Figure 13. Maximum Turn Rate Required to Hit Target (95% Probability). Only with a seeker able to detect a target from 1.15 km or more ($R_{acq} \geq 1.15$) can the maximum range requirement (6 km) be met.

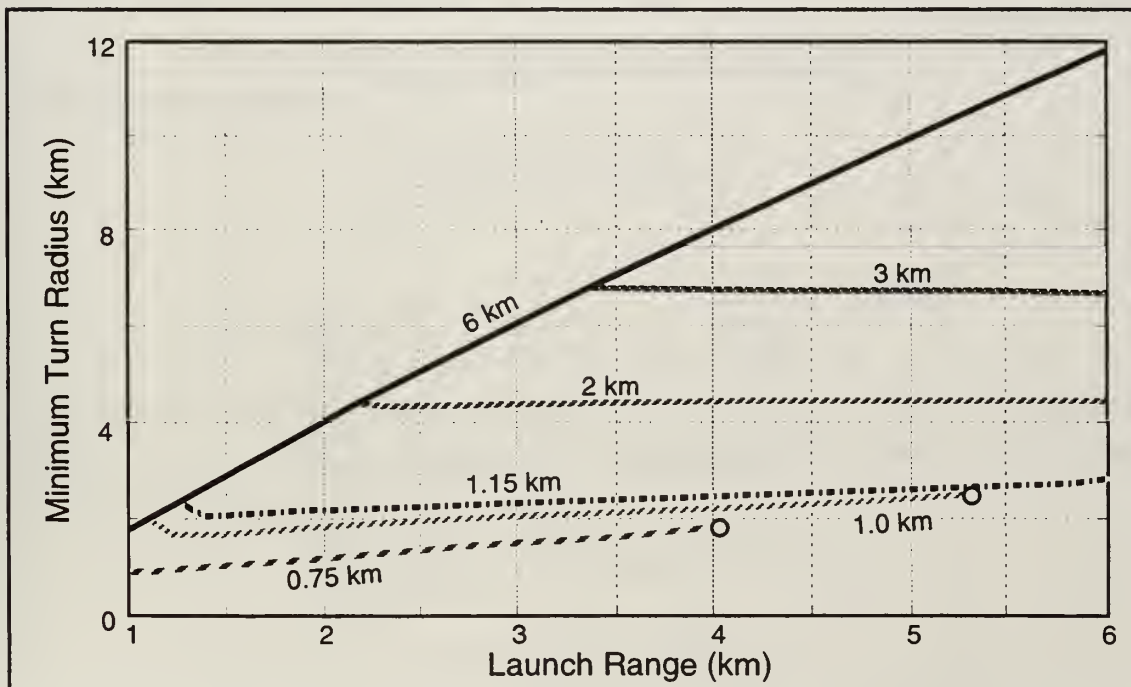


Figure 14. Minimum Turn Radius Required to Hit Target (95% Probability). Seeker acquisition ranges are indicated with the corresponding curves.

3. Steady-Turn Maneuver Analysis

Once maneuverability specifications are set, a steady-turn maneuver model can be used to size the control mechanism needed to achieve the needed turn rate or turn radius. The following paragraphs describe a computer code developed by the author to perform this task. Later a specific example for a guided rocket is presented. The MATLAB code listing with the NPS HRGK parameters is included in Appendix C.

a. Mathematical Steady-Turn Model

The purpose of this mathematical steady-turn model is to determine the thrust force and angle of attack (or sideslip angle) necessary to generate a constant acceleration turn in the horizontal. Throughout the description, the more familiar longitudinal nomenclature (loosely associated with the vertical plane) is used even though the turn is described in the directional case (loosely associated with the horizontal plane). The interchange of nomenclature is justified since, for the guided rocket or missile case, the longitudinal and directional dynamics are equivalent. A useful listing of missile aerodynamic nomenclature is included in Appendix A.

Figure 15 shows a free-body diagram for a horizontal maneuver. For a constant acceleration turn, the sum of the forces and moments can be expressed by the following equations:

$$\begin{aligned}\sum \text{Forces} &= nW = \mathbf{N} + \mathbf{T} = \bar{q}AC_{N_\alpha}\alpha + kT \\ &= \left(\frac{1}{2g_0} \rho V^2 AC_{N_\alpha} \right) \alpha + kT\end{aligned}$$

$$\begin{aligned}\sum \text{Moments} &= -\mathbf{N}X_{CP} + \mathbf{T}X_T - \mathbf{M}_q = 0 \\ &= -(\bar{q}AC_{N_\alpha}\alpha)X_{CP} + kTX_T - \bar{q}Ad\left(C_{M_q}\frac{qd}{2V}\right) \\ &= -(\bar{q}AC_{N_\alpha}\alpha)X_{CP} + kTX_T - \bar{q}Ad\left(C_{M_q}\frac{\dot{\theta}d}{2V}\right) \\ &= -(\bar{q}AC_{N_\alpha}\alpha)X_{CP} + kTX_T - \bar{q}Ad\left(C_{M_q}\frac{ngd}{2V^2}\right) \\ &= \alpha\left(-\frac{1}{2g_0}\rho V^2 AC_{N_\alpha}\right)X_{CP} + TkX_T - \frac{1}{4g_0}\rho AC_{M_q}d^2ng\end{aligned}$$

where k is a thrust multiplication factor (accounting for misalignment of the thruster and the effect of jet and free air stream interaction) and the other terms are either defined by Figure 15 or are standard terms defined in Appendix A. The moments equation uses the fact that

$$q \equiv \dot{\theta} = \frac{V}{r_T} = \frac{V}{\left(\frac{V^2}{a_z}\right)} = \frac{a_z}{V} = \frac{ng}{V}.$$

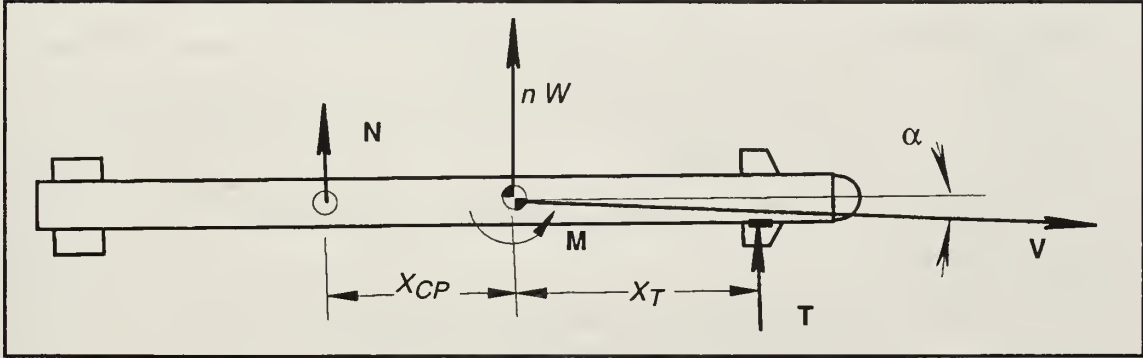


Figure 15. Plane-View, Free-Body Diagram for a Steady-Turn Maneuver (horizontal, left turn—gravity force vector pointed into the page).

The sum of forces and sum of moments equations can be rewritten as the following matrix equation:

$$\begin{bmatrix} k & \frac{1}{2g_0} \rho V^2 AC_{N_a} \\ kX_T & \left(-\frac{1}{2g_0} \rho V^2 AC_{N_a}\right) X_{CP} \end{bmatrix} \begin{bmatrix} T \\ \alpha \end{bmatrix} = \begin{bmatrix} nW \\ \frac{1}{4g_0} \rho AC_{M_q} d^2 ng \end{bmatrix}$$

which gives the thrust magnitude and angle of attack in terms of guided rocket parameters and the turn rate n . Using the relationship $r_T = V^2/ng$, the matrix equation can be expressed in terms of the turn radius as the following:

$$\begin{bmatrix} k & \frac{1}{2g_0} \rho V^2 AC_{N_a} \\ kX_T & \left(-\frac{1}{2g_0} \rho V^2 AC_{N_a}\right) X_{CP} \end{bmatrix} \begin{bmatrix} T \\ \alpha \end{bmatrix} = \begin{bmatrix} \frac{V^2 W}{gr_T} \\ \frac{1}{4r_T g_0} \rho V^2 AC_{M_q} d^2 \end{bmatrix}.$$

b. Steady-Turn Computer Code

The author has developed a computer code to implement the mathematical model described above. This code solves for the thrust and angle of attack required to achieve the required turn rate or turn radius over a range of Mach numbers. The code requires the user-supplied inputs listed and described in Table 8.

Table 8. Steady-Turn Maneuver Computer Model Inputs.

<i>Input Name</i>	<i>Input Description</i>
<i>Scenario Definition</i>	
n or r_T	Desired turn rate (g's) or turn radius (ft)
type	Indicator for computations based either on turn rate (1) or turn radius (2)
alt	Pressure altitude (ft)
Mmin, Mmax	Minimum and maximum Mach number for the calculations
<i>Rocket Configuration</i>	
Wght	Rocket total weight at maneuvering time (lb)
Dia	Rocket diameter (for reference area and length) (in)
Xcg	Rocket center of gravity (calibers from nose)
Xt	Thruster location (calibers from nose)
<i>Aerodynamic Parameters (functions of Mach)</i>	
Mach_dat	Mach values for corresponding aerodynamic parameters (vector)
CNa_dat	Rocket normal force curve slope (corresponding to <i>Mach</i>) (vector) (rad^{-1})
Xcp_dat	Center of pressure (corresponding to <i>Mach</i>) (vector) (calibers from nose)
CMq_dat	"Pitch" damping (corresponding to <i>Mach</i>) (vector) (rad^{-1})

c. NPS HRGK Example

The following provides example solutions to the equations previously developed for the steady-turn model. The examples are specific to the NPS HRGK with the guided rocket's maneuverability specifications set at 15 g's turn rate or 1.83 km (6,000 ft) turn radius. The manual calculations are for the NPS HRGK design at Mach 1.0. These calculations are done first for the turn rate specification and then for the turn radius specification. The aerodynamic coefficients are from ADAM [Ref. 12]. All computations are for 500 feet pressure altitude and use the fired rocket center of gravity (most maneuvering takes place after the 1.0 sec rocket motor burn). Because no additional data is available, the value of k (an adjustment factor for the thruster force) is assumed to be unity.

The manual calculations are followed by sample output from the steady-turn computer code.

(1) Sample Manual Calculation Based on Maximum Turn Rate.

$$\begin{bmatrix} 1 & \frac{(0.0754 \frac{\text{lbm}}{\text{ft}^3})(1114 \frac{\text{ft}}{\text{s}})^2(0.0412 \text{ ft}^2)(20.05 \text{ rad}^{-1})}{2(32.2 \frac{\text{lbm} \cdot \text{ft}}{\text{lbf} \cdot \text{s}^2})} \\ 1.79 \text{ ft} & -\frac{(0.0754 \frac{\text{lbm}}{\text{ft}^3})(1114 \frac{\text{ft}}{\text{s}})^2(0.0412 \text{ ft}^2)(20.05 \text{ rad}^{-1})}{2(32.2 \frac{\text{lbm} \cdot \text{ft}}{\text{lbf} \cdot \text{s}^2})} - 0.0824 \text{ ft} \end{bmatrix} \begin{bmatrix} T \\ \alpha \end{bmatrix} = \begin{bmatrix} 15 (22.8 \text{ lbf}) \\ \frac{(0.0754 \frac{\text{lbm}}{\text{ft}^3})(0.0412 \text{ ft}^2)(-5520 \text{ rad}^{-1})(0.229 \text{ ft})^2 15 (32.2 \frac{\text{ft}}{\text{s}^2})}{4(32.2 \frac{\text{lbm} \cdot \text{ft}}{\text{lbf} \cdot \text{s}^2})} \end{bmatrix}$$

The solution to the set of equations is:

$$\begin{bmatrix} 1 & 1200 \frac{\text{lbf}}{\text{rad}} \\ 1.79 \text{ ft} & -99.1 \frac{\text{lbf} \cdot \text{ft}}{\text{rad}} \end{bmatrix} \begin{bmatrix} T \\ \alpha \end{bmatrix} = \begin{bmatrix} 342 \text{ lbf} \\ -3.38 \text{ lbf} \cdot \text{ft} \end{bmatrix} \Rightarrow \begin{bmatrix} T \\ \alpha \end{bmatrix} = \begin{bmatrix} 13.2 \text{ lbf} \\ 0.273 \text{ rad} \end{bmatrix} = \begin{bmatrix} 13.2 \text{ lbf} \\ 15.6^\circ \end{bmatrix}$$

(2) Sample Manual Calculation Based on Minimum Turn Radius.

$$\begin{bmatrix} 1 & 1200 \frac{\text{lbf}}{\text{rad}} \\ 1.79 \text{ ft} & -99.1 \frac{\text{lbf} \cdot \text{ft}}{\text{rad}} \end{bmatrix} \begin{bmatrix} T \\ \alpha \end{bmatrix} = \begin{bmatrix} \frac{(1114 \frac{\text{ft}}{\text{s}})^2 (22.8 \text{ lbf})}{(32.2 \frac{\text{ft}}{\text{s}^2})(6000 \text{ ft})} \\ \frac{(0.0754 \frac{\text{lbm}}{\text{ft}^3})(1114 \frac{\text{ft}}{\text{s}})^2(0.0412 \text{ ft}^2)(-5520 \text{ rad}^{-1})(0.229 \text{ ft})^2}{4(32.2 \frac{\text{lbm} \cdot \text{ft}}{\text{lbf} \cdot \text{s}^2})(6000 \text{ ft})} \end{bmatrix}$$

The solution to the set of equations is:

$$\begin{bmatrix} 1 & 1200 \frac{\text{lbf}}{\text{rad}} \\ 1.79 \text{ ft} & -99.1 \frac{\text{lbf} \cdot \text{ft}}{\text{rad}} \end{bmatrix} \begin{bmatrix} T \\ \alpha \end{bmatrix} = \begin{bmatrix} 147 \text{ lbf} \\ -1.45 \text{ lbf} \cdot \text{ft} \end{bmatrix} \Rightarrow \begin{bmatrix} T \\ \alpha \end{bmatrix} = \begin{bmatrix} 5.68 \text{ lbf} \\ 0.117 \text{ rad} \end{bmatrix} = \begin{bmatrix} 5.68 \text{ lbf} \\ 6.71^\circ \end{bmatrix}$$

(3) Sample Output from Steady-Turn Computer Code. Figure 16 shows the output from a computer code developed by the author. The code computes the solution to the steady-turn equations that were manually solved in the previous paragraphs.

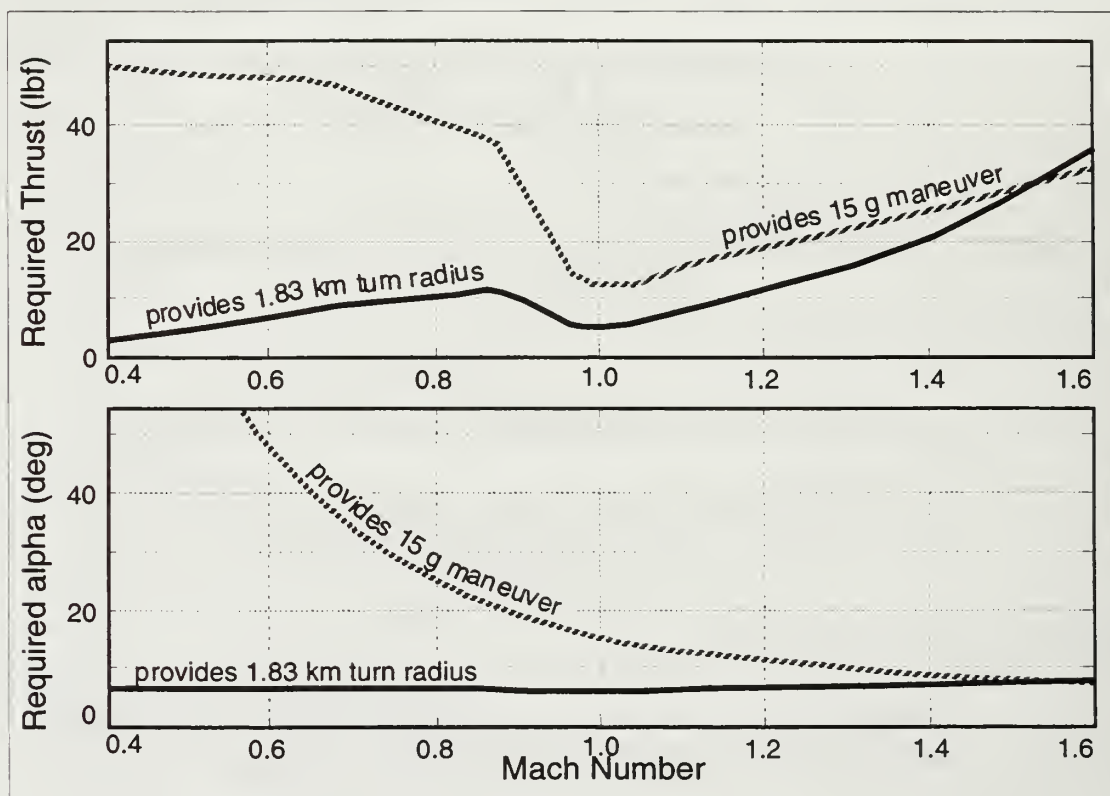


Figure 16. Required Thrust and Angle of Attack for Maximum Turn Rate (15 g's—dashed line) or Minimum Turn Radius (1.83 km—solid line) (NPS HRGK design).

From the data plotted in Figure 16, the difference in the two methods of specifying maneuverability requirements is apparent. For example, at subsonic speeds, the model predicts that the rocket could only achieve a 15 g maneuver with very high thrust and extremely high angle of attack. On the other hand, the requisite 1.83 km turn radius can be achieved at subsonic speeds with a moderate angle of attack and low thruster force.

Fortunately, 15 g maneuvers are not required when the missile has coasted down to subsonic speeds (see long range side of Figure 13, page 33). Clearly, the reasonable curve for sizing the thruster is the minimum turn radius curve (solid line). This seems reasonable since the turn radius requirements remained fairly flat over the entire gamut of launch ranges (see Figure 14).

Designing to the minimum turn radius and given the fact that the rocket has slowed down to nearly Mach 1.3 by the first kilometer of flight, the thruster can be sized to provide 10 to 15 pounds of thrust. A design with higher thrust early in the flight would be ideal, since the short-range, high-speed scenario is the most demanding.

4. Probabilistic Approach

The maneuverability analysis performed in the previous subsections was based on the statistical (probabilistic) flyout of the rocket but a deterministic, worst-case target motion. Another approach to determining the needed level of maneuverability would be to apply a statistical model to the target motion as well as the flyout. This latter approach would give valuable insight into the reasonableness of the worst-case approach taken above. This type of purely probabilistic approach was needed for the seeker field of view analysis, which is described next.

C. SEEKER FIELD OF VIEW

The seeker's field of view¹ was another early consideration for the NPS HRGK design. Again, this design specification could be derived from top-level system requirements and simple mathematical models. A possible approach to determining the needed seeker field of view was alluded to in the maneuverability analysis section. This section will briefly discuss that approach and its results. Then a probabilistic approach with its results will be discussed in greater detail.

1. Analysis with "Worst-Case" Target Motion Model

The two-dimensional scenario described in subsection III.B.1. *Turn Rate and Turn Radius Methodology* provides a means for calculating the needed HRGK seeker field of view. The equations shown in Figure 11 (page 29), can be used to determine the field of view that keeps a stationary target within the seeker's field of view with some specified level of confidence (for example, 95%) up until the target can be detected and a turn toward the target can be initiated. As discussed in the earlier subsection, the equations shown in Figure 11 can be solved iteratively to determine the required field of view for a moving target (see Figure 12, page 31).

¹ The seeker's field of regard—meaning the total area covered by a fixed or scanning seeker—is the actual consideration, but for a strapped-down seeker, the field of view and field of regard can be used interchangeably. This thesis uses the term field of view.

Unfortunately, the target motion model used for the maneuverability analysis is a worst-case example. (The target crosses at maximum velocity in the opposite direction of the statistical flyout and pointing errors. Furthermore, after detection, the target turns in at 45° which creates the need for a still larger field of view. See Figure 12.)

The required field of view results shown in Figure 17 for the NPS HRGK were obtained using the worst-case target motion model and the computer code inputs discussed in subsection III.B.2. *NPS HRGK Turn Rate and Turn Radius Analysis* (page 30). The values are for half field of view and are shown as a function of launch range and for various seeker acquisition ranges. For example, with a maximum launch range and a seeker acquisition range of 1.5 km, a $\pm 48^\circ$ seeker field of view would be needed to assure (95%) that the target stays in the field of view up until a turn can be initiated. (With a stationary target, only a $\pm 29^\circ$ seeker field of view would be needed.)

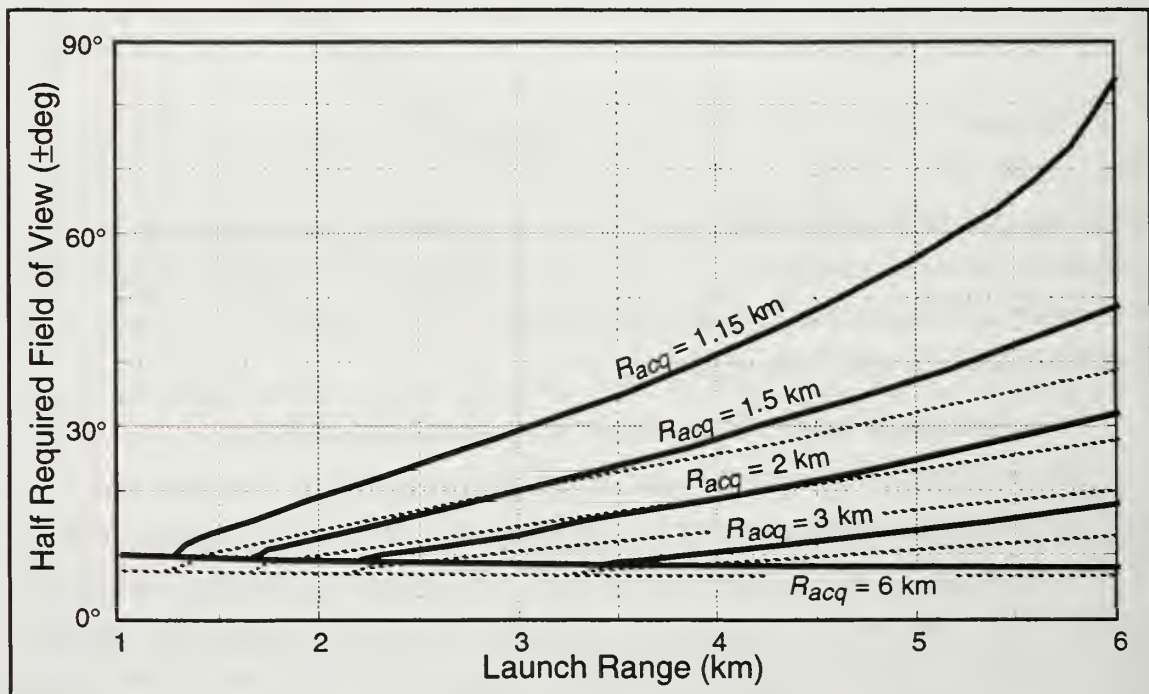


Figure 17. Required Field of View Results for 95% Probability of Target Staying in Field of View with Worst Case Target Motion. (Corresponding field of view requirements for a stationary target are indicated with dashed lines.)

From the curves in Figure 17, it is clear that longer launch ranges require larger fields of view (after longer flyouts, the rocket's cross-track error and the target's motion

away from the rocket will be larger). Shorter acquisition range seekers also require larger fields of view.

Unfortunately, the indicated field of view sizes for long range launches and short range seekers are unattainably large, especially for a strapped-down, semi-active laser spot homing seeker like that on the NPS HRGK. The worst-case target motion model is unacceptable, and so, a probabilistic approach must be taken.

2. Analysis with Probabilistic Target Motion Model

The probabilistic target motion model used for the seeker field of view analysis is based on a *distribution* of target positions. In this analysis, the probability of the seeker acquiring a target is derived from an assumed seeker field of view and the probabilistic distributions for the rocket and the target. The methodology for defining a seeker field of view specification with this approach is developed in this subsection. The resulting specifications for the NPS HRGK are also presented. The MATLAB code developed by the author to perform this analysis is included in Appendix C.

a. Computer Model Inputs

The inputs required for the probabilistic seeker field of view analysis are listed and described in Table 9.

Table 9. Seeker Field of View Analysis Inputs.

<i>Input Name</i>	<i>Input Description</i>
<i>Seeker Descriptions</i>	
FOVmin, max	Minimum and maximum seeker half field of views (deg)
R _{acq}	Specific seeker's maximum target acquisition range (vector) (km)
<i>Unguided Errors and Weapon System Delays</i>	
Pnt	Launcher pointing error at time of launch—1 σ (degrees)
B	Ballistic unguided flyout error—1 σ (milliradians)
G _D	Guidance delay (time after launch before guidance is possible) (sec)
t _D	Target identification delay (from initial acquisition until start of turn) (sec)
<i>Missile and Target Motion</i>	
RL	Range to target at launch (single value) (km)
Time	Time values for missile range and velocity time profiles (vector) (sec)
	Missile range profile (distances corresponding to <i>Time</i>) (vector) (m)
V _{Tmin} , V _{Tmax}	Minimum and maximum target speed (mph)

b. Target Motion Model

The probabilistic seeker field of view analysis uses a simple distribution model for target motion. The target's speed is assumed to be constant and uniformly distributed between the user-supplied inputs, V_{Tmin} and V_{Tmax} . Its bearing, ϕ , is also assumed to be constant and to be uniformly distributed between 0° and 360° . Figure 18 shows a plane view of possible target locations after time, t_T (the flyout time before the rocket starts its turn to the target). The figure also includes the corresponding probability density function for the target's cross-track position, x . This function provides the probability of the target being at some specific cross-track position, x_T , or between two cross-track limits, x_1 and x_2 . (The y-axis indicates the direction of the rocket flyout.)

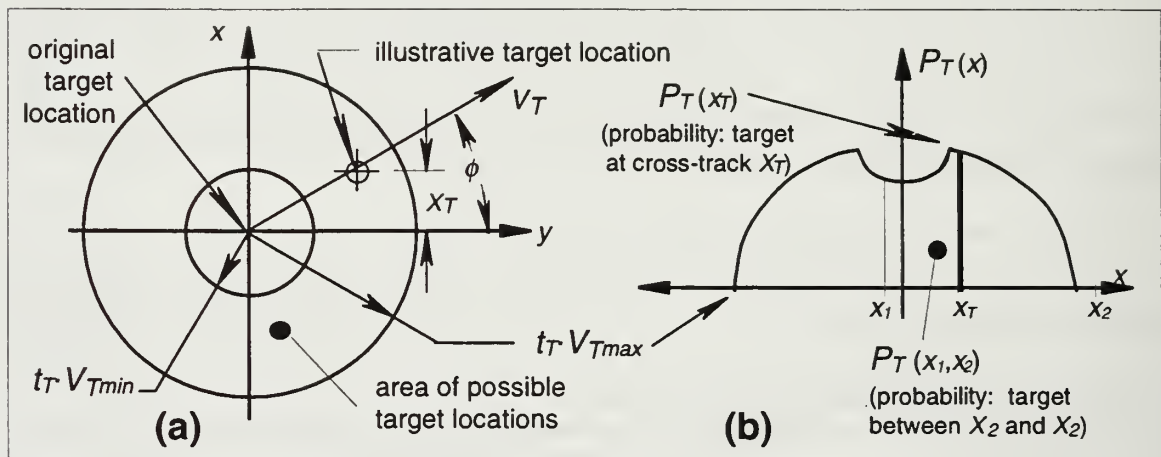


Figure 18. Target Distribution Model. (a) Plane view of possible target positions and (b) Cross-track probability density function, $P_T(x)$

c. Analysis Methodology

The methodology used to compute the probability of the target being within the HRGK field of view, has previously been documented by the author. The following paragraphs briefly summarize the methodology. In these paragraphs, the assumption is made that if the target is within the HRGK's field of view, it will be acquired; therefore, the desired quantity is the probability of acquisition, P_{acq} . The referenced technical memorandum should be consulted for a more complete description of the theory and the limitations of the simplifying assumptions. [Ref. 13]

Figure 19 shows a sample case for the probabilistic model and shows several of the variables used in the model computations. To obtain the probability of the target being within the seeker field of view ($x_1 \leq x_T \leq x_2$), the independent probabilities of

The probability of the rocket being at cross-track position x_R is

$$P_R(x) = \frac{1}{\sigma\sqrt{2\pi}} e^{\frac{-x_R^2}{2\sigma^2}}$$

¹ The field of view limits are $x_l = x_R - F$ and $x_2 = x_R + F$ where the offset, $F = R_{acq} \sin(FOV)$.

$$P_T(x_1, x_2) = \frac{A}{A_{TOT}} = \frac{\frac{\text{sign}(x_2) \cdot \min(r_2, |x_2|)}{2} \int \sqrt{r_2^2 - x^2} dx - \frac{\text{sign}(x_2) \cdot \min(r_1, |x_2|)}{2} \int \sqrt{r_1^2 - x^2} dx}{\frac{\text{sign}(x_1) \cdot \min(r_2, |x_1|)}{2} \int \sqrt{r_2^2 - x^2} dx - \frac{\text{sign}(x_1) \cdot \min(r_1, |x_1|)}{2} \int \sqrt{r_1^2 - x^2} dx} \pi (r_2^2 - r_1^2)$$

where the limits of the two integrations are set to never exceed the radius of the outer or inner circle, respectively.

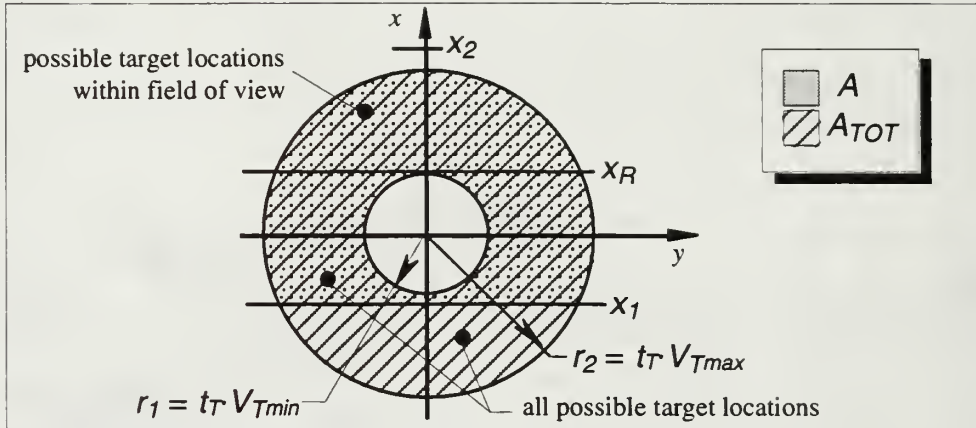


Figure 20. Possible Target Locations. The ratio of the area (A) bounded by the field of view limits— x_1 and x_2 —and the total possible area (A_{TOT}) is the probability of the target being within the two limits.

An alternative calculation of the seeker acquired area, A , is illustrated in Figure 21. The calculation method relies on the fact that since the probabilities are symmetrical about the y -axis, the calculations only need to be made for positive values of x_R ; thus x_2 will always be positive. The method involves calculating the area, A_1 , bounded by the circles, the lower field of view limit (x_2), and the y -axis as given by the equation:

$$A_1 = 2 \int_0^{\min(r_2, x_2)} \sqrt{r_2^2 - x^2} dx - 2 \int_0^{\min(r_1, x_2)} \sqrt{r_1^2 - x^2} dx$$

$$= L_1 \sqrt{r_2^2 - L_1^2} + r_2^2 \sin^{-1} \left(\frac{L_1}{r_2} \right) - L_2 \sqrt{r_1^2 - L_2^2} + r_1^2 \sin^{-1} \left(\frac{L_2}{r_1} \right).$$

Next, the area A_2 is calculated. This area is bounded by the circles, the lower field of view limit (x_1), and the y -axis, and is given by the equation

$$\begin{aligned}
A_2 &= 2 \int_0^{L_3 = \min(r_2, |x_1|)} \sqrt{r_2^2 - x^2} dx - 2 \int_0^{L_4 = \min(r_1, |x_1|)} \sqrt{r_1^2 - x^2} dx \\
&= L_3 \sqrt{r_2^2 - L_3^2} + r_2^2 \sin^{-1} \left(\frac{L_3}{r_2} \right) - L_4 \sqrt{r_1^2 - L_4^2} + r_1^2 \sin^{-1} \left(\frac{L_4}{r_1} \right).
\end{aligned}$$

Finally, the area A_2 is subtracted from A_1 if x_1 is greater than zero (Figure 21 (a)) or added to A_1 if x_1 is less than zero (Figure 21 (b))— $A = A_1 - \text{sign}(x_1) \cdot A_2$.

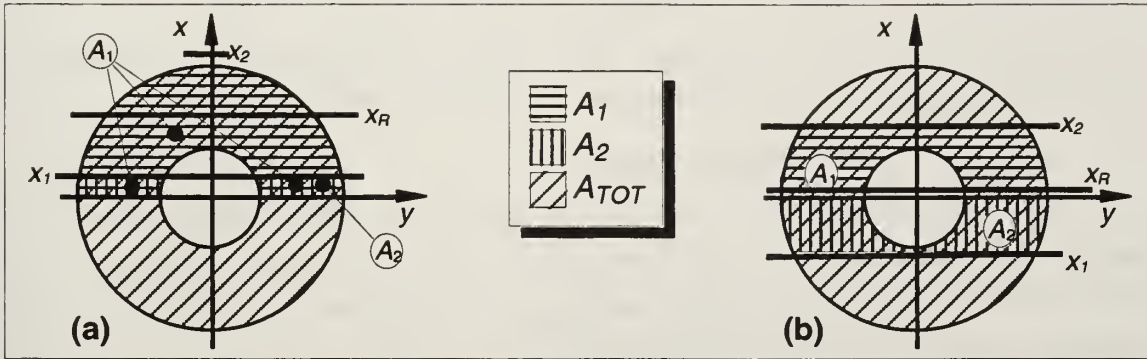


Figure 21. Alternative Method for Computing Target Distribution Area within Seeker Field of View Limits. ($A = A_1 - \text{sign}(x_1) \cdot A_2$.)

Now, the probability of the rocket being at a specific cross-track and the target being within the HRGK's field of view can be expressed as the joint probability $P_{acq}(x_R) = P(x_R, x_1 \leq x_T \leq x_2) = P_R(x_R) \cdot P_T(x_1, x_2)$. The total probability of the rocket having the target in its field of view for any flyout is the integral of this joint probability. These probabilities are illustrated in Figure 22. The actual method for computing the probability of acquisition is described in the following paragraphs.

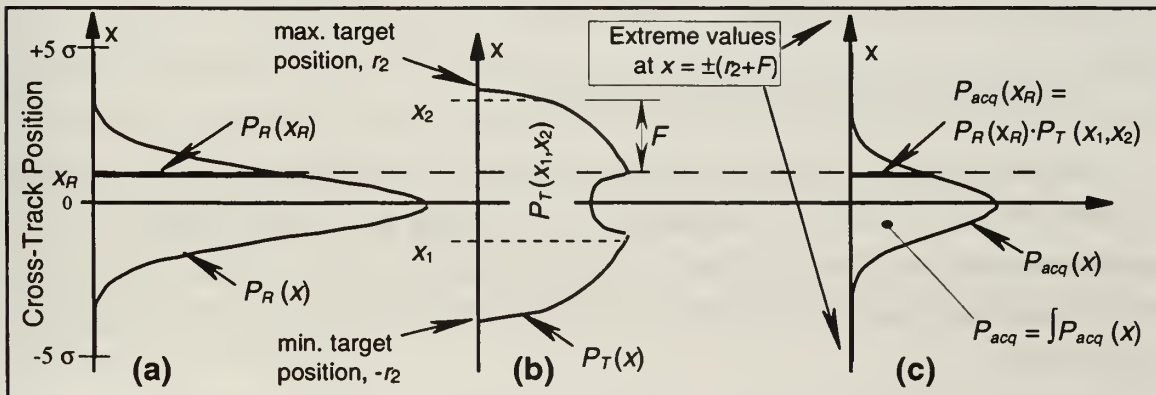


Figure 22. Probability Density Functions. (a) Rocket cross-track error, (b) Target cross-track position, and (c) Probability of acquisition.

d. Computer Code Description

The MATLAB computer code developed to determine the probability of target acquisition¹ includes a MATLAB script file and a MATLAB function. (Appendix B briefly describes the difference between script files and functions.) The script file sets the user inputs, determines the rocket's cross-track error standard deviation, sets the seeker offset (F), calculates the integral of the joint probability $\int P_R(x) \cdot P_T(x \pm F) dx$ from zero to an upper bound, and plots the results. The MATLAB function is called by the integration scheme in the script file and returns values for the joint probability ($P_{acq}(x) = P_R(x) \cdot P_T(x \pm F)$). These functions are all performed over a range of fields of view and for several seeker acquisition ranges. Both the script file and the function are included in Appendix C.

e. NPS HRGK Results

The computer code results for the NPS HRGK design case are shown in Figure 23. The results are for the maximum launch range case (6 km) as this is the most stressing case. All other input parameters are set as in previous analyses. The target speed is uniformly distributed between 20 to 60 miles per hour. The results show that a 95% probability of having the target in the field of view at time, t_T , can be obtained with fields of view slightly *smaller* than those that would be required for the same results against stationary targets. For example, with a seeker acquisition range of 1.5 km, a $\pm 25^\circ$ seeker would provide a 95% probability of acquisition against the probabilistic target model. But, against a stationary target, a $\pm 29^\circ$ seeker would be required for the same confidence (Figure 17, page 40). The probabilistic moving target model results in a smaller field of view because of the possibility of the target moving in the same direction as the rocket cross-track error is allowed. This possibility increases the probability of having the target within the field of view, even with a slightly smaller field view.

D. COMMENTS AND OBSERVATIONS

In concluding this chapter on preliminary sizing analyses, several observations are appropriate. These include (1) a discussion of the benefits and data that came from the computer models, (2) a word of caution about the limitations of the models, and (3) a listing of additional work that could be done to expand the usefulness of the preliminary sizing models.

¹ Actually the probability of the target being within the cross-track limits of the seeker's field of view.

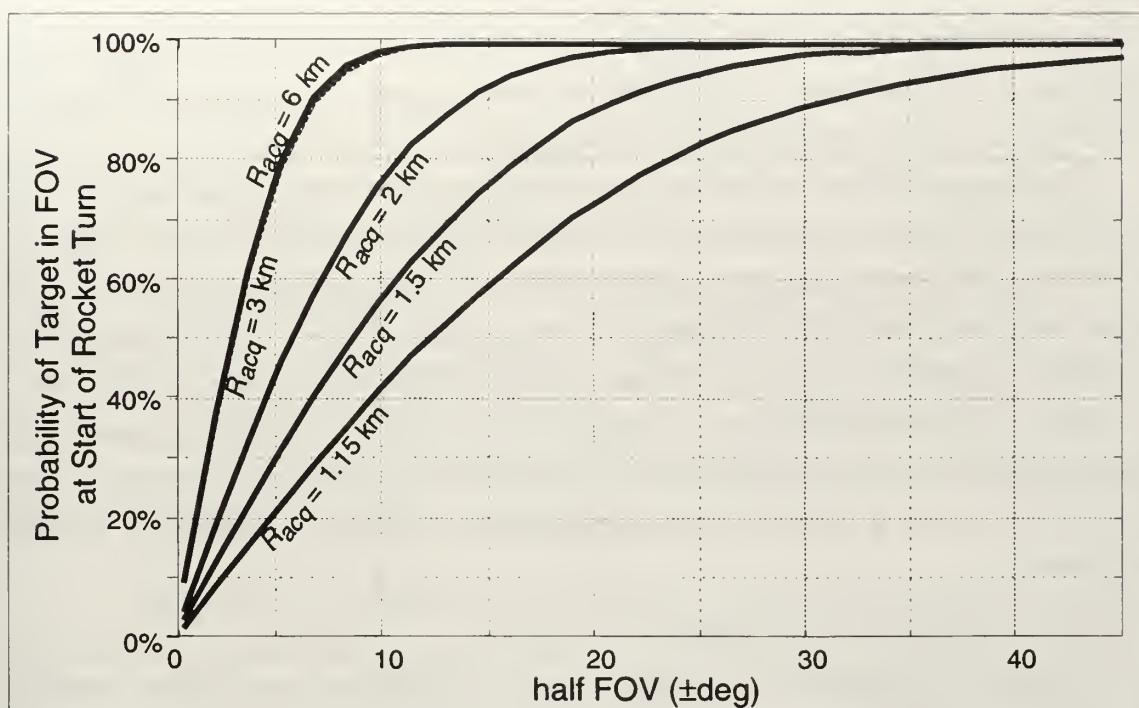


Figure 23. Probability of Target in Field of View for Maximum Launch Range (6 km).

1. Additional Data from Modeling

The primary purpose of the computer models discussed in this chapter was to give the designer a better understanding of how the system requirements affect different design specifications. However, the codes not only facilitate the “flow-down” of requirements, but they also provide additional insights into the design of the system. In the case of the NPS HRGK design, several observations were made from the use of the preliminary sizing codes. The following paragraphs site some examples.

From the length, weight, and center of gravity analysis it was determined early in the design that the launcher center of gravity constraint is not binding for any design within the maximum weight and length constraints. Thus, the kit’s center of gravity can be placed to provide the best combination of performance and packaging without concern for the launcher’s center of gravity. In a general case, a designer can use this type of knowledge to move through design iterations without making calculations regarding the non-binding constraints. Then, as the final design is approached, calculations can be made to verify the preliminary assessments.

Another good example of additional information gained from the models is the minimum required seeker acquisition range. The required seeker range was inadvertently

discovered by trying several seeker acquisition ranges in the maneuverability analyses. The final seeker range specification could be derived based on any of the three target motion types (stationary, worst-case, or uniformly distributed).

The maneuverability and field of view analyses provided other general insights into the effect of the system requirements. For example, from the analyses it became apparent that the minimum launch range requirement defines the maneuverability specification and that the maximum launch range requirement drives the seeker field of view specification. This insight is useful in determining design tradeoffs with relaxed system requirements. For example, if the minimum range requirement for the NPS HRGK were increased to 2 km, the effect on the seeker would be minimal, but the affect on the thruster design would be significant. Knowing this the designer can determine the value of relaxing the system requirement.

2. Limitations of Models

Despite the usefulness of the codes discussed in this chapter, some caution must be applied when using these and other mathematical or computer models. Model outputs are sometimes skewed or erroneous because of (1) the nature of the model with its simplifying assumptions or (2) because of the model's sensitivity to incorrect inputs. Examples of both these error sources are abundant in the NPS HRGK analyses.

For example, both the maneuverability and the field of view analyses used a two-dimensional model for a three dimensional problem. Implied in these models is the assumption that the azimuth-related maneuverability and field of view requirements outweigh the elevation-related requirements. In reality, the HRGK must execute significant maneuvers in both yaw *and* pitch (at the same time) to prosecute a target as it appears in the seeker's field of view. Furthermore, the field of view sizing may well be defined by the requirement to look down at a target rather than the requirement to look to the left or right for a target. These possibilities are not accounted for in the two-dimensional model.

Another example of potentially incorrect modeling concerns the appropriateness of the target motion model. The constant heading and speed with uniform distributions may be an appropriate target motion model for short time of flight attacks against sluggish ground targets. However, this type of target motion model would *not* be appropriate in a surface-to-air scenario where the target may have evasive maneuver capability. In general, any target motion model must allow for a reasonable, worst-case evasive maneuver.

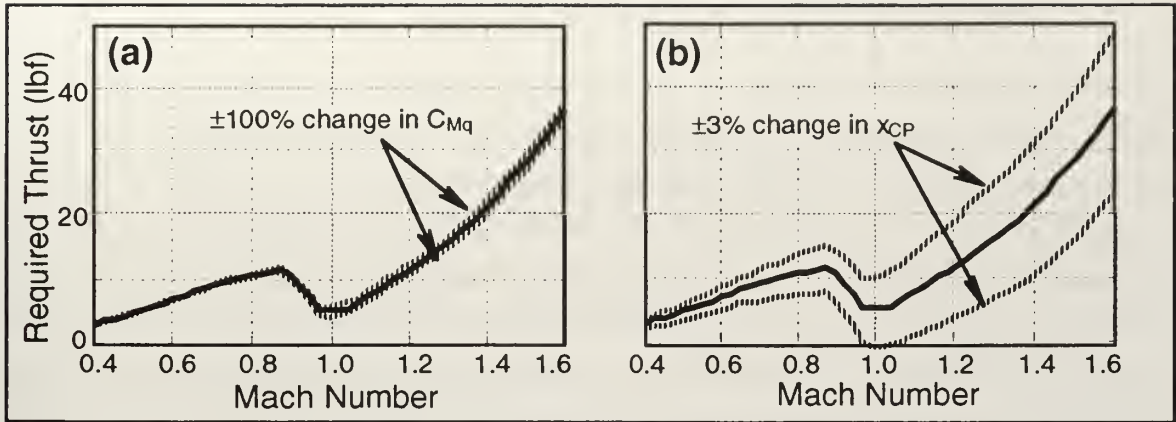


Figure 24. Sensitivity Analysis of the Steady-Turn Maneuver Model for Thruster Sizing. (a) $C_{Mq} \pm 100\%$ and (b) $x_{CP} \pm 3\%$.

Finally, Figure 24 illustrates the importance of sensitivity analysis and the potential for erroneous results due to incorrect inputs. The figure shows data from the control thruster sizing analysis with variations in the steady-turn model parameters. The plot on the left (a) shows the effect of $\pm 100\%$ changes in C_{Mq} . Doubling or zeroing the parameter produces only minor changes in required control thrust. Clearly, the thrust required is very insensitive to changes in C_{Mq} . On the other hand, the plot on the right shows the impact of $\pm 3\%$ changes in x_{CP} . The small changes in this input parameter affect the required control thrust significantly.

Another point of interest illustrated in the above example is the importance of parameter selection. In the NPS HRGK case, the parameter x_{CP} is measured from the nose of the guided rocket and varies between 28.5 and 31.8 inches as a function of Mach number. Small percentage changes in x_{CP} result in large percentage changes in the rocket's static margin (the small distance between the x_{CP} and the x_{CG}). In fact, the $\pm 3\%$ change in x_{CP} produces between a $\pm 22.7\%$ and $\pm 86.5\%$ change in static margin. Although either x_{CP} or static margin could be used as model inputs, the model sensitivity to percent changes in the two parameters would vary significantly.

3. Additional Work

The computer models developed by the author could be modified to produce new or refined models. The addition of probabilistic target motion to the turn rate and turn radius code would provide useful data. The analysis of elevation plane considerations would also be helpful in the guided rocket design. A model that could estimate both the required vertical field of view and pitch axis maneuverability would help in verifying the thruster

IV. SIX-DEGREE OF FREEDOM SIMULATION

This chapter addresses the use of detailed computer modeling in the missile design process. The chapter describes a six-degree of freedom (6DOF) simulation developed by the author for the analysis of the NPS HRGK. The HRGK 6DOF is a major modification to a simulation developed by Professor Robert (Gary) Hutchins, Electrical and Computer Engineering Department, Naval Postgraduate School, and his 1996 “Navigation, Missile, and Avionics Systems” class. The simulation was developed in SIMULINK using MATLAB functions to perform the simulation’s computations. The listings of the MATLAB functions are included in Appendix C.

Currently, the 6DOF code requires more than 20 minutes to simulate a 15 second rocket flight¹. To speed up the simulation, some of the simulation features are not yet fully implemented, but the author is in the process of converting the simulation to a more efficient computation structure. This structure uses the native Simulink “S-function” and was introduced to the author by Mr. Allen Robins; Dynamics and Controls Section, Naval Air Warfare Center Weapons Division, China Lake, California. (Appendix B briefly describes the different computation structures that can be used in Simulink.) Preliminary tests by the author have shown that the use of the S-function structure can cut simulation run times by a factor of nearly 30.

This chapter begins with an overview of the simulation architecture and then addresses the functions of the major simulation components. A section of the chapter is devoted to the development of the guided rocket equations of motion. And another, presents simulation results used in the design of the NPS HRGK. The chapter ends with a few observations concerning the use of detailed simulations in the missile design process.

A. SIMULATION OVERVIEW

The HRGK 6DOF simulation is designed to be used with an initialization script file. This MATLAB file is executed prior to running the simulation. It sets up simulation parameters such as vectors with the rocket’s aerodynamic coefficients (functions of Mach) and time profiles for mass properties and the main rocket thrust. The file also sets the initial conditions for all the simulation states. When run, the simulation uses a user-selectable

¹ Silicon Graphics, Inc. Indigo II workstation

integration scheme to simulate the rocket flight. The simulation writes several output vectors to the MATLAB workspace. These outputs include the flight time, target miss distance, the guided rocket's states ($U, V, W, P, Q, R, North, East, Altitude, \phi, \theta,$ and ψ), and their time derivatives with respect to the appropriate coordinate frames.

Figure 25 shows a top-level block diagram of the HRGK 6DOF. Figure 26 and Figure 27 respectively show detailed views of the "Rocket Dynamics" and the "Parameters and Coefficients" blocks as they are currently implemented.

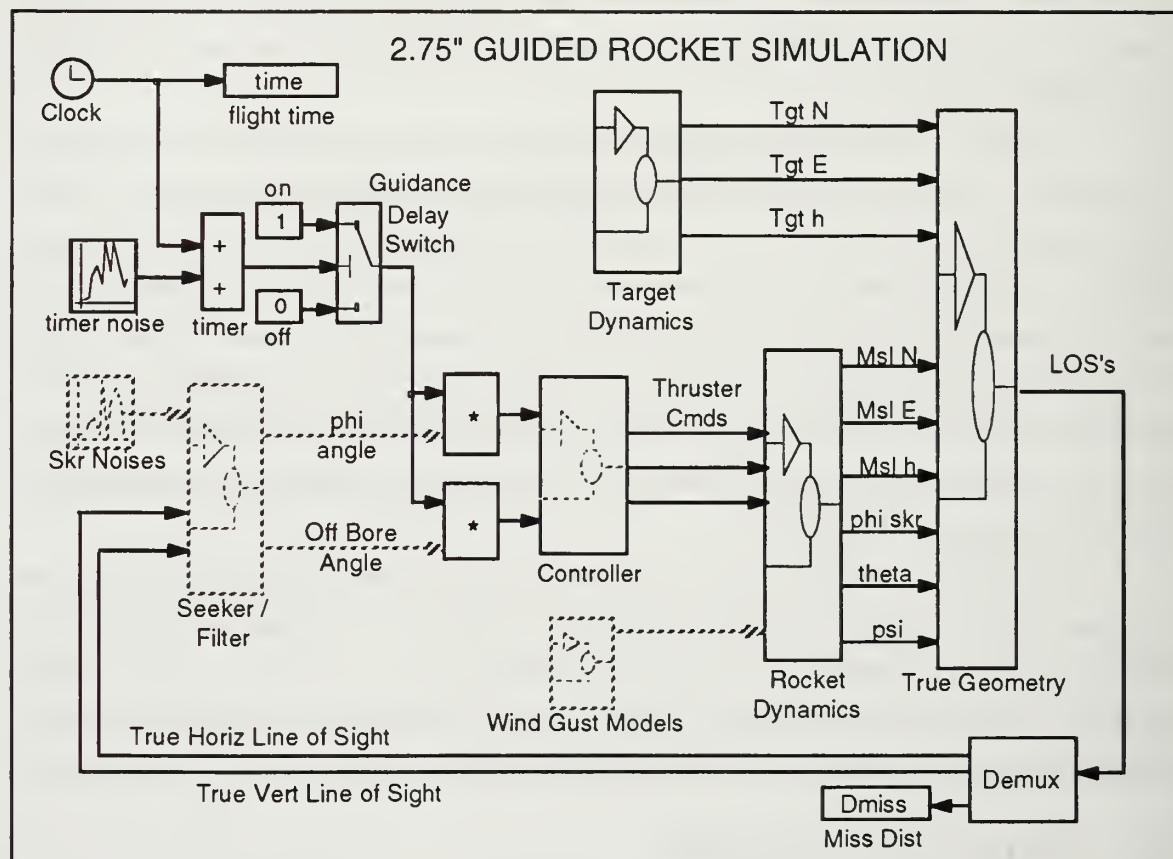


Figure 25. HRGK 6DOF Simulation Overall Block Diagram. (Dashed blocks are not yet fully implemented.)

The blocks in Figure 25 with dashed lines are not yet fully implemented. For example, the thruster control inputs are not currently generated based on seeker inputs, but rather, the thruster commands must be "hard coded" into the controller block.

Inside the Rocket Dynamics block, the time derivatives of the rocket's states are computed by a MATLAB function. The state derivatives are then integrated and feedback into

the function and other parts of the simulation. The rocket's aerodynamic and mass property parameters are determined using lookup tables in the Parameters and Coefficients block.

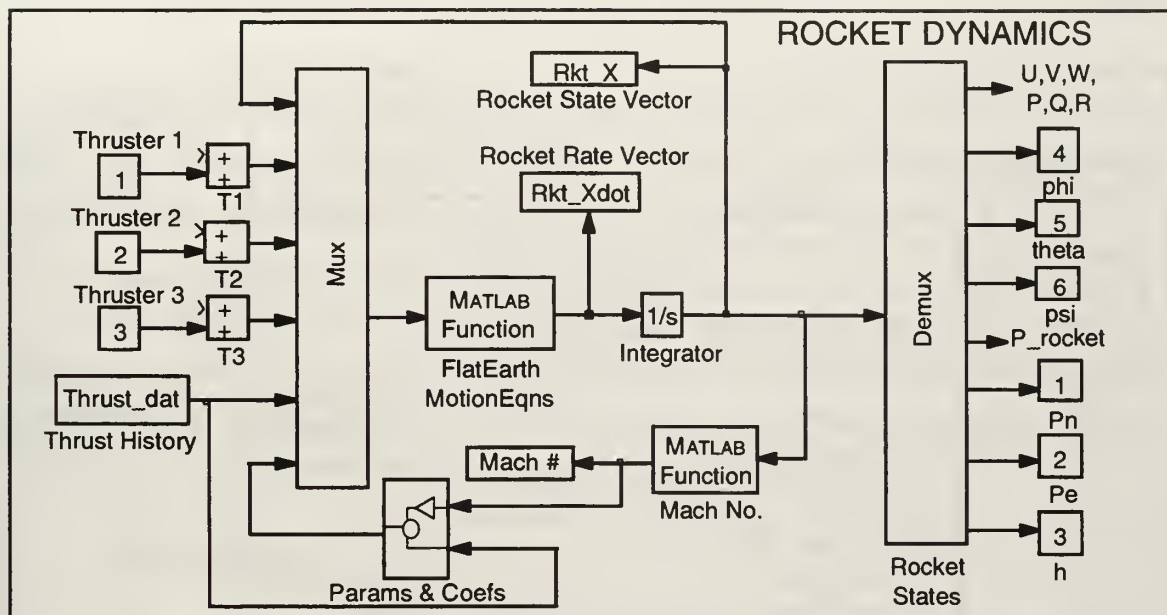


Figure 26. Detailed View of the Rocket Dynamics Block.

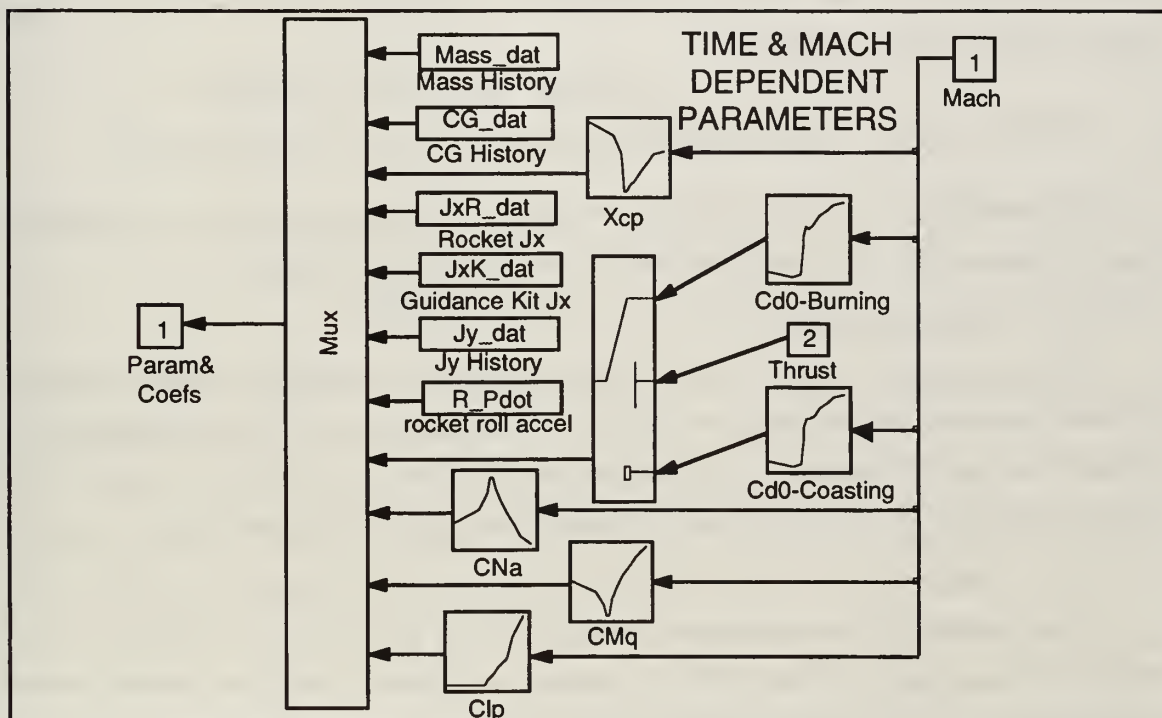


Figure 27. Detailed View of the Parameters and Coefficients Block.

Figure 28 shows the overall architecture for the simulation currently under development. Most of the components of this architecture are described in the following section.

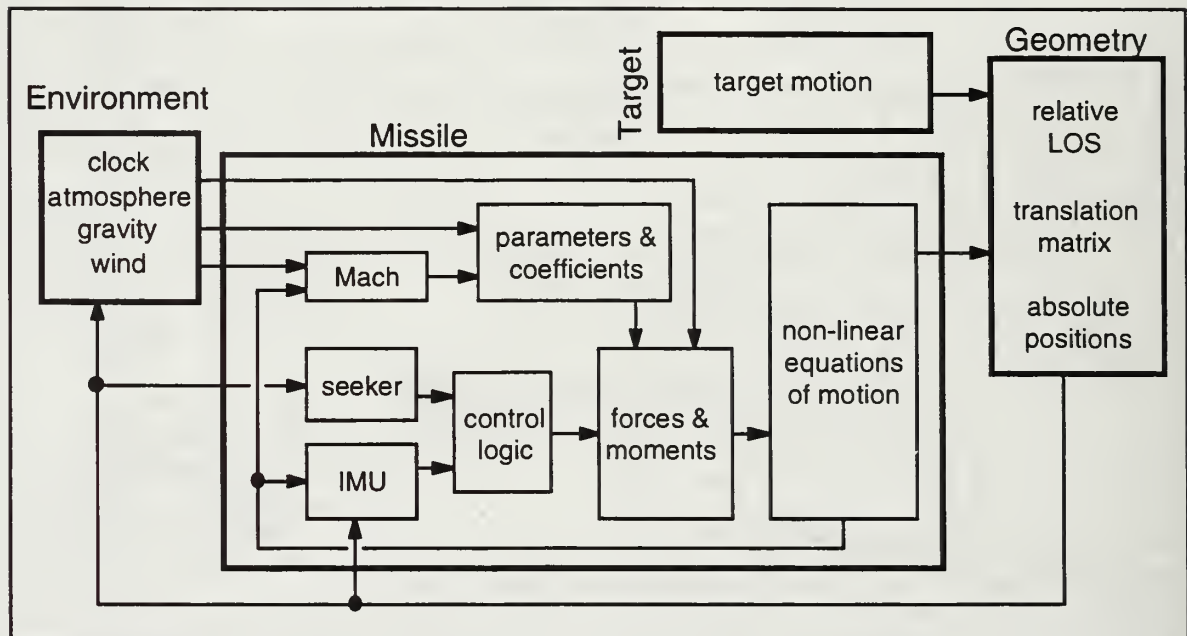


Figure 28. Future 6DOF Architecture.

B. SIMULATION COMPONENTS

The simulation shown schematically in Figure 28 is made up several components. These components are very briefly described in the following subsections.

1. Environment

The environment block simulates the environment in which the rocket operates. This block produces the simulation time and provides constant gravity. It also computes the atmospheric properties needed to calculate the Mach number and dynamic pressure. The block uses the Dryden wind gust model to produce wind gusts in pitch and yaw.

2. Missile

The missile block simulates the dynamics of the guided rocket. The block has several sub-components. These blocks are divided to align as closely as possible with actual subsystems. The missile block uses external signals and data to produce realistic seeker and IMU signals. From these signals control inputs are determined and applied to

the forces and moments sub-component. The forces and moments component computes all the body frame forces on the rocket. From these forces and moments the dynamics of the body can be determined by the flat-earth equations of motion.

3. Target Dynamics

The target block provides the target location and motion to the relative geometry block. This data allows the line of sight (between the rocket and the target) and the line of sight rate data to be calculated.

4. Relative and Absolute Geometry

The relative geometry block uses the target and rocket dynamics to solve the navigation equations (described in the following section). From the navigation equations, the absolute and relative position of the rocket and target can be computed. The line of sight and line of sight rates are also provided by the geometry block.

C. EQUATIONS OF MOTION

This section contains a brief derivation of the flat-earth equations of motion as they apply specifically to the HRGK 6DOF. The derivation is adapted from Stevens and Lewis [Ref. 15].

1. General Matrix-Form Equations

Starting with generic flat earth equations of motion:

$$\dot{\mathbf{v}}_B = -\Omega_B \mathbf{v}_B + B_B \mathbf{g}'_0 + \frac{\mathbf{F}_B}{m} \quad (\text{Force Equation})$$

$$\dot{\omega}_B = -J^{-1} \Omega_B J \omega_B + J^{-1} \mathbf{T}_B + \mathbf{H}_R \quad (\text{Moment Equation})$$

$$\dot{\Phi} = E(\Phi) \omega_B \quad (\text{Attitude Equation})$$

$$\dot{\mathbf{p}}_{NED} = B_B^T \mathbf{v}_B \quad (\text{Navigation Equation})$$

where the \mathbf{v}_B is the velocity vector, $[U \ V \ W]^T$; \mathbf{g}'_0 is the gravity vector at the surface of the earth (adjusted for the earth rotation), $[0 \ 0 \ 9.81\text{m/s}^2]^T$; \mathbf{F}_B is the force vector, $[F_x \ F_y \ F_z]^T$; ω_B is the angular rate vector, $[P \ Q \ R]^T$; \mathbf{T}_B is the torque vector, $[L \ M \ N]^T$; \mathbf{H}_R , to be defined later, is a vector to account for the gyroscopic effects of the spinning rocket motor; Φ is the Euler angle vector, $[\phi \ \theta \ \psi]^T$; \mathbf{p}_{NED} is the north-east-down frame position vector, $[p_N \ p_E \ p_D]^T$; Ω_B is the body frame angular rates cross-product matrix,

$$\Omega_B = \begin{bmatrix} 0 & -R & Q \\ R & 0 & -P \\ -Q & P & 0 \end{bmatrix};$$

B_B is the rotation matrix from the North-East-Down frame to the body frame,

$$B_B = \begin{bmatrix} 1 & 0 & 0 \\ 0 & \cos \phi & \sin \phi \\ 0 & -\sin \phi & \cos \phi \end{bmatrix} \begin{bmatrix} \cos \theta & 0 & -\sin \theta \\ 0 & 1 & 0 \\ \sin \theta & 0 & \cos \theta \end{bmatrix} \begin{bmatrix} \cos \psi & \sin \psi & 0 \\ -\sin \psi & \cos \psi & 0 \\ 0 & 0 & 1 \end{bmatrix};$$

J is the inertia matrix (with symmetry assumed about the x-axis),

$$J = \begin{bmatrix} J_x & 0 & 0 \\ 0 & J_y & 0 \\ 0 & 0 & J_y \end{bmatrix};$$

and the Euler angle function is

$$E(\Phi) = \begin{bmatrix} 1 & \tan \theta \sin \phi & \tan \theta \cos \phi \\ 0 & \cos \phi & -\sin \phi \\ 0 & \frac{\sin \phi}{\cos \theta} & \frac{\cos \phi}{\cos \theta} \end{bmatrix}.$$

The state vector is $[\mathbf{v}_B^T \ \omega_B^T \ \mathbf{F}^T \ \mathbf{p}_{\text{NED}}^T]^T$. Now the forces and moments need to be defined for the HRGK case.

2. Forces and Moments

The aerodynamic forces and moments are functions of Mach number and can be expressed by the coefficients and their derivatives. The following summarizes the forces and moments computed in HRGK 6DOF:

$$F_x \approx T - \bar{q}A \left(C_{D_0} + \frac{C_N^2}{C_{N_\alpha}} \right) \quad (\text{Axial Force})$$

$$F_y = T_y + \bar{q}A (-C_{N_\alpha} \beta) \quad (\text{Side Force})$$

$$F_z = T_z - \bar{q}A (C_{N_\alpha} \alpha) \quad (\text{Down Force})$$

$$L = \bar{q}Ad \left(\frac{C_{l_p} d}{2U} P \right) + T_R \quad (\text{Rolling Moment on HRGK})$$

$$M = T_z X_T + \bar{q} A d \left(C_{N_\alpha} \alpha X_{CP} + \frac{C_{M_q} d}{2U} Q \right) \quad (\text{Pitching Moment})$$

$$N = T_y X_T + \bar{q} A d \left(C_{N_\alpha} \beta X_{CP} + \frac{C_{M_q} d}{2U} R \right) \quad (\text{Yawing Moment})$$

where T is the rocket motor thrust; T_y and T_z are the y and z components of the reaction thruster forces, $T_z = T_1 \cos \phi + T_2 \cos(\phi + 2/3\pi) + T_3 \cos(\phi + 4/3\pi)$ and $T_y = T_1 \sin \phi + T_2 \sin(\phi + 2/3\pi) + T_3 \sin(\phi + 4/3\pi)$; and T_R is the rolling torque exerted on the HRGK by the spinning rocket motor,

$$T_R = \mu J_{X_R} \dot{P}_R$$

where μ is the coefficient of friction for the bearings, J_{X_R} is the axial moment of inertia for the rocket alone, and \dot{P}_R is the rocket motor's spin axis angular acceleration (adapted from Ref. [11]). The state P_R has to be added to the state vector, and the gyroscopic affect of the spinning rocket is added to the moment equation. The effect can be accounted for by adding the vector \mathbf{H}_R to the right-hand side of the moment equation, where \mathbf{H}_R is

$$\mathbf{H}_R = \begin{bmatrix} 0 & \frac{-R J_{x_R} P_R}{J_y} & \frac{Q J_{x_R} P_R}{J_y} \end{bmatrix}^T$$

3. HRGK Scalar Flat-Earth Equations

From the general matrix equations, the HRGK-specific scalar form of the equations can be written in terms of the defined forces and moments.

a. Force Equations

$$\dot{U} = RV - QW - g_0 \sin \theta + \frac{F_x}{m}$$

$$\dot{V} = -RU + PW + g_0 \sin \phi \cos \theta + \frac{F_y}{m}$$

$$\dot{W} = QU - PV + g_0 \cos \phi \cos \theta + \frac{F_z}{m}$$

b. Moment Equations

$$\dot{P} = \frac{L}{J_x}$$

$$\dot{Q} = \left(1 - \frac{J_x}{J_y}\right) P R + \frac{M}{J_y} - \frac{J_{x_R}}{J_y} R P_R$$

$$\dot{R} = \left(\frac{J_x}{J_y} - 1\right) P Q + \frac{N}{J_y} + \frac{J_{x_R}}{J_y} Q P_R$$

c. Kinematics Equations

$$\dot{\phi} = P + \tan \theta (Q \sin \phi + R \cos \phi)$$

$$\dot{\theta} = Q \cos \phi - R \sin \phi$$

$$\dot{\psi} = Q \sin \phi + R \frac{\cos \phi}{\cos \theta}$$

d. Navigation Equations

$$\dot{P}_N = U \cos \theta \cos \psi + V(\sin \phi \sin \theta \cos \psi - \cos \phi \sin \psi) + W(\cos \phi \sin \theta \cos \psi + \sin \phi \sin \psi)$$

$$\dot{P}_E = U \cos \theta \sin \psi + V(\sin \phi \sin \theta \sin \psi + \cos \phi \cos \psi) + W(\cos \phi \sin \theta \sin \psi - \sin \phi \cos \psi)$$

$$\dot{P}_D = -U \sin \theta + V \sin \phi \cos \theta + W \cos \phi \cos \theta$$

D. NPS HRGK RESULTS

The force and moment equations, as well as the equations of motion, are implemented in a MATLAB function which is used by the HRGK 6DOF simulation. The following subsections show two examples of how the simulation was used in the design.

1. Ballistic Flight and Maximum Range (3DOF)

Early in during the NPS HRGK design process, the HRGK simulation was simplified to only include the three dimensions of the rocket's longitudinal dynamics. (The gyroscopic effects of the spinning rocket were also ignored.) Using the simplified 3DOF, the results shown in Figure 29 were obtained. These results confirmed that the HRGK-equipped rocket could meet the time to target and the maximum range requirements.

2. Pulse Width Modulated Turn Rate (6DOF)

Later in the design, the affect of thruster pulse width modulation was investigated using the HRGK 6DOF. Two simulations were run. The first simulated the missile flight

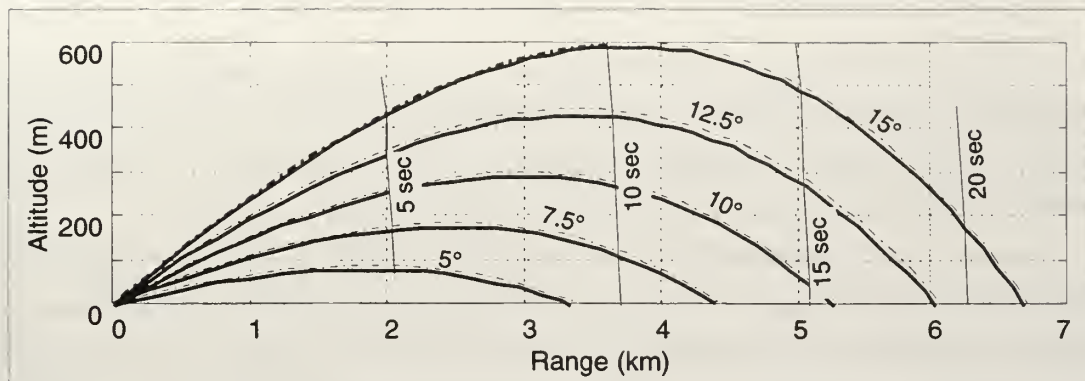


Figure 29. HRGK-Equipped Rocket Ballistic Trajectories. Ground launch at sea level with various launch elevation angles. Solid lines are for cold rocket motor, dashed lines are for hot rocket motor, and flight times are indicated.

with a constant thruster force from the appropriate side only. The second used a pulsed sequence of all three thrusters, but with a longer pulse on the appropriate side. The results for the two runs are shown in Figure 30. From the analysis, it was determined that constant thrust does not generate satisfactory maneuvers. (In fact, in the simulation, the rocket began “cartwheels” without making substantial changes in cross-track). On the other hand, the pulsed control generated an adequate maneuver while maintaining a somewhat reasonable side slip angle, β .

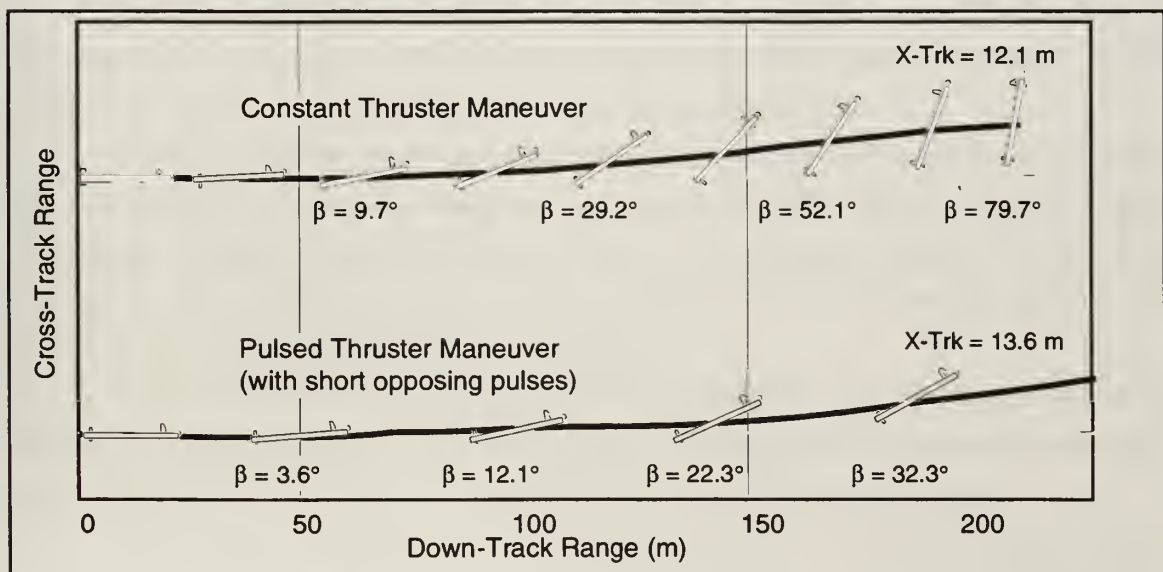


Figure 30. Sustained and Pulsed Thruster Maneuvers. Flight paths and headings indicated for a 0.8 second maneuver.

E. OBSERVATIONS

As designs become more refined and leave the conceptual phases, high fidelity simulations becomes more important. In the case of the NPS HRGK, the 6DOF simulation was helpful in performing some detailed analyses. Nevertheless, the time required per simulation run precluded the use of the simulation in many cases.

Fast, modular simulations that can be easily modified for various designs are desirable design tools. In many cases, lower-order simulations (3DOF or 5DOF) meet all the needs of the designer. For example, the 3DOF version of the HRGK simulation had sufficient fidelity to be used in the maximum range and time to target analyses. Unfortunately, other analyses required a 6DOF so that the roll of the seeker and the gyroscopic effects of the spinning rocket could be observed.

If the restructuring of the HRGK simulation provides the expected improvement in run time, this simulation would become a much more useful design tool. With run times of only a minute or so, several design iterations could be evaluated quickly.

V. CONCLUSIONS AND RECOMMENDATIONS

The purpose of this thesis is to provide documentation for the several computer codes developed by the author during the design and analysis of the NPS HRGK. The thesis is also intended to provide insights concerning the use of modeling in the design and analysis processes. Several germane points can be made in conclusion.

First, models with differing levels of complexity are appropriate during different phases of the design. Models used in the analysis of conceptual and preliminary designs are usually the simplest while those models used in design refinement are more complicated. COEA-related modeling is essential throughout the design process to ensure that the design meets the system's cost effectiveness goals.

Second, simplistic models can be used to ensure the flow down of system requirements into design specifications. In this way, the models help ensure a design driven by the requirements. Often these simple models provide great insight into additional aspects of the design problem allowing several critical specifications to be defined in the earliest phases of the design.

Third, modeling in the design process should include the appropriate mix of probabilistic and worst-case conditions. These two types of models can provide very different results which must be judiciously evaluated.

Finally, knowing the sensitivity of a model to variations in parameters is critical to the proper use of the model in decision making. Sensitivity analyses or "what-if" studies must be performed to ensure the modeling is providing reliable data.

In addition to these concluding points several recommendations for follow-on work are also appropriate. First, the design and analysis of the NPS HRGK would have been facilitated by simple MATLAB codes that allow the early aerodynamic sizing of the kit. Such a program would be helpful in evaluating the effect of nose shape and canard size and shape on the range of the HRGK-equipped rocket.

Additional work is also needed to include a probabilistic target motion model in the maneuverability analysis code. The development of models that evaluate the required pitch maneuverability and the required elevation field of view would also be useful.

Finally, the modification of the HRGK simulation to make it a generic 6DOF simulation would be very useful for future missile design work. The Simulink architecture can offer fast modular simulations that can be easily modified to meet future users' needs.

APPENDIX A. MISSILE AERODYNAMICS NOMENCLATURE

Many of the aerodynamic coefficients, stability derivatives, and various other terms and symbols used in this thesis are defined below. The nomenclature closely follows that used by Chin [Ref. 16] with some adaptations like that used by Blakelock [Ref. 17] and by Howard [Ref. 18]. It is worth noting two significant differences between terms associated with missiles and those associated with traditional aircraft. First, most missile coefficients are referenced to the missile's diameter or its cross-sectional area (normal to the longitudinal axis) rather than a wing chord or a planform area. Second, normal and axial force coefficients, C_N and C_A , (aligned to the body-axis system) are used rather than the lift and drag force coefficients, C_L and C_D , (in the stability axis system). When the missile's angle of attack (α) is small there is very little difference between the two systems, but for significant angles of attack, the relationship given in the following equations should be used.

$$C_A = C_D \cos \alpha - C_L \sin \alpha$$

$$C_N = C_L \cos \alpha - C_D \sin \alpha$$

Reference Dimensions

A or S_π	Cross-sectional area of missile body (5.94 in ²)
d	Diameter of missile body (2.75 in)
L	Missile length (68.75 in)
X_{cg}	Distance from nose tip to center of gravity on missile (27 to 31.7 in)

Flight Conditions

α	angle of attack
β	side slip angle
M	Freestream Mach number
V_i	Freestream air speed
ρ	Freestream air density
\bar{q}	Dynamic pressure ($\frac{1}{2} \rho V_i^2$)

Aerodynamic Coefficients*

C_L	Coefficient of lift, $\frac{\text{Lift}}{qS_\pi}$
C_N	Normal force (N) coefficient, $\frac{N}{qS_\pi}$
C_M	Pitching moment (M) coefficient, $\frac{M}{qS_\pi d}$
C_A	Axial force (A) coefficient, $\frac{A}{qS_\pi}$
C_D	Drag force (D) coefficient, $\frac{D}{qS_\pi}$
C_{D0}	Drag force coefficient at zero lift
C_{DN}	Coefficient of drag due to normal force (D_N), $\frac{D_N}{qS_\pi}$

Static and Dynamic Derivatives*

$C_{N\alpha}$	Normal force coefficient per radian of angle of attack, $\frac{\partial C_N}{\partial \alpha}$
$C_{M\alpha}$	Pitching moment coefficient per radian of angle of attack, $\frac{\partial C_M}{\partial \alpha}$
C_{Mq}	Pitching moment coefficient per radian/sec of pitch rate, $\left(\frac{2U}{d}\right) \frac{\partial C_M}{\partial \alpha}$

Missile "States"

U, V, W	Body axis velocities (x, y, and z-axes)
P, Q, R	Body-axis angular rates (about the x, y, and z-axes)
ϕ, θ, ψ	Euler Angles (roll, pitch, yaw)
P_N, P_E, P_D	Flat Earth Positions (North, East, Down)
h	height ($-P_D$)

* Directional coefficients and derivatives (e.g.; $C_Y, C_{\bar{N}}, C_{Y\beta}, C_{\bar{N}\beta}, C_{\bar{N}r}$) are assumed equal to their longitudinal counterparts (e.g.; $C_N, C_M, C_{N\alpha}, C_{M\alpha}, C_{Mq}$; respectively).

APPENDIX B. NOTES ON MATLAB AND SIMULINK

A. MATLAB

MATLAB is a high-performance numeric computation and visualization computer software package. It is essentially a high-level programming language that is especially tailored for the manipulation of matrices. (see *MATLAB Reference Manual* and *MATLAB User's Guide*)

MATLAB commands can either be invoked in an interactive mode at the keyboard or through MATLAB script files. Another type of file is the MATLAB function. Both the script and function files are labeled with an “m” extension at the end of the file name and are commonly called M-files.

A script M-file can run as a stand alone “batch” file invoking MATLAB commands when the file is executed. On the other hand, a function M-file is called from within script files or from the keyboard. A function can be called with or without arguments and can return computed values when completed.

Variables declared or set in a script file or at the keyboard are available throughout the MATLAB “workspace.” These variables are common and can be accessed by other script files. On the other hand, variables declared in a function M-file are local variables and are not available in the workspace. Furthermore, functions do not have access to workspace variables unless the variables are passed to the function or are declared as “global” in both the workspace and in the function.

The standard syntax used in the first line of a function M-file is

```
function y = func(u)
```

where “function” is the MATLAB function indicator, y is the variable that will be passed back, u is the input, and *func* is the name of the function (*func.m*).

Files that are written in C or FORTRAN can be converted into executable MATLAB files with a “.mex” extension by using the “cmex” or “fmex” commands. (see *MATLAB External Interface Guide*) Mex-files have the advantage of running faster than normal M-files.

B. SIMULINK

Simulink is a dynamic system simulation software package and an extension to MATLAB. Simulink offers many ready-made blocks that can be assembled graphically to model a dynamic system. Two special Simulink blocks allow tremendous flexibility in modeling systems. (see *Simulink User's Guide*)

The first is the MATLAB function block. This block when placed in a block diagram will execute the commands in the indicated M-file function. So for example, the equations of motion for a system could be placed in a M-file function. This function would have inputs from simulink that include the states and the control input. The function would then output the states' time derivatives which could then be integrated and then passed back the MATLAB function.

This method runs extremely slow!

The second more useful block is the S-function block. This block calls either a M-file or a Mex-file that is specifically structured to run efficiently in Simulink (see *Simulink 1.3 Release Notes*). Chapter 4 of *Simulink 1.3 Release Notes* outline the procedure for creating Mex-files from C codes for use in fast running Simulink models.

Additionally, simulink models that do not contain M-file references (that use Mex-files in the S-function blocks) can be turned into stand-alone, accelerated, executable code using Simulink's Real-Time Workshop (see *Real-Time Workshop User's Guide*).

APPENDIX C. MATLAB CODE LISTINGS

This appendix provides listings of the following MATLAB computer codes which were discussed in this thesis:

- Single-Shot Probability of Kill
- Length, Weight, and Center of Gravity
- Turn Rate and Radius
- Steady-Turn Maneuver
- Seeker Field of View
- 6DOF Codes
 - Initialization Code
 - Aerodynamics Data
 - Equations of Motion
 - Line of Sight
 - Mach

The user-defined inputs in the codes are denoted with bold-face type.

C. SINGLE-SHOT PROBABILITY OF KILL

```
% Single Shot Pk using "Cookie Cutter" methodology
% W. Mark Wonnacott, Naval Postgraduate School, May 1997, corrected/revised Aug 1997
%%%%%%%%%%%%%%%%%%%%%%%%%%%%%%%%%%%%%%%%%%%%%%%%%%%%%%%%%%%%%%%%%%%%%%%%INPUTS
% Terminal Dive Angle (deg relative to horizontal)
dive = 20;
% CEPs to be used in computations (for a single CEP set CEP_min equal to CEP_max)
CEP_min = .5; % minimum CEP (m) to be used
CEP_max = 100; % maximum CEP (m) to be used
% Target Size (m), Prob. of Kill given Hit, & Desired Prob. Kill
L = 5.5; H = 2.0; W = 2.5; Pkh = .90; PkD = .95; trgt='Light Arm. (AirDef)';
L = 5.5; H = 2.0; W = 2.5; Pkh = .80; PkD = .60; trgt='Light Armor (APC)';
L = 8.0; H = 2.5; W = 2.5; Pkh = 1; PkD = .50; trgt='Large Truck';
L = 14.; H = 1.5; W = 4.5; Pkh = .70; PkD = .75; trgt='Patrol Boat';
%%%%%%%%%%%%%%%%%%%%%%%%%%%%%%%%%%%%%%%%%%%%%%%%%%%%%%%%%%%%%%%%%%%%%%%%INPUTS
% Elevation and Crossrange Projected Dimensions (1:Head on & 2:Broadside)
Y1 = H*cos(dive*pi/180)+L*sin(dive*pi/180);
X1 = W;
Y2 = H*cos(dive*pi/180)+W*sin(dive*pi/180);
X2 = L;

%CEPs in desired range
if CEP_min<=0, CEP_min=eps; end %CEP_min set to allowable small number
if CEP_max<=0, CEP_max=eps; end %CEP_max set to allowable small number
if CEP_min>CEP_max, temp=CEP_min; CEP_max=CEP_min; CEP_min=temp; end
```

```

CEPs = logspace(log10(CEP_min),log10(CEP_max));
sigmas = CEPs/1.1774; %corresponding sigmas,1-D miss distances (m)
S = sigmas*sqrt(2)*2; %normalized half sigmas for MATLAB
% Probability of Hit (equal (50%) prob. of broadside or head-on encounter)
Ph = 0.5*(erf(Y1./S).*erf(X1./S)) + 0.5*(erf(Y2./S).*erf(X2./S));
% Probability of Single Shot Kill
PkSS = Pkh*Ph;

% Number of Weapons Needed to Achieve Desired Prob. of Kill
N = log(1-PkD)./log(1-PkSS);

figure (1) % Single-Shot Probability of Kill
semilogx (CEPs,PkSS,'-'), grid on
axis([CEP_min,CEP_max,0,1])
xlabel('CEP (m)'), ylabel('Single Shot Probability of Kill')

figure (2) % Number of Weapons per Kill
loglog (CEPs,N,'-'), grid on
axis([CEP_min,CEP_max,1,1000])
xlabel('CEP (m)'), ylabel(['Number of Rockets for Pk = ',num2str(PkD)])

figure (3) % Relative Cost for Equal Cost/Kill
Nc = max(1,ceil(N));
[X,Y]=stairs(CEPs,Nc(1)./Nc);
plot (X,Y,'-'), grid on
axis([CEP_min,CEP_max,0,1])
xlabel('CEP (m)'), ylabel('Relative Weapon Cost')

```

D. LENGTH, WEIGHT, AND CENTER OF GRAVITY

```

%=====
% GUIDED Rocket Center of Gravity as a Function of Kit Weight
%=====
% W. Mark Wonnacott, Naval Postgraduate School, May 1997

%%% Design Space Paramters
Wk1 = linspace(1,8); % assumed kit mass range (lbm)
Lk1 = [5,10,13.625,Lmax-Lr]; % specific kit lengths (in)
Dk1 = [.05,.07,.0865,.1,.15]; % specific kit densities (lbm/in^3)
Cgk1= 1/3; % kit Cg from nose (fraction of kit length)

dia = 2.75; % kit diameter (in)
area= pi*(dia/2)^2; % kit cross section area (in^2)

```

```

%%%% Constraint Parameters
Lmax= 72;           % max total length
Wmax= 30;           % max total weight
CgL = 1/3;          %pod forward Cg limit(frac of lug spacing back from front lug)

%%%% Rocket Parameters
Lr = 55.125;        % rocket length
CgR_live = 29.96;   % live rocket Cg (inches from base)
CgR_burn = 33.55;   % fired rocket Cg (inches from base)
WR_live = 22.95;    % live rocket mass (lbm)
WR_burn = 15.73;    % fired rocket mass (lbm)

%%%% Launcher Pod Parameters
Llug7 = 43.2;       % front lug from back of launcher-7 (in)
Llug19= 43.4;       % front lug from back of launcher-19 (in)
Cg7 = Llug7-(CgL)*14; % constraint cg (e.g. within middle half of lug space)
Cg19=Llug19-(CgL)*14; % constraint cg (e.g. within middle half of lug space)
Cgpod = 32.6;       % loaded pod Cg from back w/o kits (in)
Wpod7 = 196.2;      % loaded pod(7) mass w/o kits (lbm)
Wpod19= 516.0;      % loaded pod(19) mass w/o kits (lbm)

% (VARIOUS DENSITY CURVES PLOTTED)
% =====
Wk = Wk1'*ones(1,length(Dk1)); % matrix of kit masses
Lk = Wk(:,1)*(1./(area*Dk1)); % matrix of kit lengths (in)
Cgk= Lr+(1-Cgk1)*Lk;          % kit Cg locations (inches from base)

Mk = Wk.*Cgk;                 % Moment about base due to kit (lbm in)

% centers of gravity are calculated from base in inches
Cg_live = (WR_live*CgR_live+Mk)./(WR_live+Wk);
Cg_burn = (WR_burn*CgR_burn+Mk)./(WR_burn+Wk);

% centers of gravity are changed to calibers from nose
Cg_live = ((Lr+Lk)-Cg_live)/dia;
Cg_burn = ((Lr+Lk)-Cg_burn)/dia;

%figure
figure (1),
    plot (Wk(:,1), Cg_live), grid on
    title ('Live Round with Kit')
    ylabel ('Cg (Calibers from nose)')
    xlabel ('kit weight (lbm)')
    hold on

```



```

figure (2),
    plot (Wk(:,1), Cg_burn), grid on
    title ('Fired Round with Kit')
    ylabel ('Cg (Calibers from nose)')
    xlabel ('kit weight (lbm)')
    hold on

% (VARIOUS LENGTH CURVES PLOTTED)
% =====
Lk = Lk1; % specific kit lengths (in)
Dmin = 0.8*min(Dk1); % lower limit on assumed density range
Dmax = 1.2*max(Dk1); % upper limit on assumed density range
Dk = linspace(Dmin,Dmax); % assumed kit density range (lbm/in^3)
Dk = Dk'*ones(1,length(Lk)); % matrix of kit densities
Wk = area*Dk(:,1)*Lk; % matrix of kit masses (lbm)
Cgk= Lr+(1-Cgk1)*Lk; % kit Cg locations (inches from base)
Cgk= ones(length(Wk),1)*Cgk; % matrix of Cg locations

Mk = Wk.*Cgk; % Moment about base due to kit (lbm in)

% centers of gravity are calculated from base in inches
Cg_live = (WR_live*CgR_live+Mk)./(WR_live+Wk);
Cg_burn = (WR_burn*CgR_burn+Mk)./(WR_burn+Wk);

% centers of gravity are changed to calibers from nose
Cg_live = ((Lr+ones(length(Wk),1)*Lk)-Cg_live)/dia;
Cg_burn = ((Lr+ones(length(Wk),1)*Lk)-Cg_burn)/dia;

figure (1),
    plot(Wk,Cg_live)
    plot([(Wmax-WR_live)*ones(1,2)], [1,20]) %max weight constraint
figure (2),
    plot(Wk,Cg_burn)
    plot([(Wmax-WR_live)*ones(1,2)], [1,20]) %max weight constraint

% (POD CENTER OF GRAVITY CONSTRAINT)
% =====
Wk = Wk1'*ones(1,2); % matrix of kit masses
%length from loaded pod (w/o kits) cg to constraint Cg (in)
L1 = ones(length(Wk),1)*([Cg7,Cg19]-Cgpod);
% loaded pod weights (lbm)
Wp = ones(length(Wk),1)*[Wpod7,Wpod19];
X = ones(length(Wk),1)*[7,19]; % number of kits per pod
% length from rocket nose back to front lug
% (assume rocket base 4" from back of pod)
Lt = ones(length(Wk),1)*[Lr-Llug7+4,Lr-Llug19+4];

```

```

% Solve for allowable kit length
Lk = (1/(1-Cgk1))*((Ll.*Wp)/(X.*Wk)-Lt);

Cgk= Lr+(1-Cgk1)*Lk;           % kit Cg locations (inches from base)

% center of gravity calculated from base in inches
Cg_live = ((WR_live*CgR_live)+(Cgk.*Wk))./(WR_live+Wk);
Cg_burn = ((WR_burn*CgR_burn)+(Cgk.*Wk))./(WR_burn+Wk);

% center of gravity changed to calibers from nose
Cg_live = ((Lr+Lk)-Cg_live)/dia;
Cg_burn = ((Lr+Lk)-Cg_burn)/dia;

figure (1),
    plot(Wk,Cg_live)
    axis([1.8,7.2,7.8,14])
    %hold off
figure (2),
    plot(Wk,Cg_burn)
    axis([1.8,7.2,6.8,13])
    %hold off

```

E. STEADY-TURN MANEUVER

```

% This m-file computes thrust required, T, for certain load factor, n
% (g's), in a steady turn for various Mach numbers. The load factor is
% achieved using a thruster forward of the CG.
%
% The inputs include:
%   Scenario Definition:
%       n:   desired load factor (g's)
%       rt:  desired turn radius (ft)
%       alt: altitude (ft) (std day assumed)
%       Mmin: min Mach number
%       Mmax: max Mach number
%   Rocket Configuration:
%       Wght: rocket mass (lbm)
%       Dia: rocket cross-section diameter (in) (for ref area and length)
%       Xcg: rocket center of gravity in calibers from nose
%       Xt:  thruster location in calibers from nose
%   Aerodynamic Parameters:
%       CNa: normal force coefficient per radian of alpha [f(Mach)]
%       Xcp: center of pressure location in calibers from nose [f(Mach)]
%       CMq: moment coefficient per rad/sec of pitch rate [f(Mach)]
%       (Aero Paramaters are linearly interpolated between points in table)

```

```

% Code uses normal force and pitch moment equations:
%   Fz = nW = N + T = (Qbar)*S*CNa*alpha + T, and
%   M = 0 = -N*(Xcp-Xcg) + T*(Xcg-Xt) - CMq*q*(Dia/2V)*Qbar*S*Dia
%       {since, q = theta-dot = V/R = V/(V^2/n) = n/V
%       and N = (Qbar)*S*CNa*alpha}
%   M = (Qbar*S*CNa*alpha)(Xcp-Xcg) + T*(Xcg-Xt) - CMq*n*(Dia^2/V^2)*Qbar*S
% The two equations are solved for the unknowns, alpha and T, using several
% values of Mach number.

% W. Mark Wonnacott, Naval Postgraduate School, May 1997
clear, close all

% INPUTS
% =====
% Scenario Definition
n = 15; % desired load factor (g's)
Rt = 6000; % desired min turn radius (ft)
req_type = 2; % requirement (1:turn rate, 2:turn radius)
alt = 500; % std day pressure altitude (ft MSL)
Mmin= 0.4; % minimum Mach number for calculations
Mmax= 1.6; % maximum Mach number for calculations
% Rocket Configuration (based on burned-out, 30 lbm, 68.75" rocket)
Wght = 22.78; % rocket mass (lbm)
Dia = 2.75; % reference length (in)
Xcg = 10.0; % CG in calibers from nose
Xt = 2.2; % thruster location in calibers from nose
% Aerodynamic Parameters (based on final config 68.75"-w/ 3 case#8 strakes)
%
% Mach# CNa Xcp CMq
aero_table = [0 15.0616 11.52547 -4166.814
0.6614 16.41589 11.32152 -4556.4946
0.866 18.10928 11.01214 -5041.0303
0.9682 20.04303 10.36514 -5518.2495
1 20.05156 10.35951 -5519.5352
1.0308 20.05156 10.35951 -5519.5352
1.118 18.91632 10.45431 -4859.3901
1.25 17.51701 10.5577 -4376.4146
1.4142 16.10659 10.68451 -3938.8662
1.6008 14.68889 10.88046 -3541.0081
1.8028 13.47025 10.99184 -3202.1553
2.0156 12.38573 11.05396 -2916.2678];
Mach_dat= aero_table(:,1); % Mach numbers
CNa_dat = aero_table(:,2); % Body Normal Force per Radian Alpha
Xcp_dat = 1.03*aero_table(:,3); % Center of Pressure in calibers from nose
CMq_dat = aero_table(:,4); % Pitching Moment per rad/sec of Pitch Rate

```

```

% CONSTANTS
g0 = 32.17; % Gravity Constant.
Temp0 = 518.67; %surface temperature (°R)
Pres0 = 14.696*144; %surface pressure (lbf/ft^2)
B_atm = 0.003566; %temp lapse rate (°R/ft)
R_air = 53.35; %gas constant (ft lb/(lbm °R))
k_air = 1.4; %specific heat ratio

% INTERMEDIATE CALCULATIONS
% Speed of Sound
temp = Temp0-B_atm*alt; % temperature at altitude (°R)
pres = Pres0*(1-B_atm*alt/Temp0)^(1/R_air/B_atm); %pressure @ alt (lb/ft^2)
rho = pres/(R_air*temp); % density at altitude (lbm/ft^3)
Vs = sqrt(k_air*R_air*temp*g0); % speed of sound (ft/sec)
% Rocket Config
d = Dia/12; % reference length (ft)
S = pi*d^2/4; % reference area (ft^2)
XT = (Xcg -Xt)*d; % thruster location from CG (ft)
XP_dat = (Xcp_dat-Xcg)*d; % center of pressure location from CG (ft)
Fz = n * Wght; % normal force (lb)
% Mach numbers and speeds
% adjust min and max Mach to table values
Mmin = max(min(Mach_dat),Mmin); % min Mach number to be used
Mmax = min(max(Mach_dat),Mmax); % max Mach number to be used
kmax = 50; % number of Mach numbers to be used
Mach = linspace(Mmin,Mmax,kmax); % vector of Mach numbers to be used

% THRUST AND ALPHA CALCULATIONS FOR EACH MACH NUMBER
for k = 1:kmax
    V = Mach(k)*Vs; % rocket speed (ft/s)
    QS = S * 1/(2*g0)*rho*V^2; % (dyn pres-lb/ft^2)(ref area-ft^2) (lb)
    CNa = interp1(Mach_dat,CNa_dat,Mach(k)); %CNa for Mach#
    Xcp = interp1(Mach_dat,XP_dat,Mach(k)); %Xcp for Mach#
    CMq = interp1(Mach_dat,CMq_dat,Mach(k)); %CMq for Mach#
    A = [QS*CNa, 1;
        -QS*CNa*Xcp, XT];
    if req_type == 2,
        B = [(V^2*Wght)/(g0*Rt); % RHS vector for turn radius
            (1/2)*QS*CMq*d^2/Rt];
    else
        B = [Fz; (1/2)*QS*CMq*n*g0*(d/V)^2]; % RHS vector for turn rate
    end
    X = inv(A)*B; % solution vector
    a(k) = X(1)*180/pi; % alpha in degrees
    T(k) = X(2); % required thrust in pounds
end

```



```

subplot (2,1,1)
    plot (Mach,T,'r'), grid on
    xlabel('Mach Number')
    ylabel('Required Thrust (lbf)')
    hold on
subplot (2,1,2)
    plot (Mach,a,'r'), grid on
    xlabel('Mach Number')
    ylabel('Required alpha (deg)')
    hold on

```

F. SEEKER FIELD OF VIEW

```

% This m-file calculates the probability of a target being in the
% seeker field of view, FOV (deg), for for several seeker acquisition
% ranges (Racq) and fields of view. Only single launch range is used.
%
% inputs include:  Launcher Pointing Error, Pnt (deg) - 1 sigma
%                  Missile unguided ballistic error, B (mils) - 1 sigma
%                  Missile distance time profile, (km) (function of fly out time)
%                  Guidance time delay, Gd (sec)
%                  Time delay for target ID, td (sec)
%                  Min and Max Target Speed (mph)
% also required are:
%                  Seeker acquisition ranges (km) - (vector)
%                  Min and Max FOV (deg)
%                  Launch Range (km)

% Mark Wonnacott, April 1997
% Naval Postgraduate School
clear, close all

%% Target Description
VTmin = 20;           % (mph) min target speed
VTmax = 60;           % (mph) max target speed

%% Missile Configuration Inputs
% Launcher Pointing Error
Pnt = 3;              % (deg- 1 sig) initial pointing error
% Unguided Missile Ballistic Error
B = 12;               % (mills- 1 sig) meters error per km flight
% Guidance Delay
Gd = 1.0;              % (sec) max range delay(no guidance for 1 sec)
% Delay time to ID target
td = 5*1/8;           % (sec) 5 laser pulses received at 8 Hz

```

```

% Seeker Field of View
FOVmin = .5; % (deg) min half FoV
FOVmax = 45; % (deg) max half FoV
% Seeker Acquisition Range
Racq = [1.15,1.5,2,3,6]; % (km) parametric seeker acquisition ranges
% Launch Range
RL = 6; % (km) maximum launch range
% Missile Speed Table
Time = [0,0.22,0.89,1.02,1.67,... %flight time (s)
        2.52,4.96,7.91,11.24,14.88,18.8,22.99,27.3];
Dist = [0,0.01,0.2,0.27,0.6,1,2,3,4,5,6,7,8]; %flight dist (m)

%% Inputs converted to usable variables
VTmin2 = VTmin/2237; % min target speed (mph->km/s)
VTmax2 = VTmax/2237; % max target speed (mph->km/s)
PntR = Pnt*pi/180; % initial pointing error (deg->rad)
Bkm = B/1000; % X-trk error (km per km flight)
kmax = length (Racq); % number of seeker acq. ranges
mmax = 30; % number of FOV's
FOV = linspace(FOVmin,FOVmax,mmax)*pi/180; % FOV's (deg->rad)
Rg = interp1(Time,Dist,Gd); % unguided flyout range (km)

Pacq = zeros(kmax,mmax); % pre-set Pacq matrix size

for k = 1:kmax % calculations for each Racq
    for m = 1:mmax % calculations for each FOV
        D = Racq(k)*cos(FOV(m)); % detection range (trgt @ FOV limit)
        F = Racq(k)*sin(FOV(m)); % max x-trk offset for FOV
        if RL-Rg > D
            Rd = RL - D; % range flown before detection
        else
            Rd = RL - Rg; % range flown when guided flight begins
        end
        tD = interp1(Dist,Time,Rd); % time at detection
        tT = tD + td; % time at start of turn
        Rt = interp1(Time,Dist,tT); % distance flown at start of turn
        s = Rt*sqrt(tan(PntR)^2+(Bkm)^2); %1 sig X-trk error at start of turn
        r1 = tT * VTmin2; % min target motion at start of turn
        r2 = tT * VTmax2; % max target motion at start of turn

        L5 = min(5*s, r2+F); % integration upper limit
        %% Integration of Pr(Xr)*Pt(Xr-F,Xr+F)
        %% from 0 to L5 done using 'quad8' (Pacq function in 'ProbAcq')
        Pacq(k,m) = 2*quad8('ProbAcq',0,L5,0.01,[],F,s,r1,r2);
    end
end
end

```

```

FOV = FOV*180/pi;           % field of view changed back to degrees
figure
plot (FOV,Pacq), grid on
title (['Vt = ',num2str(VTmin),' -> ',num2str(VTmax),'] mph'))
legend(num2str(Racq(1)),num2str(Racq(2)),num2str(Racq(3)),num2str(Racq(4)),num2str(Racq(5)))
ylabel ('Probability of Target in FOV'),
xlabel('half FOV ( $\pm$ deg)')

```

ProbAcq Function

```

function Pacq = ProbAcq(Xr,F,s,r1,r2)

% Returns the product of the assumed probability of the rocket being
% approximately at a certain cross-track position, Xr, and the
% probability of the target being between  $\pm F$  to either side of
% the rocket position (seeker's FOV limits).
% The probabilities are based on the 1-sigma rocket cross-track error-s
% and the min and max possible target cross-track motion-r1 and r2.
%
% This function has to take Xr as a vector and output Pacq as a vector!!!

% W. Mark Wonnacott, Naval Postgraduate School, 1997

if r1 == 0; r1 = 0.0001; end           % avoid division by zero

Prkt = 1/(s*sqrt(2*pi))*exp(-Xr.^2./(2*s^2)); %normal distribution of rocket

% Find probability of target in FOV extremes (Pt(x1,x2)) for each Xr
for k = 1:length(Xr)
    x = Xr(k);           % step through each rocket x-trk position
    X1 = x - F;           % extreme bound of FOV
    X2 = x + F;           % extreme bound of FOV
    if X1 > r2             % weapon farther out than possible for target
        Ptgt(k) = 0;
    elseif X1 < -r2        % all possible target locations inside FOV
        Ptgt(k) = 1;
    else
        % compute area bounded r1 & r2 circles, fly-out axis, and X2
        L1 = min(X2,r2);   % limit of intgrt'n for r2 circle
        L2 = min(X2,r1);   % limit of intgrt'n for r1 circle
        Ala = L1*sqrt(r2^2-L1^2) + r2^2*asin(L1/r2); %bounded area in r2 circle
        Alb = L2*sqrt(r1^2-L2^2) + r1^2*asin(L2/r1); %bounded area in r1 circle
        A1 = Ala-Alb;
    end
end
Pacq = Ptgt;

```

```

% compute area bounded r1 & r2 circles, fly-out axis, and X1
L3 = min(abs(X1),r2);
L4 = min(abs(X1),r1);
A2a = L3*sqrt(r2^2-L3^2) + r2^2*asin(L3/r2);
A2b = L4*sqrt(r1^2-L4^2) + r1^2*asin(L4/r1);
A2 = A2a-A2b;

A = A1-sign(X1)*A2;
Ptgt(k) = A / (pi*(r2^2-r1^2));
end
end

Pacq = Prkt.*Ptgt*100;
return, end

```

G. 6DOF CODES

1. Simulation Initilization

```

% File Initializes Simulation
clear
data_out = [2001,5];

%%% Missile INITIAL CONDITIONS (6 DOF Flight)
%%% (u,v,w,p,q,r,phi,theta,psi,p_rocket,pn,pe,ph)

% ground launch initial conditions
Msl_Xo = [0;0;0;0;0;0;0;10*pi/180;0;0;0;0;0];
% target pointing after 12 sec flight (10° elev launch) trgt @ 5000m
%Msl_Xo = [285;0;0;0.03;.01;0;0;-.383;0;-125.6;4230;0;310];%theta =0.0246
% straight and level cruise after 12 sec flight
%Msl_Xo = [300;0;0;0;0;0;0;0;0;-125.6;0;0;300];
%%% Target INITIAL CONDITIONS (6 DOF Flight)
%%% (Pn, Pe)

Tgt_Xo = [5000;00];
T_Vn = 0;
T_Ve = 0;
Talt = 0;

Aerodat % weight and aero data file for 2.75" HRGK-equipped rocket

```


2. Aerodat

% This File Contains Look-up Table Data

% 2.75" Rocket with Final Design Guidance Kit

global g0 Temp0 Pres0 B_atm R_air S d Sd Xt mu rho c;

%CONSTANTS & CONVERSIONS

%%% Conversions

in2m = 39.37; %inches per meter

lb2kg = 2.2046; %pounds per kilogram

%%% Gravity

g0 = 9.81; % Gravity Constant, g'0, in m/s^2.

%%% Atmospheric Data:

Temp0 = 288.15; %surface temperature (K)

Pres0 = 101330; %surface pressure (Pa)

B_atm = 0.00650; %temp lapse rate (°C/m)

R_air = 287.0; %gas constant (N m/(kg K))

% =====

% Guidance Package Parameters

% =====

radius = 2.75/2/in2m; %Guidance Package Radius (m)

GP_Mass0 = 7/lb2kg; %Initial Guidance Package Mass (kg)

GP_Massf = 7/lb2kg; %Final Guidance Package Mass (kg)

GP_Lngth = 13.625/in2m; %Guidance Package Length (m)

Xt = 6.6/in2m; %Thruster Location from Nose (m)

mu = 0.006; %Rocket to Kit Coefficient of Friction

GP_CG0 = 8.5/in2m; %Initial Guidance Package CG from nose (m)

GP_CGf = 8.5/in2m; %Final Guidance Package CG from nose (m)

GP_Jxx0 = ... %Aprox.Initial Axial Moment of Inertia (kg m^2)

GP_Mass0*radius^2/2;

GP_Jxxf = ... %Aprox.Final Axial Moment of Inertia (kg m^2)

GP_Massf*radius^2/2;

GP_Jyy0 = ... %Aprox.Initial Transverse M. of I. (kg m^2)

GP_Mass0*(GP_CG0-GP_Lngth/2)^2 + GP_Mass0*GP_Lngth^2/12;

GP_Jyyf = ... %Aprox.Final Transverse M. of I. (kg m^2)

GP_Massf*(GP_CGf-GP_Lngth/2)^2 + GP_Massf*GP_Lngth^2/12;

FlyTime = 30; %Approximate Flyout Time Bound (sec)

```

% =====
% Rocket Parameters from IHSP 89-289, Mk-66 Data Book
% =====
d = 2.75/in2m;                %Rocket Diameter (m)

R_Mass0 = 22.95/lb2kg;         %Initial Rocket Mass (kg)
R_Massf = 15.73/lb2kg;         %Final Rocket Mass (kg)
R_Lngth = 55.125/in2m;         %Rocket Length (m)

R_CG0 = ...                    %Initial Rocket CG from nose (m)
    R_Lngth-29.96/in2m + GP_Lngth;
R_CGf = ...                    %Final Rocket CG from nose (m)
    R_Lngth-33.55/in2m + GP_Lngth;

R_Jxx0 = 26.2/(lb2kg*in2m^2);  %Initial Axial Moment of Inertia (kg m^2)
R_Jxxf = 19.7/(lb2kg*in2m^2);  %Final Axial Moment of Inertia (kg m^2)

R_Jyy0 = 6248/(lb2kg*in2m^2);  %Initial Transverse M. of I. (kg m^2)
R_Jyyf = 5008/(lb2kg*in2m^2);  %Final Transverse M. of I. (kg m^2)

BurnTime = 1.05;               %Average Rocket Motor Burn Time (sec)

ThrustHot_dat=...              %Thrust Time History (sec & lbf for 150°F)
[0.00 0                        0.40 1520                        0.85 1800
0.05 1600                      0.45 1560                        0.90 1700
0.07 1700                      0.50 1610                        0.95 600
0.10 1690                      0.55 1650                        1.00 200
0.15 1600                      0.60 1700                        1.05 40
0.20 1530                      0.65 1730                        1.10 10
0.25 1500                      0.70 1750                        1.15 0
0.30 1490                      0.75 1780                        FlyTime 0];
0.35 1510                      0.80 1800

ThrustCold_dat=...             %Thrust Time History (sec & lbf for -50°F)
[0.00 0                        0.4 1380                        0.85 1680
0.05 1150                      0.45 1350                        0.9 1760
0.07 1300                      0.5 1340                        0.95 1750
0.1 1380                      0.55 1350                        1.00 1600
0.15 1400                      0.6 1350                        1.05 700
0.2 1400                      0.65 1400                        1.1 100
0.25 1400                      0.7 1440                        1.15 0
0.3 1390                      0.75 1500                        FlyTime 0];
0.35 1400                      0.8 1590

ThrustHot_dat(:,2) = ThrustHot_dat(:,2)*g0/lb2kg;
ThrustCold_dat(:,2) = ThrustCold_dat(:,2)*g0/lb2kg;

```

```

% =====
% Reference Area/Length and Mass & Moment Time Histories
% =====
S = pi*(d^2)/4; % Cross-Sectional Area (Ref Area-m^2)
Sd = S*d; % Ref Area x Ref Length (m^3)

t = [0; BurnTime; FlyTime]; %time vector for time histories

Mass_dat = [t, [R_Mass0+GP_Mass0 % Mass Time History (sec & kg)
               R_Massf+GP_Mass0
               R_Massf+GP_Massf]];

cg0=(R_CG0*R_Mass0+GP_CG0*GP_Mass0)/(R_Mass0+GP_Mass0);
cg1=(R_CGf*R_Massf+GP_CG0*GP_Mass0)/(R_Massf+GP_Mass0);
cg2=(R_CGf*R_Massf+GP_CGf*GP_Massf)/(R_Massf+GP_Massf);
CG_dat = [t, [cg0 % CG History (sec & m from nose)
              cg1
              cg2]];

Jx0 = R_Jxx0+GP_Jxx0;
Jx1 = R_Jxxf+GP_Jxx0;
Jx2 = R_Jxxf+GP_Jxxf;
Jx_dat = [t, [Jx0 % Axial M. of I. History (kg m^2)
              Jx1
              Jx2]];

JxR_dat = [t, [R_Jxx0; R_Jxxf; R_Jxxf]];
JxK_dat = [t, [GP_Jxx0; GP_Jxx0; GP_Jxxf]];

Jy0 = R_Jyy0+R_Mass0*(R_CG0-cg0)^2+GP_Jyy0+GP_Mass0*(GP_CG0-cg0)^2;
Jy1 = R_Jyyf+R_Massf*(R_CGf-cg1)^2+GP_Jyy0+GP_Mass0*(GP_CG0-cg1)^2;
Jy2 = R_Jyyf+R_Massf*(R_CGf-cg2)^2+GP_Jyyf+GP_Massf*(GP_CGf-cg2)^2;
Jy_dat = [t, [Jy0 % M. of I. History (kg m^2)
              Jy1
              Jy2]];

% Rocket Roll Acceleration History
R_Pdot = ... % Rocket Roll Accel (rev/s/s)
    [0 0 1.8 -8.0 5.8 -4.5
     0.5 45.0 2.0 0.0 6.2 -12.5
     0.6 100.0 2.4 2.0 6.6 -10.0
     0.9 15.0 3.0 7.5 7.0 -7.0
     1.0 -50.0 3.6 8.5 8.0 -4.0
     1.2 -120.0 4.0 9.5 9.5 0.0
     1.4 -92.0 4.4 7.5 12. 1.0
     1.6 -34.0 5.6 0.0 21. 0.1];
R_Pdot(:,2) = R_Pdot(:,2)*2*pi; % converted to rad/s/s

```

```

%=====
% Aerodynamics Data from ADAM's MADR
%=====
Mach_dat = ...
    [0                1.0000                1.4142
      0.6614          1.0308                1.6008
      0.8660          1.1180                1.8028
      0.9682          1.2500                2.0156];

%Static Coefficient/Derivative Components Based on Mach Number Vector
%-----
Cd0Coast_dat = ... % Skin, Wave, and Base Drag (rocket coasting)
    [0.52292          0.83218                1.09629
      0.48521          1.0067                1.13922
      0.51417          1.00424                1.16393
      0.75708          1.02549                1.17799];

Cd0Burn_dat = ... % Skin and Wave Drag (rocket burning)
    [0.42291          0.73219                0.90267
      0.38521          0.81307                0.95226
      0.41417          0.81061                0.99252
      0.65708          0.83187                1.02295];

CNa_dat = ... % Body Normal Force per Radian Alpha or Beta
    [15.0616          20.05156                16.10659
      16.41589          20.05156                14.68889
      18.10928          18.91632                13.47025
      20.04303          17.51701                12.38573];

CP_dat = ... % Center of Pressure in Calibers
    [11.52547          10.35951                10.68451
      11.32152          10.35951                10.88046
      11.01214          10.45431                10.99184
      10.36514          10.5577                11.05396];

CP_dat = CP_dat*d;

%Dyanamic Coefficients/Derivatives Based on Mach Number Vector
%-----
CMq_dat = ... % Pitching damping per Radian/sec of Pitch Rate
    [-4166.814        -5519.5352            -3938.8662
      -4556.4946        -5519.5352            -3541.0081
      -5041.0303        -4859.3901            -3202.1553
      -5518.2495        -4376.4146            -2916.2678];

Clp_dat = ... % Roll damping (HRGK only) /Radian/sec of Roll Rate
    [-7.513           -7.513                -6.7529
      -7.513           -7.513                -6.453
      -7.513           -7.2767                -5.5802
      -7.513           -7.0348                -4.7831];

```


3. Equations of Motion

```

function xo = MotionEqns(uo)
%%%%%%%%%%%%%%%%%%%%%%%%%%%%%%%%%%%%%%%%%%%%%%%%%%%%%%%%%%%%%%%%%%%%%%%%
%%% This Function computes the Flat-Earth, Body Axes,
%%% 6-DOF Dynamics Equations for a
%%% Thruster-Controlled Missile
%%%%%%%%%%%%%%%%%%%%%%%%%%%%%%%%%%%%%%%%%%%%%%%%%%%%%%%%%%%%%%%%%%%%%%%%
%%% Adapted for rolling airframe, thrust control, and
%%% variable aero coefficient and missile parameters by
%%% W. Mark Wonnacott, March 1997
%%% Naval Postgraduate School
%%% Adapted from the G. Hutchins' Code for EC 4330.
%%%%%%%%%%%%%%%%%%%%%%%%%%%%%%%%%%%%%%%%%%%%%%%%%%%%%%%%%%%%%%%%%%%%%%%%
%%% Original Code by R. G. Hutchins, 10 December 1996
%%% Thanks to
%%%      Rob King and Mark Wonnacott for aero assistance
%%%%%%%%%%%%%%%%%%%%%%%%%%%%%%%%%%%%%%%%%%%%%%%%%%%%%%%%%%%%%%%%%%%%%%%%
%%% The State Vector is defined as:
%%%      Body-Axes Velocities
%%%      x(1) = U,  speed along missile axis, x direction
%%%      x(2) = V,  speed of sideslip, y direction
%%%      x(3) = W,  speed along z direction ("Down")
%%%      Body-Axes Angular Velocities
%%%      x(4) = P,  roll rate
%%%      x(5) = Q,  pitch rate
%%%      x(6) = R,  yaw rate
%%%      Euler Angles
%%%      x(7) = phi,  roll relative to vertical down
%%%      x(8) = theta,  pitch
%%%      x(9) = psi,  yaw
%%%      Rocket Rolling
%%%      x(10) = Pr, rocket roll rate
%%%      Location Variables
%%%      x(11) = Pn,  Position North of (0,0,0)
%%%      x(12) = Pe,  Position East of (0,0,0)
%%%      x(13) = h,  Height
%%% The input vector is defined as:
%%%      u(1) = T1,  thrust from thruster #1
%%%      u(2) = T2,  thrust from thruster #2
%%%      u(3) = T3,  thrust from thruster #3
%%%      u(4) = T,  thrust through the missile x axis

```

```

%%%Other Missile Parameter Inputs(functions of Mach or time):
%%%   P(1) = mass, missile mass (kg) [f(t)]
%%%   P(2) = Xcg,missile Cg (m from nose) [f(t)]
%%%   P(3) = Xcp, center of pressure (m from nose) [f(M)]
%%%   P(4) = JxR rocket MofI about long axis(kg m^2)
%%%   P(5) = JxK kit MofI about long axis(kg m^2)
%%%   P(6) = Jy=Jz, missile MofI-y or z axes [f(t)]
%%%   P(7) = PdotR, rocket roll accel (rad/s/s)[f(t)]
%%% Aero Coefficients/Derivatives(functions of Mach or time):
%%%   C(1) = Cd0,zero alpha drag coefficient
%%%   C(2) = CNa,normal force /rad alpha (lift curve slope)
%%%   C(3) = CMq,pitch damping per rad/sec pitch rate
%%%   C(4) = Clp,roll damp per rad/sec roll rate (HRGK)
%%%%%%%%%%%%%%%%%%%%%%%%%%%%%%%%%%%%%%%%%%%%%%%%%%%%%%%%%%%%%%%%%%%%%%%%
%%% Related Quantities
%%%   alpha,      Angle of Attack
%%%   beta,       Sideslip Angle
%%%   Tz,         Resultant Vert. Thrust (up, -z dir.)
%%%   Ty,         Reultant Side Thrust (y direction)
%%%   Vt,         Missile Speed
%%%   Temp,       Air Temperature (K) [f(altitude)]
%%%   Pres,       Air Pressure (Pa) [f(altitude)]
%%%   Rho,        Air Density (Kg/m^3) [f(altitude)]
%%%   qbar,       Dynamic Pressure = 1/2 rho(h) Vt^2
%%%   L,          missile length (m)
%%%   d,          missile diameter (m) (ref length)
%%%   S=pi*d^2/4, missile cross-sectional area(m^2)(ref area)
%%%   mu,         rocket to kit coefficient of friction
%%% Aerodynamic Forces
%%%   CN = CNa*alpha => N=CN*qbar*S+Tz      Normal Force (=Lift)
%%%   CY = -CNa*beta => Y=CY*qbar*S+Ty      Sideslip Force
%%%   CD = Cd0 + CN^2/CNa => D=CD*qbar*S    Drag Force
%%% Aerodynamic Moments
%%%   CLbar = Clp*P*d/(2*U),
%%%   => Lbar = CLbar*qbar*S*d              Kit Roll Moment
%%%   CM = CNa*alpha(Xcg-Xcp) + CMq*Q*d/(2*U)
%%%   => M = CM*qbar*S*d + Tz(Xcg-Xt)      Pitch Moment
%%%   CNbar = CNa*beta(Xcg-Xcp) + CMq*Q*d/(2*U)
%%%   => Nbar = CNbar*qbar*S*d + Ty(Xcg-Xt) Yaw Moment
%%%%%%%%%%%%%%%%%%%%%%%%%%%%%%%%%%%%%%%%%%%%%%%%%%%%%%%%%%%%%%%%%%%%%%%%
%%%%%%%%%%%%%%%%%%%%%%%%%%%%%%%%%%%%%%%%%%%%%%%%%%%%%%%%%%%%%%%%%%%%%%%%
%%% Declare Global Variables
global g0 Temp0 Pres0 B_atm R_air S d Sd Xt mu;

```

```

%%% Define State Variables from Inputs
x = uo(1:14);
%%% Body-Axes Velocities
U = x(1);      % speed along missile axis, x
V = x(2);      % speed of sideslip, y direction
W = x(3);      % speed along z direction ("Down")
%%% Body-Axes Angular Velocities
P = x(4);      % roll rate
Q = x(5);      % pitch rate
R = x(6);      % yaw rate
%%% Euler Angles
phi = x(7);     % roll
theta = x(8);   % pitch
psi = x(9);     % yaw
%%% Rocket Rolling
Pr = x(10);     % rocket roll rate
%%% Location Variables
Pn = x(11);     % Position North of (0,0,0)
Pe = x(12);     % Position East of (0,0,0)
h = x(13);      % Height

%%% Define Control Variables from Inputs
u = uo(14:17);
T1 = u(1);      % thrust from thruster #1
T2 = u(2);      % thrust from thruster #2
T3 = u(3);      % thrust from thruster #3
T = u(4);       % thrust through the missile long. axis

%%% Other Missile Parameter Inputs (time or Mach dependent):
Param = uo(18:24);
mass = Param(1); %missile mass (kg)
Xcg = Param(2);  %missile Cg (m from nose)
Xcp = Param(3);  %missile CP (m from nose)
JxR = Param(4);  %rocket M of I about long axis(kg m^2)
JxK = Param(5);  %kit M of I about long axis(kg m^2)
Jy = Param(6);   %missile MofI about y or z axes(kg m^2)
PdR = Param(7);  %rocket roll acceleration (rad/s/s)
%%% Define Mach Number Dependent Coefficients/Derivatives
C = uo(25:28);
Cd0 = C(1);      %zero alpha drag coefficient
CNa = C(2);      %normal force /rad alpha (lift curve slope)
CMq = C(3);      %pitch damping per rad/sec pitch rate
Clp = C(4);      %roll damping (kit only) per rad/sec roll

```

```

##### Define the Forces and Moments

%%% Related Quantities
% speed quantities
Vxz2 = U^2 + W^2;
Vt2 = Vxz2 + V^2;
Vt = sqrt(Vt2);
% atmospheric
temp = Temp0-B_atm*h;
pres = Pres0*(1-B_atm*h/Temp0)^(g0/R_air/B_atm);
rho = pres/(R_air*temp);
qbar = .5*rho*Vt2;
% control thrusts
Ty = T1*cos(phi) + ...
    T2*cos(phi+2/3*pi) + T3*cos(phi+4/3*pi);
Tz = T1*sin(phi) + ...
    T2*sin(phi+2/3*pi) + T3*sin(phi+4/3*pi);
% angles of attack
alpha = atan2(W,U);
beta = atan2(V,sqrt(Vxz2));

%%% Forces
CN = CNa*alpha;           % normal force coefficient
Fz = -qbar*S*CN - Tz;     % normal force
CY = -CNa*beta;          % side force coefficient
Fy = qbar*S*CY + Ty;      % side force
CD = Cd0 + (CN^2+CY^2)/CNa;% drag force coefficient
Fx = T - qbar*S*CD;       % drag force

%%% Moments
Cl = Clp*P*d/(2*U+.001);  % roll moment coefficient
Lbar = qbar*Sd*Cl + mu*JxR*PdR; % roll moment on kit
CM = CNa*alpha*(Xcg-Xcp) + ... %pitch moment coefficient
    CMq*Q*d/(2*U+.001);
M = qbar*Sd*CM + Tz*(Xcg-Xt); % pitch moment
Cn = -CNa*beta*(Xcg-Xcp) + ... % yaw moment coefficient
    CMq*R*d/(2*U+.001);
Nbar = qbar*Sd*Cn + Ty*(Xcg-Xt); % yaw moment

```



```
%%% Compute the Time Derivatives from Flat-Earth Equations
```

```
%%% Force Equations
```

```
Ud = R*V - Q*W - g0*sin(theta) + Fx/mass;
Vd = -R*U + P*W + g0*sin(phi)*cos(theta) + Fy/mass;
Wd = Q*U - P*V + g0*cos(phi)*cos(theta) + Fz/mass;
```

```
%%% Moment Equations
```

```
Pd = Lbar/JxK;
Prd = PdR;
Qd = (1-JxK/Jy)*P*R + M/Jy - (JxR/Jy)*R*Pr;
Rd = (JxK/Jy-1)*P*Q + Nbar/Jy + (JxR/Jy)*Q*Pr;
```

```
%%% Kinematic Equations
```

```
phid = P + tan(theta)*(Q*sin(phi) + R*cos(phi));
thetad = Q*cos(phi) - R*sin(phi);
psid = (Q*sin(phi)+R*cos(phi))/cos(theta);
```

```
%%% Navigation Equations
```

```
Pnd = U*cos(theta)*cos(psi) + ...
      V*(sin(phi)*sin(theta)*cos(psi) - cos(phi)*sin(psi)) +...
      W*(cos(phi)*sin(theta)*cos(psi) + sin(phi)*sin(psi));
Ped = U*cos(theta)*sin(psi) + ...
      V*(sin(phi)*sin(theta)*sin(psi) + cos(phi)*cos(psi)) +...
      W*(cos(phi)*sin(theta)*sin(psi) - sin(phi)*cos(psi));
hd = U*sin(theta) - V*sin(phi)*cos(theta) - ...
     W*cos(phi)*cos(theta);
```

```
%%%%%%%%%% Define the output vector
```

```
%%% Body-Axes Accelerations
```

```
xo(1) = Ud;           % acc along missile axis,x direction
xo(2) = Vd;           % acc of sideslip, y direction
xo(3) = Wd;           % acc along z direction ("Down")
```

```
%%% Body-Axes Angular Accelerations
```

```
xo(4) = Pd;           % roll acc
xo(5) = Qd;           % pitch acc
xo(6) = Rd;           % yaw acc
```

```
%%% Euler Angle Rates
```

```
xo(7) = phid;         % d phi/dt
xo(8) = thetad;       % d theta/dt
xo(9) = psid;         % d psi/dt
```

```
%%% Rocket Rolling Equations
```

```
xo(10) = Prd;         % rocket spin acceleration
```

```
%%% Location Variable Rates
```

```
xo(11) = Pnd;         % Position North of (0,0,0) rate
xo(12) = Ped;         % Position East of (0,0,0) rate
xo(13) = hd;          % Height rate
```

4. Line of Sight

```

function yo = LineofSight(uo)
%%%%%%%%%%%%%%%%%%%%%%%%%%%%%%%%%%%%%%%%%%%%%%%%%%%%%%%%%%%%%%%%%%%%%%%%
%%% This Function computes the seeker frame LOS,
%%% from the tangent plane coordinates
%%% W. Mark Wonnacott, May 1997
%%% Naval Postgraduate School
%%%%%%%%%%%%%%%%%%%%%%%%%%%%%%%%%%%%%%%%%%%%%%%%%%%%%%%%%%%%%%%%%%%%%%%%
%%%  INPUTS
%%%      Position Differences Xt-Xm
%%%      u(1) = N,          delta north
%%%      u(2) = E,          delta east
%%%      u(3) = H,          delta height
%%%      Euler Angles
%%%      u(4) = phi,        seeker roll relative to vertical down
%%%      u(5) = theta,      rocket pitch relative to horizontal
%%%      u(6) = psi,        rocket yaw relative to north
%%%  OUTPUTS Seeker LOS
%%%      y(1) = alpha,      off-boresight angle
%%%      y(2) = beta,       angle from seeker's ref. roll position (down)
%%%      y(3) = R,          slant range to target
%%%%%%%%%%%%%%%%%%%%%%%%%%%%%%%%%%%%%%%%%%%%%%%%%%%%%%%%%%%%%%%%%%%%%%%%
%%% Define Tangent Plane LOS Offsets
      N = uo(1);          % north distance to target
      E = uo(2);          % east distance to target
      D = uo(3);          % down distance to target
%%% Define Rocket Euler Angles
      phi = uo(4);        % seeker roll relative to vertical down
      theta = uo(5);      % rocket pitch relative to horizontal
      psi = uo(6);        % rocket yaw relative to north
%%% Transformation Matrices (NED to XYZ-body)
      C1 = [cos(psi)    sin(psi)    0;
            -sin(psi)   cos(psi)    0;
              0          0          1];
      C2 = [cos(theta)  0    -sin(theta);
              0          1      0;
            sin(theta)  0    cos(theta)];
      C3 = [ 1          0          0;
              0        cos(phi)  sin(phi);
              0       -sin(phi)  cos(phi)];
      X=C3*C2*C1*[N;E;D];
      Offbore = atan2(sqrt(X(2)^2+X(3)^2),X(1));
      pointing= atan2(X(3),X(2));
      R = sqrt(X(1)^2+X(2)^2+X(3)^2);

      yo(1) = Offbore;    yo(2) = pointing;    yo(3) = R;

```

5. Mach Number

```
function M = Mach(uo)
%%%%%%%%%%%%%%%%%%%%%%%%%%%%%%%%%%%%%%%%%%%%%%%%%%%%%%%%%%%%%%%%%%%%%%%%
%%% This function computes the Mach Number as a function of
%%% component velocities and altitude
%%%%%%%%%%%%%%%%%%%%%%%%%%%%%%%%%%%%%%%%%%%%%%%%%%%%%%%%%%%%%%%%%%%%%%%%
%%% W. Mark Wonnacott, March 1997
%%% Naval Postgraduate School
%%%%%%%%%%%%%%%%%%%%%%%%%%%%%%%%%%%%%%%%%%%%%%%%%%%%%%%%%%%%%%%%%%%%%%%%
%%% INPUTS:
%%%   Body-Axes Velocities
%%%       x(1) = U,   speed along missile axis, x direction
%%%       x(2) = V,   speed of sideslip, y direction
%%%       x(3) = W,   speed along z direction ("Down")
%%%       x(13)= h,   altitude (m)
%%% Related Quantities
%%%       Vt,        Missile Speed (m/s)
%%%       Temp,       Air Temperature (K) as function of altitude
%%%       Pres,       Air Pressure (Pa) as function of altitude
%%%       Rho,        Air Density (Kg/m^3) as function of altitude
%%%%%%%%%%%%%%%%%%%%%%%%%%%%%%%%%%%%%%%%%%%%%%%%%%%%%%%%%%%%%%%%%%%%%%%%
%%%%%%%%%%%%%%%%%%%%%%%%%%%%%%%%%%%%%%%%%%%%%%%%%%%%%%%%%%%%%%%%%%%%%%%%

%%% Declare Global Variables
global g0 Temp0 Pres0 B_atm R_air S d Sd Xt;

%%% Define Variables from Inputs
%%%   Body-Axes Velocities
%%%       U = uo(1);    % speed along missile axis, x direction
%%%       V = uo(2);    % speed of sideslip, y direction
%%%       W = uo(3);    % speed along z direction ("Down")
%%%       h = uo(13);   % height

Vt = sqrt(U^2 + V^2 + W^2);

% atmospherics
k = 1.4;
temp = Temp0-B_atm*h;
pres = Pres0*(1-B_atm*h/Temp0)^(g0/R_air/B_atm);
rho  = pres/(R_air*temp);

c = sqrt(k*R_air*temp);

M = Vt/c;
```

LIST OF REFERENCES

1. AIAA Missile Systems Technical Committee. "Graduate Team Missile Design Competition, RFP: Hit-To-Kill Guided Rocket (HGR)." American Institute of Aeronautics and Astronautics; Reston, VA: June 1996.
2. Wonnacott, W.M; Pomerantz, B; Silva, S.L; and Nurse, N.A. "The Three and a Half Rocketeers Hit-to-Kill Rocket Guidance Kit" (design proposal for AIAA graduate student competition). Naval Postgraduate School; Monterey, CA: June 1997.
3. Foss, Christopher F. and Gander, Terry J., eds. *Jane's Military Vehicles and Logistics, 1996-97*. Jane's: 1996.
4. Foss, Christopher F., ed. *Jane's Armour and Artillery, 1996-97* (7th ed). Jane's: 1996.
5. Cullen, Tony and Foss, Christopher R., eds. *Jane's Land-Based Air Defense, 1996-97* (9th ed). Jane's: 1996.
6. Sharpe, Richard, Captain RN, ed. *Jane's Fighting Ships, 1995-96*. Jane's: 1995.
7. Washburn, Alan. "Notes on Firing Theory." Naval Postgraduate School; Monterey, CA: 1983.
8. Nicholas, Ted and Rossi, Rita, eds. *US Weapon Systems Costs, 1994* (14th ed). Data Search Associates; Fountain Valley, CA: 1994.
9. Tobin, Vince, Maj. U.S. Army and Mason, Pat, Capt. U.S. Army—AH-64 pilots. personal communications. Naval Postgraduate School; Monterey, CA: January 1997.
10. HYDRA-70/2.75 Inch Rocket Management Office. "Hydra-70 2.75 Inch Rocket System Information Handbook." US Army Armament, Munitions and Chemical Command; Rock Island, IL: April 1994.
11. Ferguson, John H., Jr. and Garvey, Paul B. "2.75-Inch Rocket Motor Mark 66 Data Book: Characteristics and Performance Data," IHSP 89-289. Naval Ordnance Station; Indian Head, MD: June 1989.
12. Hindes, John W., Jr. *Using ADAM* (3rd ed). Madison, AL: October, 1993.
13. Wonnacott, W.M. "Initial Version of the Medium Range, Antiship Weapon Analysis Program—SeaHit," NWC TM 6823. Naval Air Warfare Center Weapons Division; China Lake, CA: September 1990.
14. Advanced Systems Concepts Office. "Missile Sizing Program User's Manual." U.S. Army Missile Command; Huntsville, AL: March 1989.

15. Stevens, Brian L. and Lewis, Frank L. *Aircraft Control and Simulation*. Wiley; New York: 1992.
16. Chin, S.S.; *Missile Configuration Design*; 1961: McGraw-Hill Book Company; New York.
17. Blakelock, John H.; *Automatic Control of Aircraft and Missiles*; 2nd Ed; 1991: John Wiley & Sons, New York.
18. Howard, Richard; *AA3701: Missile Aerodynamics Class Notes*; 1995: Naval Postgraduate School; Monterey, CA.

INITIAL DISTRIBUTION LIST

1. Defense Technical Information Center 2
8725 John J. Kingman Rd., STE 0944
Ft. Belvoir, VA 22060-6218

2. Dudley Knox Library 2
Naval Postgraduate School
411 Dyer Rd.
Monterey, CA 93943-5101

3. Dr. Conrad F. Newberry 4
(Code AA/Ne)
Naval Postgraduate School
Monterey, CA 93943-5106

4. Dr. Louis V. Schmidt 1
(Code AA/Sc)
Naval Postgraduate School
Monterey, CA 93943-5106

5. Commander 4
Code 471300D (Attn: Mr. W. Mark Wonnacott)
Naval Air Warfare Center Weapons Division
1 Administration Circle
China Lake, CA 93555-6001

6. Commander 1
Code 473000D (Attn: Mr. Stephen F. Lyda)
Naval Air Warfare Center Weapons Division
1 Administration Circle
China Lake, CA 93555-6001

7. Mr. Eugene L. Fleeman 1
Boeing North American, Inc.
MS 031-FB23
3370 East Miraloma Avenue
P.O. Box 3105
Anaheim, CA 92803-3105

STUDLEY KNOX LIBRARY
NAVAL POSTGRADUATE SCHOOL
MARIETTA, GA 30043-5101

DUDLEY KNOX LIBRARY



3 2768 00341272 7